RICE UNIVERSITY

Development of a Thermoresponsive and Chemically Crosslinkable Hydrogel System for Craniofacial Bone Tissue Engineering

by

Eleftheria Leda Klouda

A THESIS SUBMITTED IN PARTIAL FULFILLMENT
OF THE REQUIREMENTS FOR THE DEGREE

Doctor of Philosophy

APPROVED, THESIS COMMITTEE:

Antonios G. Mikos, Professor (Chair)
Bioengineering and Chemical and Biomolecular Engineering

Paul S. Engel, Professor
Chemistry

K. Jane Grande-Allen, Associate Professor
Bioengineering

John A. Jansen, Professor
Radboud University Nijmegen Medical Center

F. Kurtis Kasper, Faculty Fellow
Bioengineering

HOUSTON, TEXAS

DECEMBER 2010

ABSTRACT

Development of a Thermoresponsive and Chemically Crosslinkable Hydrogel System for Craniofacial Bone Tissue Engineering

by

Eleftheria Leda Klouda

A novel injectable hydrogel system for cell delivery in craniofacial bone tissue engineering was developed in this work. The hydrogel employs a dual solidification mechanism by containing units that gel upon temperature increase to physiological temperature and groups that allow for covalent crosslinking. The successful synthesis of macromers for hydrogel fabrication was demonstrated and structure-property relations were established. The hydrophilic-hydrophobic balance of the macromers was found to be an important design criterion towards their resulting thermal gelation properties. When tested with cells *in vitro,* macromers with different molecular compositions, molecular weights and transition temperatures were all found to be cytocompatible. The introduction of a chemically crosslinkable group in the macromers resulted in hydrogels with improved stability. The effect of the addition of these highly reactive groups on cell viability was evaluated and parameters that enable viable cell encapsulation in the

hydrogels were determined. It was shown that there was a dose- and time-dependent effect of the macromers on cell viability. Increased degrees of modification were found to decrease the thermal transition temperature as well as the cytocompatibility of the macromers. Hydrogels were fabricated at physiological temperature upon physical gelation and chemical crosslinking with the addition of a thermal free radical initiator system. The swelling behavior of the hydrogels was characterized and it was found to be controlled by the chemistry of the macromer end group, the concentration of the initiator system used, the fabrication interval as well as the incubation temperature and medium. In order to evaluate the hydrogels as cell carriers, mesenchymal stems cells were encapsulated in the hydrogels over a 21-day period. Cells retained their viability over the duration of the study and exhibited markers of osteogenic differentiation when cultured with appropriate supplements. These findings hold promise for the use of these hydrogel systems for cell encapsulation in tissue engineering applications.

ACKNOWLEDGMENTS

This thesis is dedicated to my parents Stamatios and Kalliopi Klouda for providing me with all the love and opportunities I am fortunate to enjoy in my life.

This work has been supported by research grants from the National Institutes of Health. I would also like to acknowledge a fellowship from the Gerondelis Foundation.

I would like to express my appreciation to my advisor and chair of the thesis committee Dr. Antonios Mikos. Working with him has been an invaluable educational experience. I would like to thank him for the trust he showed me to explore my ideas and his guidance throughout my years in his laboratory.

I would like to thank the members of my thesis committee Dr. Paul Engel, Dr. Jane Grande-Allen, Dr. John Jansen and Dr. Kurt Kasper for being always available for advising and supporting me over the course of my work. Dr. Michael Hacker was instrumental in teaching me all about polymer synthesis and characterization and I would like to thank him for helping me initiate my research. Dr. Lawrence Alemany is gratefully acknowledged for his help and advice with NMR spectroscopy. Dr. Robert Raphael allowed me to use his lab's confocal microscope and I would like to thank him herewith.

My research experience might not have been as didactic and pleasant without the help and support from my lab mates in the Mikos laboratory over the past years. I have been

very lucky to be able to work with, learn from and call my friends the people I have collaborated with during my PhD research.

I am grateful to my parents, sister Alkisti and brother Alexandros for believing in me at all times. They encouraged me greatly even though we live in different continents. I would like to thank also my extended family and friends who have always been there for me.

My husband Ilias has shown unconditional support and never-ending patience while I have been pursuing my PhD. I can't thank him enough for helping me reach this stage of my education and life.

TABLE OF CONTENTS

LIST OF FIGURES

LIST OF TABLES

LIST OF ABBREVIATIONS

^{1}H-NMR	Proton nuclear magnetic resonance
AAm	Acrylamide
AcCl	Acryloyl chloride
AIBN	Azobisisobutyronitrile
ALP	Alkaline phosphatase
APS	Ammonium persulfate
dd water	Double distilled water
DMEM	Dulbecco's modified Eagle medium
DSC	Differential scanning calorimetry
EDS	Energy dispersive spectrometry
ECM	Extracellular matrix
FBS	Fetal bovine serum
GPC	Gel permeation chromatography
HEA	2-Hydroxyethylacrylate
LCST	Lower critical solution temperature
MACl	Methacryloyl chloride
MSC	Mesenchymal stem cell
NiPAAm	*N*-isopropylacrylamide
ODA	Octadecyl acrylate
PBS	Phosphate buffered saline
PEDAS	Pentaerythritol diacrylate monostearate

PEG	Poly(ethylene glycol)
PEG-DA	Poly(ethylene glycol) diacrylate
PEO	Poly(ethylene oxide)
PI	Polydispersity index
PNiPAAm	Poly(*N*-isopropylacrylamide)
PPO	Poly(propylene oxide)
SBF	Simulated body fluid
SEM	Scanning electron microscopy
Stat	Statistical copolymer (notation for)
TEMED	*N*,*N*,*N*′,*N*′-Tetramethylethylenediamine
TGM	Thermogelling macromer
THF	Tetrahydrofuran
TMS	Tetramethylsilane
α-MEM	Minimum essential medium, α modification

CHAPTER I

OBJECTIVE AND SPECIFIC AIMS

The overall objective of this work is the development of injectable, *in situ* forming hydrogels for application in craniofacial bone tissue engineering. The hydrogel is designed to solidify upon injection to the body at physiological temperature, employing two independent gelation mechanisms.

1. ***Synthesis and characterization of thermally responsive and chemically crosslinkable, amphiphilic N-isopropylacrylamide based macromers***
   - Synthesis of macromers that contain thermally responsive domains and chemically modifiable units that allow for covalent crosslinking.
   - Evaluation of the effects of macromer composition and hydrophilic-hydrophobic balance on the thermal gelation characteristics (i.e. lower critical solution temperature and gel stability).
   - Evaluation of the effects of a dual, physical and chemical gelation mechanism at physiological temperature employing a chemical initiator system on hydrogel stability.

2. ***Cytocompatibility evaluation of thermally responsive and chemically crosslinkable macromers***
   - Evaluation of the effects of unmodified macromer molecular composition, molecular weight and lower critical solution temperature on *in vitro* cell viability.
   - Evaluation of the effect of macromer modification with varying contents of (meth)acrylate groups on *in vitro* cell viability.

3. ***Fabrication, characterization and cell encapsulation in thermoresponsive and chemically crosslinkable hydrogels***
   - Evaluation of the effect of fabrication method and incubation temperature on the hydrogel swelling characteristics.
   - Evaluation of the effect of macromer end group chemistry (acrylate or methacrylate group) on *in vitro* hydrogel swelling and degradation.
   - Mesenchymal stem cell encapsulation in the hydrogels and evaluation of *in vitro* cellular viability, osteogenic differentiation and hydrogel mineralization.

CHAPTER II

BACKGROUND INFORMATION: INJECTABLE SYSTEMS FOR CRANIOFACIAL BONE TISSUE ENGINEERING

Abstract

Tissue engineering represents a promising strategy towards the regeneration of craniofacial bone defects. This approach relies on the delivery of a scaffold material with cells and bioactive factors and can provide significant aid in the healing of compromised tissues. The parameters that are important in the design of a biomaterial carrier are discussed. Injectable systems are particularly attractive for craniofacial bone defects as they can be administered in a minimally invasive manner and can fill irregular cavities, two factors that are important due to the unique location and shape of these defects. Among injectable, *in situ* forming hydrogels, thermoresponsive materials utilize temperature change as the trigger that determines their gelling behavior without any additional external factor. These hydrogels have been interesting for biomedical uses as they can swell under physiological conditions and provide the advantage of convenient administration.

Significance and current treatments of craniofacial bone defects

Bone loss and possible strategies towards its replacement represent some of the most common problems for surgeons nowadays. One particular challenge is represented by defects in the skull and facial bones which impose severe functional and aesthetic limitations to patients. Craniofacial bone defects can cause facial asymmetry and problems in mastication and articulation, depending on the location of the defect [1]. Furthermore, the protection of the brain and soft cranial and facial tissues may be compromised [2]. The occurrence of craniofacial defects may result from tumor resection, trauma, ischemic or infectious causes as well as congenital and developmental anomalies [1, 2].

Craniofacial bone reconstruction aims at re-establishing form and function, as well as minimizing patient morbidity and discomfort [1]. Ideally, a bone grafting material should be biocompatible and not affect unfavorably its biological environment, perform the mechanical and structural function of native bone and promote its healing. Traditional treatments include alloplastic materials (non-living) as well as homologous (from the same species), heterologous (from a different species) and autologous (from oneself) bone grafts [2]. Some alloplastic materials that have been used in craniofacial bone reconstruction over the past years include aluminum, gold, vitallium (an alloy of cobalt, chromium and molybdenum), tantalum, stainless steel, titanium, methylmethacrylate resins, polyethylene, silicone elastomers and hydroxyapatite ceramics [2]. However, limitations inherent in the use of alloplastic materials include biocompatibility issues and insufficient response to the mechanical and thermal stress of the physiologic

environment. Specifically, there is increased probability of inflammatory response, risk of infection or neoproliferative reactions. Furthermore, conventional materials are not biodegradable and lack the ability to remodel with the host tissues and organs. Another important consideration for the material is to be easy to handle and to adapt to the shape of the defect [2-4]. Biologically active implants such as demineralized bone matrix obtained from homologous or heterologous sources have shown potential for reconstructive purposes because of their high ability to induce bone growth termed as osteoinductivity [5]. However, drawbacks include the theoretical risk of disease transmission, possible immune rejection, as well as cost. Surgeons often regard autologous bone as the gold standard for a grafting material due to its potential for growth and remodeling, as well as immunocompatibility. Disadvantages associated with this approach include insufficient host tissue for repair of the defect site and possible donor site morbidity [3, 6, 7].

A more recent promising approach involves the emerging field of tissue engineering for the regeneration of bone defects. As defined by Langer and Vacanti in 1993: "Tissue Engineering is an interdisciplinary field that applies the principles of engineering and life sciences toward the development of biological substitutes that restore, maintain, or improve tissue function" [8].

Engineering complex craniofacial tissues [*]

Tissue engineering strategies rely on the use of cells, bioactive factors, and scaffolds or combinations thereof. The scaffold serves the purpose of a delivery vehicle, a space-filling agent and can be designed to be biointeractive, i.e. to be able to guide tissue regeneration. The field of tissue engineering has made significant advances over the past 15 years. Interdisciplinary research spanning basic cell biology to nanotechnology deepened our understanding of nature and enabled methods of mimicking it to augment tissue or even organ function. Research on virtually all types of tissues is being currently conducted, and products for cartilage and skin regeneration are already approved for commercial use by the Food and Drug Administration of the United States. The engineering of more complex tissues remains a challenge, but encouraging results were published in the *Lancet* in 2006, reporting the clinical success of a tissue engineered bladder [9]. Bladder tissue has distinct properties and is it difficult to restore its function with synthetic materials or grafts. Patients' own populations of smooth muscle and urothelial cells were expanded *in vitro*, seeded on bladder-shaped, biodegradable scaffolds, and implanted. Functional bladders were observed on patient follow up over a period of years, and importantly, no adverse effects on other organs, such as kidney problems, were reported. Biopsies taken from the tissue engineered bladders showed an architecture and phenotype that adequately resembled the native organs. The authors

[*] The following section was included in: J.D. Kretlow, S. Young, L. Klouda, M. Wong and A.G. Mikos, Injectable Biomaterials for Regenerating Complex Craniofacial Tissues, Advanced materials 21 (2009), 3368-3393

concluded that tissue engineering of the complex bladder is possible, however further studies are necessary to optimize the procedure for wide clinical use.

The coordinated regeneration of multiple tissues in the complex craniofacial environment requires a deeper understanding of their physiology and their remodeling characteristics. One needs to engineer complex tissues with the structural and functional characteristics of the native tissue, in a process that is not only biocompatible but also interactive with neighboring tissues at the same time. Another challenge lies in the fact that one type of tissue can be found in various structures that serve different functions and have therefore different properties. For example, the cartilaginous structures found in the craniofacial region have very distinct characteristics. It may require a certain approach to regenerate the weight-bearing, dense bilaminar structure of cartilage found in the temporomandibular joint (TMJ), and quite another to create the delicate elastic cartilage found in the ears or nose [10].

The craniofacial region, including also oral and dental tissues, is composed of skin, bone, muscle, cartilage, adipose tissue, tendons, ligaments, salivary glands and teeth. Extensive research is conducted on each of these tissues, but few studies focus on regeneration of multiple tissues in tandem. Recent advances in craniofacial tissue engineering, as summarized by Mao et al [3], include integrated bone and cartilage layers for the temporomandibular joint (TMJ) condyle, various elements of the periodontium, craniofacial bone, cranial suture-like structures as well as adipose tissue.

Tissue engineering of composite tissues such as of those found in the craniofacial region is a demanding task. One needs to account for multiple cellular phenotypes and

find a way to enhance their interactions towards tissue repair, possibly stimulating their behavior by supplying bioactive factors. Furthermore, the problem of vascularization must be solved since most tissues are strongly dependent on blood supply for growth. Creating stratified tissue architectures and achieving the physiological structure-function properties of the final tissues is the ultimate goal. The choice of a tissue engineering scaffold can significantly aid in this process, not only being a delivery vehicle for the cells and bioactive factors but also with its ability to interact and guide tissue growth. Cell-material interactions and mass transport are only some of the important parameters that need to be incorporated into the design. Additionally, one needs to consider that the location and form of craniofacial tissues requires special treatment. For this delicate region, also the aesthetic effect is important and there should ideally be minimal scar formation.

Craniofacial Bone

Tissue engineering of the cranial and facial bone is a promising technique towards the functional restoration of this tissue. Craniofacial bone serves as a protective barrier to the intercranial structures and maintains the shape of the head. Bone is a highly vascularized and cellular tissue. The extracellular matrix of bone consists of an organic component, mainly collagen, and an inorganic component. This mineral component provides the mechanical strength of the matrix [11]. Approaches towards tissue engineering of bone are numerous, and much progress has been reported in that area. It is desired that bone tissue engineering constructs are osteoconductive, i.e. are allowing the migration of cells from the surrounding bone tissues and the sprouting of existing blood vessels, and

also osteoinductive, meaning that they encourage the formation of new bone by inducing cellular differentiation and mineralization. Review articles on bone tissue engineering considerations have been extensively published [12-16]. The Mikos group and other researchers have been utilizing a synthetic biomaterial strategy, usually in conjunction with growth factors and/or cellular delivery. Synthetic polymers, ceramics or composites thereof belong to the biomaterials mostly investigated for bone tissue engineering; many of these systems being injectable as well. It is suggested that osteogenesis is strongly dependent on angiogenesis [17]. Besides the facilitated transport of nutrients, oxygen and minerals, blood vessels stimulate bone morphogenesis due to the osteogenic effects of vascular cells [18]. This association has led many researchers to investigate the incorporation of angiogenic growth factors into bone tissue engineering models [19-21]. Also potent osteogenic factors have been identified, one prominent example being bone morphogenetic protein 2 (BMP-2). This growth factor has been shown to induce ectopic bone formation, i.e. in sites where bone would normally not grow [22, 23]. As our understanding of bone cell biology and development deepens, new frontiers open up in tissue engineering. A breakthrough was the identification of mesenchymal stem cells, the progenitor cells bone tissue derives from, and their isolation from multiple sites in the body. Factors that enhance the bone-forming capacity of these cells, found in their biomechanical and biochemical environment, are currently heavily examined [24-27].

Cell delivery for engineering complex craniofacial tissues

The delivery of cells to a defect is a means to accelerate the healing process as the body would not have to rely on host cells being recruited to that site. The cell source and type is a topic of much discussion and research over the past decades, and approaches using xenogeneic, allogeneic or autologous cells have been made. There are advantages and disadvantages involved in all of these approaches, and the decision has to be made considering the application and the translation from research to the final tissue engineered product. The other big question facing researchers is the choice between already differentiated cell types and stem cells, either embryonic or adult. Stem cells have the ability to proliferate in an undifferentiated state or, with the application of certain stimuli, to differentiate into one or more cell lineages. Investigators have recognized the tremendous potential of stem cells in regenerative medicine, and given their versatility, they can offer a valuable solution for engineering complex tissues. Embryonic stem cells are isolated from embryonic or fetal tissues, and are capable of giving rise to all types of tissues [28]. Adult stem cells can be mainly categorized into hematopoietic and mesenchymal stem cells. Hematopoietic stem cells (HSC) derive from the bone marrow and are progenitor blood cells. Mesenchymal stem cells (MSC) can be found in a variety of tissues, as for example the bone marrow, the periosteum, or adipose tissue, and can differentiate into bone, cartilage, muscle, fat, and other tissues [29, 30]. Most craniofacial tissues derive from mesenchymal stem cells. A recent review article by Mao et al [3] outlines the advances in the field of craniofacial tissue engineering using stem cells.

Once in the body, stem cells will receive signals which will govern their fate. These signals can be chemical or mechanical in nature, and are provided either by the

physiologic environment or can be incorporated in the cell delivery vehicle. The mechanisms by which these signals exert their effects on stem cells are not yet fully understood. The field of tissue engineering is greatly advanced by stem cell biology findings, and tissue engineering scaffolds have been used with promising results for stem cell delivery for various tissues. The nature of injectable materials, which allows for simultaneous cell and bioactive agent encapsulation, makes them particularly attractive for this application, and so does the ability to control these scaffolds' mechanical properties, which can provide the appropriate mechanobiological environment.

Injectable hydrogel systems with or without the addition of growth factors, were shown to promote mesenchymal stem cell differentiation, with possible applications in bone and cartilage regeneration [31, 32]. By controlling the scaffolds' swelling and mechanical characteristics, appropriate signals were transduced to the cells. Also the addition of a functional group to the polymer has been shown to induce cell differentiation, as for example a group that will enhance biomineralization, helping MSC turn into bone-forming cells [33]. Yamada et al utilized the abundance of growth factors in blood platelets by delivering MSC in a platelet-rich plasma gel, observing bone formation and neovascularization *in vivo* [34]. Morphogenic factors are often co-injected with cells, but can also be applied to the cells to pre-differentiate them *in vitro* prior to administration. An example for engineering complex tissues using the latter strategy is the work of Alhadlaq et al [35]. Rat mesenchymal stem cells were treated for three to four days with either chondrogenic or osteogenic supplements and loaded in two hydrogel layers formed by photopolymerization. After four weeks *in vivo*, stratified layers of chondrogenesis and osteogenesis were observed. The authors concluded that this

approach can offer a solution for tissue engineering complex tissues using a single adult mesenchymal stem cell population.

Biomaterial scaffold design criteria [†]

Following the classic tissue engineering paradigm, cells are seeded on a biomaterial scaffold with or without the addition of chemical or mechanical stimuli. The scaffold provides a three-dimensional supporting environment for the cells and should ideally guide tissue growth. Biomaterials have been a topic of extensive research in the past decades, and a plethora of scaffolds for diverse tissue engineering applications has been developed. Having as ultimate scope the clinical translation, researchers have established certain criteria that have to be met for a material in order to be considered. Some physiologically relevant design criteria are summarized in the next paragraphs. These variables are crucial for the success of a material in a tissue engineering application and should be considered during its design. These criteria are general guidelines; they have to be reviewed and applied according to the intended usage.

[†] The following section was included in: L. Klouda, J.D. Kretlow and A.G. Mikos, Tailored biomaterials for tissue engineering needs and their clinical translation, in: Translational Approaches in Tissue Engineering and Regenerative Medicine, J.J. Mao, G. Vunjak-Novakovic, A.G. Mikos and A. Atala, editors, Artech House, Boston, 2008, 325-337

Biocompatibility

Biocompatibility as defined by D. Williams in 1999 is "the ability of a material to perform with an appropriate response in a specific application" [36]. This definition encompasses the significant fact that the response to a material will vary according to the use and situation, and also that the appropriateness of the response may vary. For tissue engineering applications, a scaffold used as a cell substrate should not elicit any undesirable effects on them, and further cause any inappropriate local or systemic responses in the host [37]. Moreover, also any potential leachable products as well as the degradation products in the case of a biodegradable scaffold must be biocompatible [38]. Therefore, the synthetic and purification processes must be adapted in order to yield biocompatible materials and remove any potentially harmful components.

Biodegradation

Biodegradation is again a parameter that varies with the application. Although there is a general consensus that biomaterials in tissue engineering represent a temporary scaffold and must be thus biodegradable, the rate of degradation strongly depends on the desired function. A material must degrade in the body in order to provide space for new tissue development, however it should maintain its structural and mechanical properties until the newly-formed tissue is able to sustain itself. This is particularly important in the case of load-bearing tissues like bone. The degradation rate of a material can be tailored during its synthesis by incorporating chemical moieties that allow for hydrolytic scission of the molecules, rendering it faster degradable in the aqueous physiologic environment. Additionally, the molecular weight as well as the crosslinking density influence

degradation in the case of polymers, and so does the presence of particulates such as ceramics [39].

Porosity

A tissue engineering scaffold needs to be porous. This requirement is two-fold, firstly because pores allow for space that can be used for cell and tissue growth, and secondly as they enable nutrient and oxygen exchange as well as waste removal. A biomaterial fabrication process can be selected to yield porous constructs, for example rapid prototyping techniques [40] and electrospinning [41]. Moreover, a porous structure can be introduced by the addition of porogens into the bulk material matrix such as micro-and nanoparticles.

Mechanical properties

Another parameter that is strongly application-dependent is the mechanical properties of the biomaterial. In the cases of cardiovascular tissues or bone for example, a scaffold has to perform well mechanically to bear the loads in the place of the diseased or missing tissue, for a period until the growing tissue can do so by itself. The mechanical properties of the surrounding matrix can influence also cellular differentiation and tissue morphogenesis [42]. There are several techniques used to produce mechanically strong materials. Starting with the materials, the initial mechanical properties as well as those over time can be examined for different existing materials. Also the synthetic process can be optimized by selecting building blocks that enhance the strength of the resulting

material as well as the fabrication process that can result in a crosslinked system or the reinforcement of a material with particles such as carbon nanotubes [43].

Biological Properties

A desirable feature for a scaffold is to be biointeractive and able to direct tissue growth. It was found that extracellular matrix (ECM) proteins containing specific peptide sequences possess adhesion domains recognized by cellular receptors [44]. In order to facilitate cellular adhesion and function, those proteins or peptide sequences alone are coupled to a biomaterial's surface. Another approach involves the design of scaffolds that release growth factors in a controllable manner, stimulating cellular proliferation and differentiation as well as tissue growth [45, 46].

Handling and delivery

Another important consideration in the design of a biomaterial for tissue engineering is its delivery method and the ease of handling. A scaffold can be either prefabricated or formed *in situ*. The first type usually requires a surgical procedure for its placement, whereas the second can be injected. Both methods have advantages and disadvantages and in most cases, the application will determine the appropriateness of each. In the case of an irregular defect for example, an injectable scaffold that will harden and form *in vivo*, filling the cavity, may be preferred. The fabrication and sterilization processes must be selected according to the desired product and in a manner that does not affect its chemical composition and properties. Furthermore, the procedure must be

characterized by reproducibility. In summary, according to the case and the tissue to be regenerated, the desired delivery method will dictate the choice of biomaterial and its properties will help identify the preferred fabrication procedure.

Injectable systems in tissue engineering [♠]

Injectable biomaterials are widely researched and hold great promise in both the fields of drug delivery and tissue engineering, largely due to the minimally invasive nature with which they can be delivered. Injectable systems in drug delivery can be used both for parenteral drug delivery or localized injection to an affected site. Drug release kinetics can be varied via altering the character and processing of the injectable biomaterial matrix or depot, and the properties (size, hydrophobicity, etc.) of the drug to be released often have a large effect on release kinetics. For a patient, injectable delivery systems offer the advantage of avoiding surgical procedures and the host of potential complications thereof to implant the drug depot or, in the case of long term drug delivery, elimination of the need for repeated doctors visits or potentially dangerous indwelling percutaneous lines. Thus a long term drug delivery system deliverable via a simple injection holds multiple benefits for patient safety and quality of life.

[♠] The following section was included in: L. Klouda*, J.D. Kretlow* and A.G. Mikos, Injectable matrices and scaffolds for drug delivery in tissue engineering, Advanced Drug Delivery Reviews, 59 (2007), 263-273 (* equal contributors)

Tissue engineering is a relatively new field that seeks to regenerate human tissues through the use of some combination of cells, bioactive molecules such as drugs or growth factors, and a biomaterial support system or scaffold. The need for such technology is readily apparent; with the continued aging of the population, the current shortage of donor organ availability will likely only grow, and strategies to address the shortage through increased donation are fraught with medical [47-50] and ethical concerns [51-55]. The ability to regenerate damaged tissues and organs to a healthy and functional state using the body's own healing capabilities and without the need for long term immune suppression represents a near ideal solution to this growing problem. Injectable materials for use in tissue engineering share the same advantages as those used in drug delivery. Additionally, in tissue engineering applications, injectable biomaterials that form scaffolds *in situ* have the advantage of being able to take the shape of a tissue defect, avoiding the need for patient specific scaffold prefabrication, which is particularly useful in the case of irregular defects. Injectable scaffolds eliminate the need for surgical interventions for delivery, and the minimally invasive procedure of injection reduces discomfort and complications for the patient. Also problems of cell adhesion and bioactive molecule delivery are overcome as, under proper conditions, they can be easily incorporated in the solution by mixing prior to injection.

Thermoresponsive hydrogels [§]

Hydrogels are composed of hydrophilic homopolymer or copolymer networks and can swell in the presence of water or physiological fluids. Chemical crosslinks (covalent bonds) or physical junctions (e.g. secondary forces, crystallite formation, chain entanglements) provide the hydrogels' unique swelling behavior and three-dimensional structure [56-58]. Hydrogels have been a topic of extensive research in the past decades and their properties as for example their high water content and the possible control over the swelling kinetics make them very attractive for biomedical applications. More specifically, *in situ* forming hydrogels can provide a means for simple, "custom-made" therapeutics and diagnostics. A polymer solution can be prepared and allowed to gel *in situ*, after photopolymerization [59, 60], chemical crosslinking [61, 62], ionic crosslinking [63] or in response to an environmental stimulus such as temperature, pH or ionic strength of the surrounding medium [64, 65]. Hydrogels that respond to temperature change are the subject of this review. Their sensitivity to the thermal environment is useful as temperature is the sole stimulus for their gelation with no other requirement for chemical or environmental treatment, and can be thus produced e.g. upon injection to the body, when temperature is increased from ambient to physiological.

[§] The following section was included in: L. Klouda and A.G. Mikos, Thermoresponsive hydrogels in biomedical applications, European Journal of Pharmaceutics and Biopharmaceutics, 68 (2008), 34-45

The phenomenon of transition from a solution to a gel is commonly referred to as sol-gel transition. Some hydrogels exhibit a separation from solution and solidification above a certain temperature. This threshold is defined as the lower critical solution temperature (LCST). Below the LCST, the polymers are soluble. Above the LCST, they become increasingly hydrophobic and insoluble, leading to gel formation. In contrast, hydrogels that are formed upon cooling of a polymer solution have an upper critical solution temperature (UCST) [65]. The sol-gel transition of thermosensitive hydrogels can be experimentally verified by a number of techniques such as spectroscopy [66-68], differential scanning calorimetry (DSC) [66, 67] and rheology [66].

There are various mechanisms behind thermogelation in aqueous solutions, and for some polymers they are still a topic of debate. Many polymers show a decrease in solubility that is attributed by changes in the overall hydrophilicity of the polymer chains upon temperature change. When a polymer is dissolved in water, there are three types of interactions that take place: between polymer molecules, polymer and water and between water molecules. For polymers exhibiting an LCST, temperature increase results in a negative free energy of the system which makes water-polymer association unfavorable, facilitating the other two types of interactions. This negative free energy (ΔG) is attributed to the higher entropy term (ΔS) with respect to the increase in the enthalpy term (ΔH) in the thermodynamic relation $\Delta G = \Delta H - T\Delta S$. The entropy increases due to water-water associations which are the governing interactions in the system. This phenomenon is the so-called hydrophobic effect [66, 69, 70]. Polymer micelle packing [71] and coil to helix transition causing network formation [72] are examples of the conformational changes that take place at the critical solution temperature. All of these result in a

reversible physical linking of the polymer chains, and gels can therefore return to solution after the thermal stimulus that caused their gelation is removed.

This chapter reviews the applications of thermosensitive hydrogels in fields of interest for pharmaceutical and biomedical scientists and engineers. It emphasizes mainly the use of hydrogels based on natural polymers, *N*-isopropylacrylamide (NiPAAM) polymers, poly(ethylene oxide)-*b*-poly(propylene oxide)-*b*-poly(ethylene oxide) (PEO-PPO-PEO) as well as poly(ethylene glycol) (PEG)-biodegradable polyester copolymers. The structure of some thermoresponsive hydrogel-forming polymers is illustrated in Figure II-1. As there are some excellent reviews [73, 74] summarizing the literature on thermosensitive hydrogels published in the past years, the scope of this work is to cover the advances in the field from 2004 until 2006.

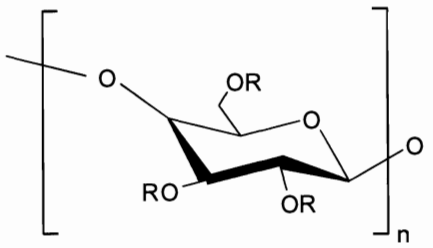

R=CH_3 or H

a) methylcellulose

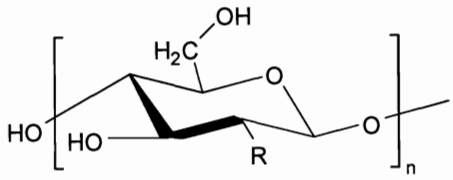

R=NH_2 or CH_2—C(=O)—NH_2

b) chitosan

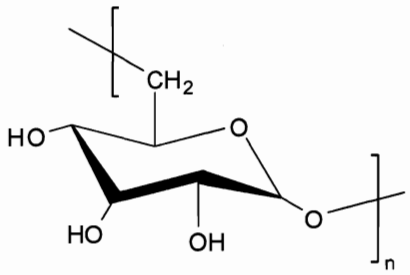

c) dextran

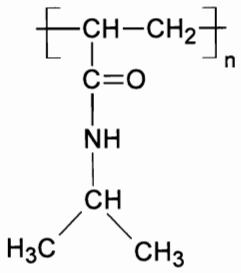

d) pNiPAAm

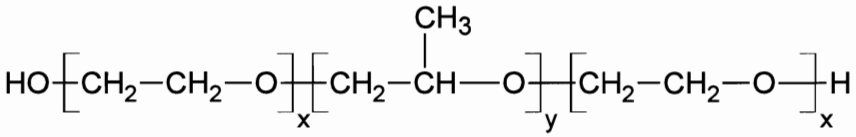

e) PEO-PPO-PEO (Pluronics®)

Figure II-1: Chemical formulas of polymers that form or are part of thermoresponsive hydrogels.

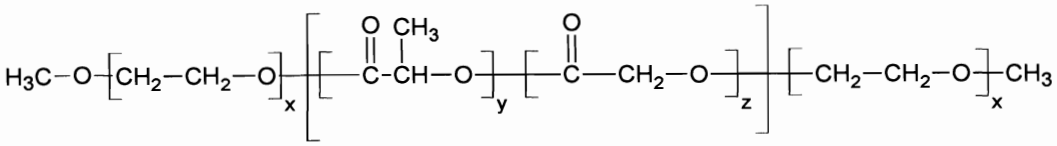

f) PEG-PLGA-PEG

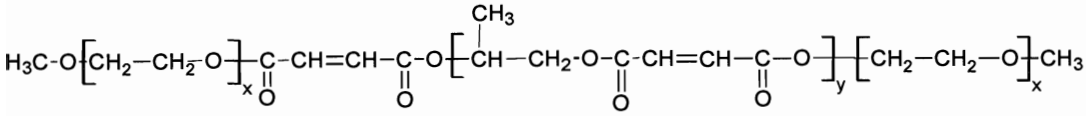

g) PEG-PPF-PEG

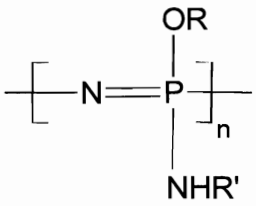

R and R' can vary

h) general structure of poly(organophosphazenes)

Figure II-1 (continued): Chemical formulas of polymers that form or are part of thermoresponsive hydrogels.

Natural polymers and derivatives

Many natural polymers have been shown to exhibit gelation upon temperature change. Researchers have used them alone or in combination with synthetic polymers to fabricate thermally responsive hydrogels with desired properties.

1. Polysaccharides

1.1 Cellulose derivatives

Cellulose is a natural polysaccharide which is insoluble in water. Substitution of the hydroxyl groups on cellulose with more hydrophobic units as methyl or hydroxypropyl groups renders the originally insoluble cellulose water soluble [66]. Methylcellulose (MC) is a cellulose derivative that has been extensively investigated for biomedical applications. It has thermoreversible gelation properties in aqueous solutions, gelling at temperatures in the range of 60-80°C and turning into a solution upon cooling [66, 75]. Liu et al. [76] have grafted methylcellulose with the synthetic *N*-isopropylacrylamide (NiPAAm), combining the thermogelling properties of both materials. It was possible to prepare fast reversibly thermogelling hydrogels by adjusting the ratios of the two components. They reported that a low percentage of methylcellulose decreases the LCST as compared to pNiPAAm, but with a high MC ratio the LCST increases. They also found that addition of MC to NiPAAM polymers enhances the mechanical strength of the hydrogel with no syneresis. The phenomenon of syneresis occurs when a hydrogel shrinks and expels previously imbibed water.

Another interesting approach towards a thermosensitive hydrogel system based on methylcellulose was recently reported by Stabenfeldt et al. [77]. As it had been shown before [78] that methylcellulose showed low protein adsorption and cell adhesion, Stabenfeldt et al. functionalized methylcellulose with the protein laminin, aiming towards the creation of a bioactive scaffold for neural tissue engineering. In order to facilitate laminin tethering, methylcellulose was oxidized prior to functionalization. They reported that the laminin-functionalized oxidized methylcellulose hydrogel promoted neuronal cell adhesion and showed higher cell viability rates than methylcellulose, oxidized methycellulose or laminin-functionalized methylcellulose. Moreover, the concentration could be adjusted so that the hydrogel exhibits a lower critical solution temperature slightly below physiological temperature.

1.2 Chitosan

Chitosan is produced with the deacetylation of chitin, which can be found in the outer skeleton of shrimp and insects, among others. We would like to refer the reader to the excellent review by Gariépy and Leroux [74] which covers the developments of thermosensitive chitosan-polyol salt hydrogels until 2004. More recently, Bhattarai et al. [79] incorporated poly(ethylene glycol) (PEG) into chitosan and were able to form a thermoreversible hydrogel with no additional crosslinking agents. Moreover, PEG grafting improved the solubility of chitosan in water, and the gelation was found to be possible in physiological pH values. The same group [80] evaluated the PEG-grafted chitosan for controlled drug release *in vitro*. Using albumin as a model protein, an initial

burst release was observed, which was followed by a steady release from the hydrogel for about three days. After this time, the remaining albumin could not be released from the hydrogel until the gel matrix was dissolved in the media. When the PEG-grafted chitosan was crosslinked *in situ* with genipin, a crosslinking agent with low cytotoxicity, quasi-linear drug release was possible for up to 40 days; however the hydrogel lost its thermoreversibility at 37°C.

Chitosan-based hydrogels have been also investigated as potential cell carriers for tissue engineering applications. A copolymer of NiPAAm and water-soluble chitosan was tested for chondrogenic differentiation of human mesenchymal stem cells (hMSC). The hydrogel showed a stable gelation at 37°C and differentiation of hMSC into chondrocytes was observed, both *in vitro* and *in vivo*. This hydrogel could be used for a minimally invasive treatment of vesicouretral reflux with an endoscopic procedure through a single injection [81]. Dang et al. [82] modified chitosan by adding hydroxybutyl groups to its hydroxyl and amino reactive sites, rendering it water soluble and thermally responsive. The resulting hydrogel could gel within seconds after exposure to physiological temperature and was sufficiently strong to be handled with, as for example to measure mechanical properties. Upon cooling, the gel returned to liquid state. Having as an ultimate goal the treatment of degenerative disc disease, the hydrogel's interaction with hMSC and cells derived from the intervertebral disc was tested. The cells were able to proliferate and produce extracellular matrix when encapsulated in the hydrogels for a period up to two weeks.

A chitosan-glycerophosphate salt (GP) hydrogel was recently tested for its potential in neural tissue engineering. This thermally responsive hydrogel, as developed

initially by Chenite et al. [83], has been shown to have good biocompatibility *in vitro*, but it hadn't been yet tested with nerve cells. Crompton et al. [84] compared the hydrogel to polylysine-functionalized chitosan-GP, with the hypothesis that the peptide polylysine might improve neuronal adhesion and neurite outgrowth. When neurons were grown in a two-dimensional culture, the functionalized hydrogel did not seem to significantly affect cell survival as compared to chitosan-GP, but it was observed that increasing concentrations of polylysine inhibited neurite outgrowth. However, when the cells were cultured in a three-dimensional functionalized gel, a geometry that is more representative of the extracellular matrix environment, in certain polylysine concentrations more cells were viable than on non-modified chitosan-GP. The authors concluded that polylysine-chitosan-GP may be a good candidate for neural tissue engineering.

1.3 Dextran

A modified precursor of the enzymatically biodegradable dextran (Dex) was formed by reaction with maleic anhydride (MA) and the Dex-MA polysaccharide was given thermoresponsive properties by photocrosslinking it with NiPAAm. The resulting hydrogel was partially biodegradable and exhibited a higher LCST than pNiPAAm due to the hydrophilic and biodegradable nature of Dex-MA. Additionally, the carboxylic end groups of Dex-MA render the hydrogel pH sensitive [85]. Another approach based on a dextran polysaccharide was reported by Huang et al [86]. A dextran macromer containing oligolactate and 2-hydroxyethyl methacrylate units (Dex-lactate-HEMA), which has hydrolytically degradable blocks, was copolymerized with NiPAAm. This hydrogel

showed an LCST close to that of pNiPAAm (approximately 32°C). Its swelling and degradation in phosphate buffered saline (PBS) were studied at 25 and 37°C. At 25°C, which is below the LCST, the hydrogels had disintegrated within two weeks, with the rate of dissolution depending on their composition. At 37°C however, the degradation was much slower due to increased hydrophobic effects. Interestingly, when the hydrogel was tested for drug delivery, it was shown that a low molecular weight drug (methylene blue) was released slower at 25°C than at 37°C, whereas the opposite was observed for a high molecular weight substance (bovine serum albumin). The authors concluded that the drug release profile depends on a number of factors, such as the temperature, the swelling and degradation characteristics of the hydrogel, as well as the interactions of the drug and the hydrogel macromolecules.

1.4 Xyloglucan

Xyloglucan is a cytocompatible polysaccharide and has exhibited thermally responsive behavior when more than 35% of its galactose residues are removed [87]. Xyloglucan gels have been used as a drug delivery vehicle for various applications [74], however there are not many data on the rheological and morphological characteristics of these hydrogels. Nisbet et al. [88] have examined the gelation properties of xyloglucan hydrogels as well as their morphology under physiological conditions. The gelation process seemed to be influenced by the presence of ions in PBS as compared to deionized water. As to the optimum concentration, it was found that 3% (wt.) xyloglucan in aqueous media possess an elastic modulus that is significantly higher than other natural

or synthetic hydrogels. Moreover, this concentration yielded a gel that could be freeze-dried and examined with scanning electron microscopy. The images showed a macroporous, interconnected, three-dimensional network.

2. Proteins

2.1 Gelatin

Gelatin is another biopolymer with thermoreversible properties. At temperatures below 25°C, an aqueous gelatin solution solidifies due to the formation of triple helices and a rigid three-dimensional network. When the temperature is raised above approximately 30°C, the conformation changes from a helix to the more flexible coil, rendering the gel liquid again [72]. As the opposite thermal behavior is desired for biomedical applications, researchers have combined gelatin with other polymers, which show thermal gelation close to body temperature. Gelatin has the advantage of allowing for easy modification on the amino acid level; moreover, it is biodegradable and biocompatible [89]. A binary-component hydrogel composed of gelatin and monomethoxy poly(ethylene glycol)-poly(D,L-lactide) (mPEG-DLLA) block copolymers was synthesized by Yang and Kao [89]. For most compositions of gelatin and mPEG-DLLA, the hydrogel was shown to flow at 37°C and gel at room temperature, however a 100 mg/mL gelatin solution underwent fast gelation at 37°C when mixed with 30% wt. mPEG-DLLA. Different hydrogel compositions were also examined for drug release kinetics with gentamycin sulfate as the model drug. At room temperature, five days or longer was necessary for 50% drug release, and the release lasted up to 40 days. At 37°C, gelatin-

mPEG-DLLA showed an even slower release profile, however after one week the release was no longer detectable due to degradation of the hydrogel matrices.

Ohya and Matsuda [90] have grafted gelatin with NiPAAm in an effort to produce a thermoresponsive extracellular matrix analogue. Aqueous solutions showed a sol-gel transition at physiological temperature when the weight ratio of pNiPAAm to gelatin chains was higher than 5.8. Smooth muscle cells were suspended in medium solutions of pNiPAAm/gelatin and subsequently incubated at 37ºC. It was shown that a low hydrogel concentration (5% w/v) and a high pNiPAAm to gelatin ratio (P/G) supported the highest cell proliferation and extracellular matrix production. The authors suggested that this was due to increased hydrophobicity caused by higher pNiPAAm ratios, which would lead to the formation of large aggregates. As a result, a higher porosity with larger pore size occurs, which comprises a favorable cell environment.

Another protein-based hydrogel was proposed by Gil et al. [91]. Gelatin was blended with silk fibroin to yield a thermoresponsive gel, which was stabilized at 37ºC by the presence of β crystals of silk fibroin. The swelling profile at temperatures below and above the helix-to-coil transformation of gelatin was evaluated, as well as the protein release from the matrices. The gel showed a higher swelling at physiological temperatures as compared to 20ºC, but also higher mass loss due to dissolution and release of gelatin.

N-Isopropylacrylamide-based systems

Hydrogels based on poly(*N*-isopropylacrylamide) (pNiPAAm) and its copolymers belong to the most intensively investigated thermoreversible systems. Recent developments on pNiPAAm-based hydrogels include their use for drug delivery [67, 68, 92, 93], cell encapsulation and delivery [94, 95] and cell culture surfaces [96]. Poly(*N*-isopropylacrylamide) is non-biodegradable and exhibits a sharp phase transition, with an LCST at about 32°C in pure water [93, 97]. Below the LCST, pNiPAAm assumes a flexible, extended coil conformation in aqueous solutions. At the LCST, it becomes hydrophobic and the polymer chains seem to collapse prior to aggregation in globular structures [69, 98]. Copolymerization of NiPAAm with a more hydrophilic monomer increases the overall hydrophilicity of the polymer, and the stronger polymer-water interactions lead to an increase in the LCST. Likewise, copolymerization with a more hydrophobic monomer results in a lower LCST than pNiPAAm [99]. Moreover, the phase transition temperature is influenced by the presence of salts [100] and pH to a certain extent [97, 100].

Coughlan and colleagues [92] evaluated the swelling and release profile of crosslinked pNiPAAm hydrogels as a function of the physicochemical properties of the loaded drugs. Dried hydrogel discs were loaded by sorption of a drug solution, the solvent was removed and the hydrogels were allowed to swell in a buffer solution. Hydrogel swelling was decreased in the presence of hydrophobic drugs and the opposite effect was observed for hydrophilic drugs. At temperatures above the LCST, the system showed contraction and deswelling, and a solubility-dependent drug pulse release was shown for hydrophobic drugs, whereas hydrophilic drugs showed a molecular weight-dependent drug pulse. The authors suggested that drug properties such as solubility, size

and chemical nature should be considered when a thermosensitive hydrogel such as pNiPAAm is chosen as a delivery vehicle.

Copolymers of NiPAAM have also been popular in attempts to yield hydrogels with thermal responsiveness and improved properties. The hydrogel potential of NiPAAM copolymers with acrylic (AA) [67, 95] and propylacrylic acid (PAA) [68] was examined. The thermoreversible p(NiPAAm-*co*-AA) hydrogel was tested as a cell and drug delivery vehicle. Chondrocytes, dexamethasone and ascorbate as differentiation factors as well as transforming growth factor β3 (TGF-β3) were encapsulated in the hydrogel and were implanted subcutaneously in mice. The chondrogenic factors were provided in order to hinder chondrocyte de-differentiation *in vivo.* After 8 weeks, significant collagen II expression as well as proteoglycan and polysaccharide production was evident, indicating that the cells had preserved their phenotype. This hydrogel in combination with the differentiation and growth factors holds promise for cartilage tissue engineering [95]. Liu [67] et al have synthesized p(NiPAAm-*co*-AA) and polymerized it with ethyl acrylate (EA) using the interpenetrating polymer network (IPN) technology. An interpenetrating polymer network is formed by hydrophilic and hydrophobic networks that are only physically interconnected, without any chemical bonding, so that individual components retain their original properties. The same group [101] had found that IPN structures are effective amphiphilic drug carriers. A pH dependence on the swelling ratio of p(NiPAAm-*co*-AA) as well as of interpenetrating polymer network with ethyl acrylate (p(NiPAAm-*co*-AA)/pEA IPN) was observed at 37ºC. This was attributed to the presence of the carboxyl group on the acrylic acid. Swelling was lower on the IPNs due to the hydrophobic pEA. The drug release kinetics of both hydrogels were evaluated using

daidzein as a model drug. P(NiPAAm-*co*-AA) showed an initial burst release, which was not observed on p(pNiPAAm-*co*-AA)/pEA IPN. It was concluded that the pEA chains in the IPN structure had a favorable effect in maintaining a slower and more stable release profile [67]. Also, copolymers of NiPAAm with propylacrylic acid (PAA) show a temperature and pH-sensitive behavior. Yin et al [68] synthesized copolymers by a reversible addition fragmentation transfer (RAFT) method, using different NiPAAm and PAA ratios. They showed that even small changes in pH can have a big effect on the LCST of the hydrogel. This feature can be useful for applications such as drug delivery, where physiological temperature and local pH differences can both act as stimuli, and for molecular switching over a desired pH range.

An interesting approach to a combination of stimuli-responsive attributes was recently proposed by Xu et al. [102] in the form of a triblock copolymer hydrogel. A poly((2-dimethyl amino)ethyl methacrylate-*co*-2-hydroxyethyl methacrylate)-*b*-poly(*N*-isopropylacrylamide)-*b*-poly((2-dimethyl amino)ethyl methacrylate-*co*-2-hydroxyethyl methacrylate) or p(DMAEMA-*co*-HEMA)-*b*-p(NiPAAm)-*b*-p(DMAEMA-*co*-HEMA) copolymer was synthesized by atom transfer radical polymerizations (ATPR). The hydroxyl groups on HEMA allowed for chemical crosslinking with glutaraldehyde through acetal formation. The hydrogel showed combined characteristics of its building blocks: Its temperature-responsive behavior was attributed to pNiPAAm and the pH-sensitivity to pDMAEMA.

The Mikos group [94] has synthesized thermogelling macromers for fabrication of a hydrogel for orthopedic tissue engineering applications. The aim was to yield a gel with better mechanical properties than most hydrophilic injectable hydrogels. This was

accomplished by incorporating a hydrophobic domain that provides cohesive interactions as well as functional groups for chemical crosslinking. A copolymer of pentaerythritol monostearate diacrylate (PEDAS), *N*-isopropylacrylamide (NiPAAm), acrylamide (AAm) and 2-hydroxyethyl acrylate (HEA) was synthesized. PEDAS contains a lipophilic side chain, and AAm and HEA can modulate hydrophilicity and add groups for subsequent acrylation and crosslinking. The thermal gelation is attributed to the NiPAAm block. Studies so far have shown that the macromers possess a thermoreversible behavior. Future work is directed into further development and characterization of the hydrogel and examination of its potential in bone regeneration.

Another issue that has to be addressed is biodegradability. Many homo-and copolymers of NiPAAm are not biodegradable [103], a fact that may prove problematic for some biomedical engineering applications. Nakayama and colleagues [93] have prepared thermally responsive, biodegradable polymeric micelles for controlled drug release. A hydrophobic block in the micelles was used to incorporate water-insoluble drugs. By combining a poly(*N*-isopropylacrylamide-*co*-*N,N*-dimethylacrylamide) (p(NiPAAm-*co*-DMAAm)) block, which has an LCST around 40°C, with poly(D,L-lactide), poly(ε-caprolactone) or poly(D,L-lactide-*co*-ε-caprolactone), which are all biodegradable and hydrophobic, the group was able to fabricate polymeric micelles with controlled dimensions and phase transition temperatures. Below the LCST, the thermoresponsive block forms the outer shell of the micelle, but upon temperature increase above the LCST, the block becomes increasingly hydrophobic and shrinks. In the case of p(NiPAAm-*co*-DMAAm)-*b*-p(D,L-lactide-*co*-ε-caprolactone) diblock copolymer, temperature increase above the LCST proved to facilitate drug release.

Polymers based on pNiPAAm have found applications in another field crucial to biomedical scientists: Their thermoresponsive behavior has been proven useful in cell culture substrates. By introducing a pNiPAAm layer on tissue culture plates, the hydrophilicity of the substrate can be modulated with a temperature switch. It is well known that most cells preferentially adhere to hydrophobic surfaces. Above its LCST (32ºC), pNiPAAm shows a hydrophobic behavior. It represents therefore a suitable surface for cell attachment and proliferation at physiological temperature. By lowering the temperature below the LCST, the culture surface becomes hydrophilic and the cells automatically detach [104]. This cell recovery technique is a good alternative to the conventional, but often damaging, enzymatic or mechanical detachment methods. Recently, Hatakeyama et al. [96] have been producing bioactive, thermoresponsive cell culture surfaces by immobilizing the cell adhesive peptide RGDS and the growth factor insulin on a NiPAAm-copolymer. *N*-Isopropylacrylamide was copolymerized with its analogue 2-carboxyisopropylacrylamide and the polymer was grafted onto polystyrene tissue culture dishes, followed by RGDS and insulin immobilization. They found that these factors increase cell adhesion and proliferation, reducing therefore culture time. When the temperature was brought to 20ºC, the cells could be easily recovered as contiguous tissue monolayers.

PEO/PPO-based systems

Triblock copolymers poly(ethylene oxide)-*b*-poly(propylene oxide)-*b*-poly(ethylene oxide) (PEO-PPO-PEO), known also as Pluronics® or Poloxamers, are another important group of synthetic polymers with a thermoreversible behavior in

aqueous solutions. By adjusting the composition, the molecular weight and the concentration, this reversible gelation can occur at physiological temperature and pH [105]. The polymers owe their amphiphilic structure to the hydrophilic ethylene oxide and the hydrophobic propylene oxide. The gelation mechanism of PEO/PPO block copolymers in aqueous solutions has been a topic of extensive investigation, and a possible explanation for this phenomenon could be given by the changes in micellar properties as a function of both concentration and temperature. Amphiphilic block copolymer molecules can self assemble into micelles in aqueous solutions. Above a certain concentration, termed as the critical micelle concentration (CMC), the polymer molecules, which were previously in solution, aggregate and form micelles. Members of the Pluronics® family which are used for drug delivery exhibit a CMC of 1 μM to 1 mM at 37°C. Moreover, the micelle formation has strong temperature dependence. Below a certain temperature, termed the critical micelle temperature (CMT), both ethylene and propylene oxide blocks are hydrated and poly(propylene oxide) is relatively soluble in water. With temperature increase, poly(propylene oxide) chains become less soluble, resulting in micelle formation [71].

As Pluronics® are commercially available in a range of molecular weights, composition ratios and forms, it would be useful to mention the nomenclature rules for these copolymers. The letter in the notation stands for liquid (L), paste (P) or flakes (F), whereas the first two numbers are an indication for the molecular weight of the PPO block and the last number is the weight fraction of the PEO block. For example, the commonly used in biomedical applications F127 has a weight percentage of 70% PEO and a molecular weight of PPO around 4000 [105].

Over the past years, these copolymers have been extensively used in applications such as drug and gene delivery [71], inhibition of tissue adhesion [106, 107] and burn wound covering [108, 109]. Newer advances in gene delivery are summarized elsewhere [110]. Pluronics® represent a bio-inert environment, imparted by the hydrophilicity and flexibility of PEO chains [111]. Therefore, most cells do not grow on these polymers, which have been used as tissue adhesion barriers. However, it was shown that Pluronics® can be a good substrate for hematopoietic stem cells, supporting their culture and preservation more than conventional tissue culture dishes [112, 113]. Recently, the use of Pluronic® F127 (synonymous to poloxamer 407) was reported for tissue engineering applications. This polymer has been found to have a rapid gelation at 37°C (after one-minute incubation, 30% solution in cell culture medium) [114]. F127 was evaluated as a scaffold for lung tissue engineering, showing promising results on tissue growth with low inflammatory response [115]. Weinand and colleagues [114] tested a β-tricalcium phosphate (β-TCP) scaffold, using a F127 hydrogel to facilitate cell delivery and distribution for an *in vitro* study aiming at bone regeneration. They reported that F127 was no longer present in the channels of the β-TCP scaffold after one week in culture and seemed to have degraded. Bone tissue growth was only weakly induced, and the constructs showed lower stiffness than other hydrogel (fibrin, collagen I) composites evaluated.

In general, Pluronic® F127 has been found to have inadequate mechanical integrity which makes it inappropriate for certain biomedical applications. The hydrogels show a low viscosity, which has as consequences poor mechanical strength, high permeability and limited stability with quick dissolution [116, 117]. Cohn and colleagues proposed two new mechanisms to create copolymers based on Pluronic® F127 with

improved mechanical properties. In both cases they relied on the principle of a multiblock backbone with the addition of covalently bound repeating units. This way, the macromolecular structure and orientation could be controlled. The first involved the polymerization of F127, with hexamethylene diisocyanate as a chain extender, forming poly(ether-urethanes). The second relied on the covalent binding of poly(ethylene glycol) and poly(propylene glycol), which as such do not possess thermogelling properties at physiological temperatures, using phosgene as a coupler and forming poly(ether-carbonates). Both newly synthesized polymers exhibited significantly higher viscosities than F127 at 37°C, and the poly(ether-urethanes) displayed much slower drug release kinetics than the original polymer [116]. The group developed the idea of thermoresponsive PEO/PPO polymers with improved mechanical behavior further in the next years. Their strategies included i) introduction of end groups that would allow for *in situ* chemical crosslinking after thermal gelation, such as carbon-carbon double bonds [118], ethoxysilane groups [117, 119] and methacrylate groups [119] ii) synthesis of poly(ethylene oxide) and poly(propylene oxide) block copolymers using diacyl chloride as a coupling agent [120] iii) synthesis of PEO/PPO copolymers with incorporation of ε-caprolactone [120, 121] or lactide [121] oligoester segments prior to chain extension. The latter approach yielded biodegradable hydrogels due to hydrolytic cleavage of the ester bonds.

The need for more stable hydrogels was identified also by Cellesi et al. [122-124]. Their approach mimicked the natural thermal gelation of alginate by relying on the occurrence of a physical mechanism, imparted by the thermosensitive nature of Pluronics®, followed by an irreversible chemical mechanism, due to covalent

crosslinking by the reaction of groups at the termini of the copolymer. They named their gelation approach "tandem process" due to the cooperative action of both mechanisms.

Pluronic® polymers were functionalized with acrylic moieties and thiols at their end groups and were subsequently gelled at 37°C, where a Michael-type addition took place and allowed for a slower chemical curing. It was found that these polymers were biocompatible, and so was their gelation process, which can be performed at physiological temperature and pH, allowing for encapsulation of sensitive drugs and cells [123]. In order to limit steric hindrance phenomena, a similar method was followed with Tetronic® polymers, which are thermosensitive tetra-armed Pluronic® analogues [124]. By adjusting the molecular weight of the precursors and the functionalization (therefore also the crosslinking density), the final mechanical and transport properties of the "tandem" polymers can be controlled [122, 124]. Moreover, the "tandem" method allows for easy processing of the polymers, for example into spherical beads and hollow capsules [122].

Other synthetic polymers

1. PEG/Biodegradable polyester copolymers

The copolymerization of hydrophilic, biocompatible poly(ethylene glycol) (PEG) with biodegradable and biocompatible polyesters has yielded some interesting hydrogel systems. Thermoresponsive properties were given by the appropriate adjustment of the hydrophobic polyester block and the PEG block length.

In 1997, Jeong [125] and colleagues reported the synthesis of injectable poly(ethylene glycol)-*b*-poly(D,L-lactic acid-*co*-glycolic acid)-*b*-poly(ethylene glycol) (PEG-PLGA-PEG) triblock copolymers. These polymers were biocompatible, biodegradable and exhibited a sol-gel transition. The use of high molecular weight-PLGA combined with low molecular weight-PEG resulted in a hydrogel with quick gelation at physiological temperature. The combination of hydrophobic/hydrophilic units created a surfactant behavior of the polymers in water, facilitating thus also the solubilization of hydrophobic drugs. *In vivo* studies showed sufficient mechanical properties and integrity for longer than a month [126]. More recently, Chen et al. [127] developed a triblock PLGA-PEG-PLGA-based system for the controlled release of testosterone. Testosterone is water-insoluble and so far, its delivery systems included patches, creams, gels, injectables and implants [128]. A slower *in vitro* release of testosterone was observed for copolymers with longer PLGA blocks, possibly due to the slower degradation of these hydrophobic units. The thermosensitive polymers showed a controlled, linear release for a period of three months.

Another recent approach towards a thermoresponsive system involved the synthesis of a multiblock copolymer with a biodegradable polyester. Alternating multiblock poly(ethylene glycol)/poly(L-lactic acid) (PEG/PLLA) copolymers were produced. It was shown that sol-to-gel transition was depending on both the total molecular weight (MW) and the MW of each building block. *In vitro* and *in vivo* gelation studies determined that a copolymer with a total MW of 6700 daltons and 600/1300 (MW of PEG/PLLA blocks respectively) holds potential as an injectable carrier for biomedical applications in terms of transition temperature and modulus at 37°C [129].

The Mikos group has proposed the combination of methoxy poly(ethylene glycol) (mPEG) with poly(propylene fumarate) (PPF) and the synthesis of a mPEG-PPF-mPEG triblock copolymer [130]. Copolymers exhibited an LCST depending on the molecular weight of mPEG, and it was shown that their LCST was strongly influenced by the presence of salts. Moreover, the presence of the fumarate double bonds on PPF can allow for chemical crosslinking, thus enhancing the stability of the hydrogels. Recently, this hydrogel was evaluated for articular cartilage tissue engineering [131]. Chondrocytes were encapsulated in the hydrogel at 37°C and subsequently tested for their phenotypic characteristics. It was found that chondrocytes cultured in PEG/PPF hydrogels proliferated and produced significant levels of proteoglycans and collagen type II, which are both markers of the chondrocytic phenotype. When compared to cells cultured in agarose and alginate hydrogels, two materials widely studied for chondrocyte delivery, proliferation levels in PEG/PPF were similar, however proteoglycan and collagen production was lower. Supplement of the bone morphogenic protein 7 in PEG/PPF hydrogels was also shown to increase chondrocyte proliferation, but not proteoglycan synthesis.

2. Poly(organophosphazenes)

Current advances on poly(organophosphazenes) include their use as drug [132, 133] and cell [134] delivery systems. Poly(organophosphazenes) grafted with mPEG and amino acid esters were reported as a new class of biodegradable and thermosensitive polymers in 1999 [103]. Sohn and colleagues [135] developed a correlation for the LCST of these

polymers as a function of their molecular structure, which comprises hydrophilic (PEG) and hydrophobic (amino acid esters) side groups. The polymers showed a sustained release profile for both hydrophobic [133] as well as hydrophilic [132] drugs for over three and two weeks respectively. Also their use as cell carriers holds promise, as shown recently. Hepatocytes cultured in poly(organophosphazene) hydrogels were able to maintain good viability and liver-specific activity for a period of four weeks [134].

Conclusions

Extensive research over the past years in biomaterials and tissue engineering has yielded promising results towards the regeneration of damaged or lost tissues. One commonly encountered problem that might benefit from this emerging strategy is craniofacial bone defects, for which no ideal solution exists yet. Combined progress in cell biology and biomaterials science has identified suitable cell sources as well as materials and the parameters that need to be tailored for each application. Injectable hydrogel systems have been used as space filling agents and for cell and bioactive molecule delivery. Considering the potentially sensitive nature of the cells and drugs to be delivered, thermoresponsive hydrogels may provide the additional advantage of a mild and quick gelation method in response to temperature change from ambient to physiological, without the use of external solidification factors.

CHAPTER III

SYNTHESIS AND CHARACTERIZATION OF THERMORESPONSIVE AND CHEMICALLY CROSSLINKABLE, AMPHIPHILIC POLY(*N*-ISOPROPYLACRYLAMIDE)-BASED MACROMERS ‡

Abstract

In this study, we synthesized and characterized a series of macromers based on poly(*N*-isopropylacrylamide) that undergo thermally induced physical gelation and, following chemical modification, can be chemically crosslinked. Macromers with number average molecular weights typically ranging from 2000 – 3500 Da were synthesized via free radical polymerization from, in addition to poly(*N*-isopropylacrylamide), pentaerythritol diacrylate monostearate, a bifunctional monomer containing a long hydrophobic chain, acrylamide, a hydrophilic monomer, and hydroxyethyl acrylate, a hydrophilic monomer used to provide hydroxyl groups for further chemical modification. Results indicated that the hydrophobic-hydrophilic balance achieved by varying the relative concentrations of comonomers used during

---

‡ This chapter has been published as follows: M.C. Hacker, L. Klouda, B.B. Ma, J.D. Kretlow and Antonios G. Mikos, Synthesis and Characterization of Injectable, Thermally and Chemically Gelable, Amphiphilic Poly(*N*-isopropylacrylamide)-Based Macromers, Biomacromolecules 9, (2008), 1558-70

synthesis was an important parameter in controlling the transition temperature of the macromers in solution and stability of the resultant gels. Storage moduli of the macromers increased over four orders of magnitude once gelation occurred above the transition temperature. Furthermore, chemical crosslinking of these macromers resulted in gels with increased stability compared to uncrosslinked controls. These results demonstrate the feasibility of synthesizing poly(*N*-isopropylacrylamide)-based macromers that undergo tandem gelation and establish key criteria relating to the transition temperature and stability of these materials. The data suggest that these materials may be attractive substrates for tissue engineering and cellular delivery applications as the combination of mechanistically independent gelation techniques used in tandem may offer superior materials with regard to gelation kinetics and stability.

Introduction

One of the primary problems facing researchers and clinicians in the broad field of tissue engineering and regenerative medicine is the fabrication of biomaterial substrates that provide appropriate three-dimensional architecture, mechanical support, and the ability to deliver both cells and growth factors tailored to a specific tissue of interest. *In situ* gel formation is a concept of great interest for tissue engineers as it enables the delivery of a hydrogel matrix encapsulating cells and growth factors to defects of any shape using minimally invasive surgical techniques [136, 137].

So far, no ideal technique toward achieving *in situ* gel formation exists. Various natural and synthetic polymers have been chemically modified with moieties for

chemical crosslinking, including acrylic esters, methacrylic esters, cinnamoyl esters [138], fumaric esters [137], and vinylsulfone [139], to yield injectable biodegradable matrices [140]. *In situ* gel formation by radical polymerization of electron-poor olefins can be induced photochemically or thermally without harming encapsulated cells [141, 142]. However, only low concentrations of radical initiators and crosslinking agents are tolerated by encapsulated cells [142, 143], and thus certain important parameters such as gelation kinetics, crosslinking densities and resulting mechanical properties of the hydrogels can only be varied to a limited extent without compromising the cytocompatibility of the process.

Polymeric materials that respond to a variety of environmental stimuli such as changes in temperature, pH, osmotic pressure, ionic strength, pressure, and electric or magnetic field [136, 144, 145] have become attractive materials in biotechnology and medicine [144] and represent a viable approach to developing *in situ* gelling biomaterials. Temperature-sensitive hydrogel-forming polymers are among the most common of such materials and have been extensively studied as temperature-regulated drug delivery systems [74, 146-149] and injectable matrices for tissue engineering [56, 136, 150]. While soluble below a characteristic temperature, solutions of these polymers undergo thermally induced, entropically driven phase separation above their lower critical solution temperature (LCST).

Cytocompatible chemical gelation protocols typically yield firm hydrogels after several minutes, while thermally induced gelation of thermosensitive polymer solutions occurs almost instantaneously once the LCST is reached. For cell encapsulation applications, thermosensitive polymers must possess an LCST below 37°C and the thermally aggregated polymer chains have to retain a significant amount of water.

Polymer classes from which certain representatives have been shown to meet these characteristics include copolyethers of poly(ethylene glycol) (PEG) and poly(propylene glycol) [151], copolyesters of PEG and poly(lactic acid) [152] or poly(propylene fumarate) [131], homo- and copolymers of poly(organophosphazenes) [153], and copolymers of poly(*N*-isopropylacrylamide) (pNiPAAm) [154, 155]. PNiPAAm undergoes a sharp and reversible phase transition at an LCST of 32°C, but when used at the physiological temperature of 37°C, linear pNiPAAm collapses substantially and precipitates as a separate phase. pNiPAAm copolymers containing small amounts of hydrophilic molecules, such as acrylic acid, PEG or hyaluronic acid, however, demonstrated reversible gelation around body temperature without significant syneresis [156-158]. Another method to stabilize pNiPAAm copolymers above the LCST is to copolymerize the monomers in the presence of a crosslinker to yield polymer networks [150], which in part limits the injectability of the materials [149]. Despite this limitation, combining functional groups within a macromolecule such that in solution there is physical gelation in response to physiological temperature upon injection and radical crosslinking at a slower kinetic rate *in situ* is a concept that can yield superior materials with regard to gelation kinetics and ultimate mechanical properties. In addition, control over hydrogel properties might be improved through the combination of two mechanistically and kinetically independent gelation techniques. The few studies that have explored such tandem gelation concepts for biomedical applications have used modified pNiPAAm-based and polyether-type thermogelling materials that were chemically cured after physical *in situ* gelation by Michael-type addition reactions between thiols and acrylates [123, 159, 160].

This study describes the synthesis of novel injectable pNiPAAm-based thermogelling macromers that are modified with olefinic moieties available for chemical crosslinking *in vivo* and that contain biocompatible hydrophobic domains. This design is expected to yield novel water-soluble environmentally responsive amphiphiles that not only combine two independent gelation mechanisms but also incorporate hydrophobic domains for mechanical reinforcement and increased hydrophobicity of the thermogelled and crosslinked hydrogel matrix. A radical polymerization strategy is proposed to copolymerize the thermosensitive component *N*-isopropylacrylamide (NiPAAm) with other acrylic monomers to yield the functional amphiphiles. Pentaerythritol diacrylate monostearate (PEDAS), a bifunctional monomer consisting of the biocompatible tetrafunctional alcohol pentaerythritol esterified with two acrylic acids and stearic acid, a natural, metabolically resorbable fatty acid, provides the hydrophobic domain and NiPAAm the thermogelling properties, while acrylamide (AAm) was selected as a hydrophilic comonomer to adjust the transition temperature of the macromer, and 2-hydroxyethyl acrylate (HEA) was introduced to increase the number of hydroxyl groups available for chemical modification to yield chemically crosslinkable macromers. This study presents a protocol to yield water-soluble thermogelling amphiphilic macromers composed of PEDAS, NiPAAm, AAm, and HEA. Specifically, two series of macromers, one consisting of poly(PEDAS-*stat*-NiPAAm-*stat*-AAm) terpolymers and the other poly(PEDAS-*stat*-NiPAAm-*stat*-AAm-*stat*-HEA) copolymers, with different comonomer ratios were synthesized and characterized by nuclear magnetic resonance (NMR) spectroscopy and gel permeation chromatography (GPC). Solutions of the macromers were characterized for their phase transition properties by differential scanning

calorimetry (DSC) and oscillation rheology. Macroscopic gelation studies were performed to identify the thermodynamic stability of the thermogels. Candidate amphiphiles were (meth)acrylated to yield chemically crosslinkable thermogelling macromers, which were then analyzed for chemical composition and crosslinking characteristics. Thermally and chemically crosslinkable macromers are presented that are potential building blocks for novel hydrogel systems with improved mechanical properties for orthopedic applications.

Materials and Methods

Materials

Pentaerythritol diacrylate monostearate (PEDAS), octadecyl acrylate (ODA), *N*-isopropylacrylamide (NiPAAm), poly(NiPAAm) (pNiPAAm), acrylamide (AAm), 2-hydroxyethylacrylate (HEA), 2,2′-azobis(2-methylpropionitrile) (azobisisobutyronitrile, AIBN), acryloyl chloride (AcCl), methacryloyl chloride (MACl), anhydrous sodium carbonate, 4-methoxyphenol, ammonium persulfate (APS), and *N,N,N′,N′*-tetramethylethane-1,2-diamine (TEMED) were purchased from Sigma-Aldrich (Sigma, St. Louis, MO) and used as received. The solvents tetrahydrofuran (THF), diethyl ether and acetone were obtained from Fisher Scientific (Pittsburgh, PA) in analytical grade and were used as received unless stated differently. THF used during macromer (meth)acrylation was dried by refluxing over a potassium/sodium alloy for 3 days under nitrogen and distilled prior to use.

Methods

Macromer synthesis. Statistical copolymers were synthesized from PEDAS, NiPAAm, AAm, and HEA using free radical polymerization (Figure III-1). A statistical copolymer is defined as a copolymer with an irregular (statistical) distribution of repeating units [161]. Thermogelling macromers (TGMs) of various compositions were obtained by dissolving the acrylic monomers at corresponding molar comonomer ratios in THF at 60°C under nitrogen and initiating polymerization through the addition of AIBN (1.5 mol%). In a typical experiment, 3 g of PEDAS and corresponding amounts of comonomers were dissolved in 250 mL THF. The reaction was continuously stirred at 60°C over 16 - 18h and then refluxed for an additional 2h while the nitrogen atmosphere was maintained. The product was isolated by rotoevaporation and precipitation in cold diethyl ether. The filtrate was dried, dissolved in THF for a second time and again precipitated in diethyl ether. Precipitating the product in ether twice has been shown efficient to remove unreacted monomers and low molecular weight oligomers during method development. The final product was vacuum dried at ambient temperature and ground to a fine powder. Table III-1 summarizes the different TGMs that were synthesized and characterized.

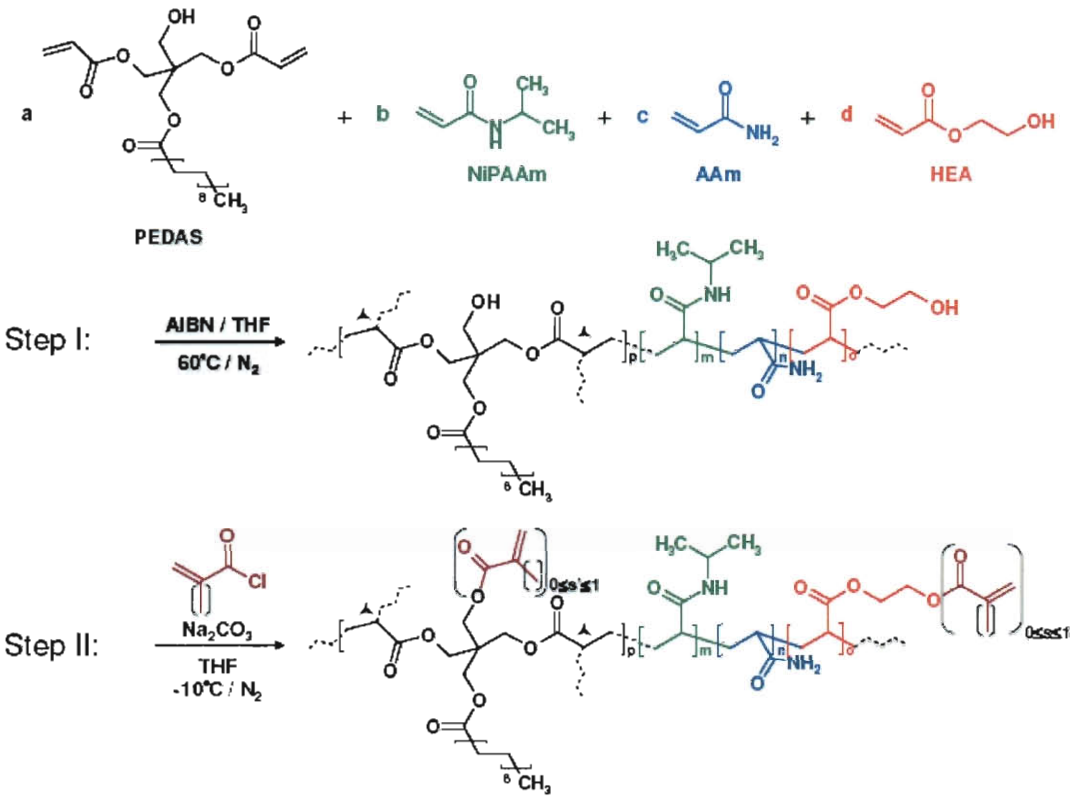

Figure III-1: Synthetic scheme for thermogelling macromers by radical copolymerization (Step I). The resulting macromer is a branched statistical copolymer. The schematic illustration of its structure is very simplified recognizing that a PEDAS repeating unit can be part of two linear chains thus contributing to the branched structure of the macromer (⅄ indicates possible branching sites). All copolymers in this study are synthesized from a comonomer ratio of a:(b+c+d) = 1:20. Theoretically, three out of four indices (p,m,n,o) could equal zero in possible products. In the ideal case, the ratio p:m:n:o equals a:b:c:d. (Meth)acrylate moieties that enable chemical crosslinking of the macromer are introduced in the second reaction step. Pendant hydroxyl groups that can be reacted in this methacrylation step are found in the PEDAS and HEA repeating units of the macromer and will be converted to different degrees (s, s').

Table III-1: Compositions and molecular weight characteristics of thermogelling macromers

Theoretical molar composition	**Actual molar comonomer feed (based on 1 mol PEDAS)**	**^{1}H-NMR results (based on 1 mol PEDAS)**	**GPC results**	
PEDAS:NiPAAm: AAm:HEA	NiPAAm:AAm:HEA (b:c:d in Figure III-1)	NiPAAm:AAm:HEA (m:n:o in Fig. III-1)	Mn [Da]	PI
		Effect of AAm content		
1/20/-/-	20.0/-/-	20.7/-/-	2660 ±130	3.4±0.2
1/18.5/1.5/-	18.6/1.6/-	19.1/2.1/-	2450 ±280	2.6±0.2
1/18/2/-	18.0/2.0/-	18.9/2.4/-	1870 ± 30	2.5±0.3
1/17/3/-	17.0/3.0/-	16.4/2.1/-	1860 ±260	2.7±0.2
1/16/4/-	16.0/4.1/-	13.3/4.2/-	1690 ± 80	2.7±0.1
1/14/6/-	13.9/6.0/-	10.0/5.2/-	1470 ±250	6.9±2.1
		Effect of HEA content		
1/16/-/4	15.9/-/4.0	17.5/-/5.8	3050 ±140	2.9±0.2
1/15.4/1/3.6	15.4/1.0/4.2	17.0/1.3/3.2	3810 ±260	3.0±0.3
1/15.4/2/2.6	15.3/2.0/2.6	17.4/1.8/2.0	2070 ± 90	2.7±0.1
1/15.4/2.6/2	15.4/2.7/2.2	15.0/3.1/2.8	2030 ±190	2.9±0.2
1/15.4/3/1.6	15.1/3.0/1.9	14.0/4.0/0.9	1930 ±120	2.9±0.4
1/15/3.5/1.5	15.2/3.5/1.5	15.8/3.1/2.0	2110 ± 60	3.7±0.6
1/14/3/3	14.0/3.0/3.0	15.2/2.0/3.4	2630 ±200	2.9±0.0
1/13.5/3.5/3	13.4/3.5/3.0	11.6/6.6/2.2	2770 ± 80	2.7±0.2
		Control		
ODA/15.4/3/1.6	15.4/3.1/1.7	15.5/5.1/1.8	2450 ± 80	2.1±0.0

Macromer (meth)acrylation. Methacrylated TGMs (TGM-MA) or acrylated TGMs (TGM-Ac) were obtained through the conversion of TGMs with MACl or AcCl in anhydrous THF in the presence of anhydrous sodium carbonate as scavenger for any acidic byproducts. In a typical reaction, 5 g of vacuum dried TGM, 2.5 g of sodium

carbonate, and approximately 120 mg of 4-methoxy phenol as radical inhibitor were weighed into a three neck flask, which was subsequently purged with nitrogen and sealed against moisture. The nitrogen stream was maintained throughout the entire reaction. THF (75 mL) was added through a septum and the polymer was dissolved under vigorous stirring. Thereafter, the reaction was chilled to below -10°C using an ice-sodium chloride bath. As soon as the temperature dropped below -10°C, the (meth)acrylation agent (MACl or AcCl) was added dropwise by means of a plastic syringe with needle through the septum. This addition step was controlled by the reaction temperature which was maintained below -10°C at any time. Following the addition of the (meth)acrylation agent, the mixture was stirred for another 16 - 18 h during which the ice was allowed to melt and the mixture warmed up to ambient temperature. The reaction mixture was filtered to remove any salt. Subsequently, the polymer solution was carefully concentrated by rotoevaporation, diluted with acetone, and again concentrated until almost dry. Enough acetone was added to redissolve the polymer. The solution was precipitated in cold diethyl ether. This step allows also for the removal of the radical inhibitor 4-methoxy phenol which is soluble in diethyl ether. The (meth)acrylated TGM was isolated by vacuum filtration and finally dried under vacuum at ambient temperature.

Proton nuclear magnetic resonance spectroscopy (^{1}H-NMR). ^{1}H-NMR spectra were obtained using a 400 MHz spectrometer (Bruker, Switzerland). Sample materials were dissolved in $CDCl_3$ (typical concentration: 20 mg/mL) that contained 0.05% tetramethylsilane (TMS) as internal shift reference. All postacquisition data processing was performed with the MestRe-C NMR software package (Mestrelab Research S.L.,

Spain). The free induction decay (FID) was Fourier transformed, manually phased, referenced using the TMS signal, baseline corrected, and integrated. To improve signal-to-noise, line broadening of 1.5 Hz was applied during transformation of the FID when meth(acrylated) TGMs were analyzed. To determine the comonomer composition of the macromers relative to PEDAS, the spectra were typically integrated between 0.85 and 0.94 ppm (I1), 0.95 and 1.24 ppm (I2), 1.25 and 1.34 ppm (I3), 1.35 and 2.45 ppm (I4), and between 3.50 and 4.50 ppm (I5) (Fig. III-2). I3, which was attributed to 28 (b in Fig. III-2) out of the 32 methylene protons of the stearate chain in PEDAS was set to 28. Consequently, I1, which represents the methyl protons in PEDAS (a in Fig. III-2), yielded values ranging between 2.8 and 3.4. It was found that the use of I3 instead of I1 as internal standard yielded more accurate results because I3 comprises a higher number of protons. The relative molar contents of the comonomers NiPAAm, AAm and HEA were calculated from the values obtained for I2, I4, and I5 according to the following equations (indices m, n, and o refer to Figure III-1):

$$I2 = 6 \cdot n_m(\text{NiPAAm}) \quad (1)$$

$$I4 = 11 + 3 \cdot n_m(\text{NiPAAm}) + 3 \cdot n_n(\text{AAm}) + 3 \cdot n_o(\text{HEA}) \quad (2)$$

$$I5 = 8 + n_m(\text{NiPAAm}) + 5 \cdot n_o(\text{HEA}) \quad (3)$$

Integral I2 comprises the 6 methyl protons of the N-isopropyl group of NiPAAm (p in Fig. III-2) (equation 1). I5 measures the methine proton of the latter functional group (i in Fig. III-2), the 8 methylene protons of pentaerythrityl core in PEDAS (e,f in Fig. III-2) as well as the 5 protons of the hydroxyethyl residue of HEA (l,m,h in Fig. III-

2) (equation 3). I4 summarizes the 4 methylene protons on C2 and C3 of the fatty acid in PEDAS (c,d in Fig. III-2), the free hydroxyl proton in PEDAS (g in Fig. III-2), the 6 protons of the polymerized acrylic moieties of PEDAS, as well as 3 protons from each of the other copolymerized monomers NiPAAm, AAm, and HEA (x,y in Fig. III-2) (equation 2).

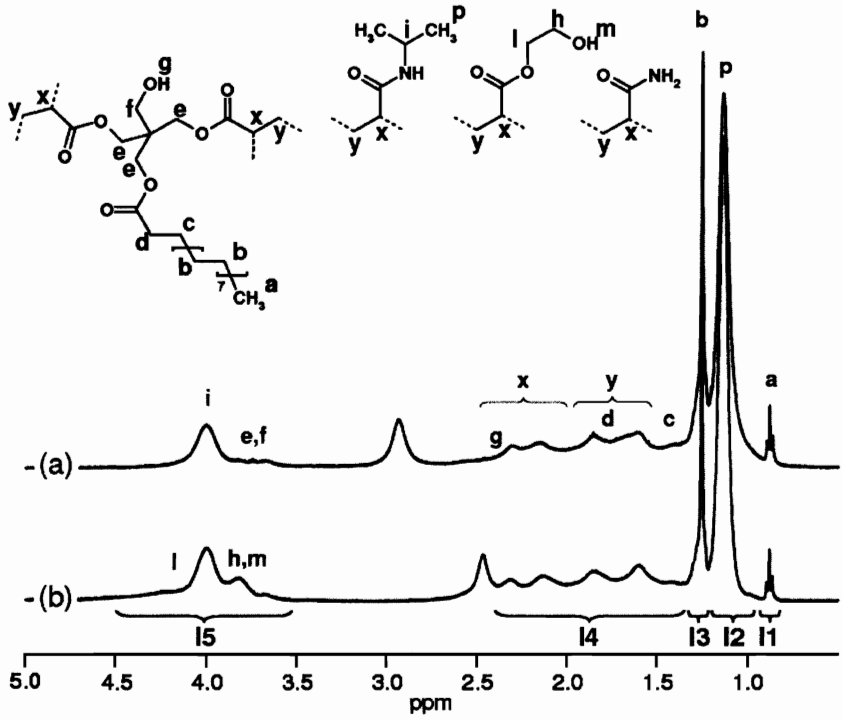

Figure III-2: ^{1}H-NMR spectra of (a) poly(PEDAS$_1$-*stat*-NiPAAm$_{16}$-*stat*-AAm$_4$) and (b) poly(PEDAS$_1$-*stat*-NiPAAm$_{16}$-*stat*-HEA$_4$). The letters assigned to the peaks correspond to the protons at the positions labeled in the structural elements of the copolymers. I1 - I5 represent the integrals used to determine macromer composition.

TGM conversion upon (meth)acylation was also determined relative to PEDAS. The integral I3 (1.25 - 1.34 ppm) was set to equal 28 protons. The signals derived from the olefinic protons of the acrylate (typically: 5.9 ppm, 6.2 ppm, and 6.5 ppm) or methacrylate groups (typically: 5.6 ppm, 6.15 ppm) were integrated individually and the upfield signal (5.9 ppm (TGM-Ac) or 5.6 ppm (TGM-MA)) was quantified to obtain the degree of (meth)acrylation relative to PEDAS. The olefinic signals located further downfield often overlapped with the broad signal of the -NHR proton (6 - 7 ppm) of NiPAAm, which lead to falsely increased signal integrals.

Gel Permeation Chromatography (GPC). Molecular weight distributions of the different TGMs and (meth)acrylated TGMs were determined by GPC. A GPC system consisting of an HPLC pump (Waters, model 510, Milford, MA), an autosampler/injector (Waters, model 717) and a differential refractometer (Waters, model 410) equipped with a series of analytical columns (Styragel® guard column 20 mm, 4.6 x 30 mm; Styragel® HR3, 5 mm, 4.6 x 300 mm; Styragel® HR1 column, 5 mm, 4.6 x 300 mm (all Waters) was used with degassed chloroform (HPLC grade, Sigma) as the eluent at a flow rate of 1.0 mL/min. Samples were prepared in chloroform at a concentration of 25 mg/mL and filtered prior to analysis. Macromer number average molecular weight (Mn), weight average molecular weight (Mw), and polydispersity index (PI) were determined relative to polystyrene. Three samples of each material were prepared and analyzed.

Rheological characterization. All rheological measurements were performed on a thermostated oscillating rheometer (Rheolyst AR1000, TA Instruments, New Castle, DE,

USA) equipped with a 6 cm steel cone (1 degree). TGMs were dissolved at the desired concentration, 10% (w/v) unless otherwise stated, in sterile minimum essential media (α modification; α-MEM) (Sigma) and kept on an orbital shaker over 24h at room temperature. In case the transition temperature of the macromer solution was below 25°C, samples were shaken in a cold room (4°C) until the polymers were dissolved. The dynamic viscoelastic properties of the solutions, namely the dynamic moduli, storage modulus (G') and loss modulus (G''), complex viscosity ($|\eta^*|$), and loss angle (δ), were recorded using the TA Rheology Advantage™ software (TA Instruments) at a gap size of 26 μm. When an oscillatory strain with frequency ω is applied, the complex viscosity is defined as: $\eta^* = (G''/\omega) - i\,(G'/\omega)$.

Gelation properties and transition temperatures. In a typical experiment, TGM and control samples were loaded, cooled to 5°C, pre-sheared at a rate of 1 s^{-1} for 1 min, and equilibrated for 15 min at 5°C. The viscoelastic properties of the samples were then recorded during a temperature sweep from 5°C to 65°C at a rate of 1°C/min at an observing frequency of 1 Hz and a displacement of $1x10^{-4}$ rad. To characterize the phase transition temperature of the TGM solution, different characteristic temperatures were determined. Upon thermogelation different rheological properties show characteristic changes during the temperature sweep. The initial change in viscoelastic properties is characterized by an increase of G' over G'' resulting in a decrease of the phase angle δ. T_δ characterizes the temperature at the first inflection point of the temperature-phase angle curve. During thermogel formation the viscosity of the system increased notably. T_η describes the location of the inflection point of the temperature-complex viscosity curve.

Reversibility of the thermogelation. Samples were loaded, cooled to 10°C, pre-sheared at a rate of 1 s^{-1} for 1 min, and equilibrated for 5 min at 10°C. The viscoelastic properties of the samples were then recorded during a set of different steps with a solvent trap installed. To gel the samples, a temperature sweep from 10°C to 37°C was performed at a rate of 4°C/min with a frequency of 1 Hz and a displacement of $1x10^{-4}$ rad (step I). The samples were kept at 37°C for 2 min while maintaining frequency and displacement at 1 Hz and $1x10^{-4}$ rad, respectively (step II). For the next 2 min at 37°C the displacement was increased to $1.5x10^{-3}$ rad (step III). Thereafter, the temperature setting was automatically changed to 15°C and a time sweep was recorded over 90 min at a frequency of 1 Hz and a displacement of $1.5x10^{-3}$ rad (step IV). In a typical experiment, the temperature had equilibrated at 15°C after around 2.0 min into the time sweep. G' and $|\eta^*|$ were analyzed at 15°C in step I, at the end of step II and after 60' during step IV.

Macromer crosslinking. The cone-plate setup described above including the solvent trap was used to compare the gelation properties of solutions from (meth)acrylated TGMs with and without chemical initiation. Solutions of different (meth)acrylated TGMs with a concentration of 10% (w/v) were prepared in α-MEM and loaded on the rheometer at 15°C. Before the geometry was lowered to gap size, TEMED and APS solution (100 mg/mL in water) were added to reach final concentrations of 20 mM each. In control samples without chemical initiation, equal amounts of TEMED and water were added. The samples were pre-sheared at a rate of 1 s^{-1} for 1 min at 15°C before the viscoelastic properties were recorded in a two step protocol. A temperature sweep from 15°C to 37°C was performed at a rate of 5°C/min with a frequency of 1 Hz and a displacement of $1x10^{-4}$ rad (step I). Thereafter, the thermogel properties were

monitored at 37°C over 30 min while maintaining oscillation frequency and displacement (step II). For samples with a transition temperature below 20°C, the temperature sweep (step I) was started at 10°C. For sample comparison the complex viscosities of the different samples were determined at 15°C during step I and at the end of step II (30' at 37°C).

Differential Scanning Calorimetry (DSC). The transition temperature of different TGM solutions was also determined by DSC. Solutions of different macromers (10% w/v) were prepared in sterile α-MEM as described for the rheology samples and 20 μL were pipetted in an aluminum sample pan (TA Instruments, Newcastle, DE) and capped. Thermograms were recorded on a TA Instruments DSC 2920 equipped with a refrigerated cooling system against an empty sealed pan as reference. In a typical run, the oven was equilibrated at 5°C for 10 min and then heated to 80°C at a heating rate of 5°C/min. For samples with a transition temperature below 20°C, the measurements were performed between -5°C and 50°C. The transition temperature (T_{DSC}) of the TGM solution was determined as the "onset at inflection" of the endothermic peak in the thermogram using the Universal Analysis 2000 software provided with the DSC system. DSC has been shown to yield phase separation temperatures that are comparable to values obtained by optical cloud point measurements and UV turbidimetry [69, 162]; methods that are typically used to determine the LCST of a polymer solution. All DSC experiments were performed in triplicate.

Thermogel stability. TGM solutions (10% w/v) in α-MEM were prepared as described above and pipetted (450 μL) into glass vials, which were finally capped airtight. The vials were placed in an incubator at 37°C and analyzed after 2h and 24h. Following macroscopic observation of the thermogels, any supernatant was removed carefully using a syringe with needle. The amount of aspirated solvent was determined gravimetrically on an analytical scale and recorded relative to the amount of media that could be removed from control vials that had been filled with 450 μL plain α-MEM. The relative amount of supernatant represents a means to characterize the amount of syneresis of the corresponding thermogel.

Statistics. Unless otherwise stated, all experiments were conducted in triplicate and the data were expressed as mean ± standard deviation (SD). Single-factor analysis of variance (ANOVA) in conjunction with Tukey's Post Hoc test was performed to assess the statistical significance ($p < 0.05$) within data sets.

Results & Discussion

Macromer design

Statistical copolymers of different comonomer ratios were synthesized from PEDAS, NiPAAm, AAm, and HEA in a free radical polymerization reaction initiated by AIBN in THF (Figure III-1). The main design criteria behind the amphiphilic NiPAAm-based macromers were the incorporation of a hydrophobic moiety to improve intermolecular cohesion and hydrogel mechanics in the long run; the introduction of

hydrolytically labile bonds to foster macromer biodegradability; the presence of thermoresponsive domains and of functional groups that can be modified to enable chemical crosslinking of the macromers. Hydrophobicity has been described as an important design criterion for polymers in bone tissue engineering [163]. Hydrophobic domains also contribute to cell-biomaterial interactions and can improve the mechanical properties of a material. Lipids and fatty acids are hydrophobic building blocks that have become popular in biomaterial research due to their biocompatibility, metabolic elimination and renewability [164-166]. PEDAS was selected as a hydrophobic building block as it contains the natural fatty acid stearic acid. Further components of PEDAS are the biocompatible alcohol pentaerythritol and two acrylic moieties that allow for the incorporation of PEDAS in copolymers synthesized by radical polymerization. The ester functionalities in PEDAS are potentially prone to hydrolysis. Other polymeric pentaerythritol esters have shown reasonable tissue compatibility and biodegradation [167]. PEDAS, therefore, was intended to function as a hydrophobic acrylic building block that mediates degradability to the copolymers. NiPAAm served as a well established building block for thermoresponsive polymers [156]. PNiPAAm is characterized by a LCST around 32°C and is known to show extensive phase separation at higher temperatures. To form stable hydrogels, NiPAAm has been copolymerized with hydrophilic comonomers or crosslinked [56]. Since copolymerization with the hydrophobic comonomer PEDAS would decrease the transition temperature, AAm was selected as a non-ionic, hydrophilic acrylic monomer to compensate for the hydrophobic contribution of PEDAS and adjust the hydrophilic-hydrophobic balance of the resulting macromer. Through HEA, free hydroxyl groups can be introduced into the macromer that are available for chemical

modification. Acrylation or methacrylation of the hydroxyl group would lead to crosslinkable macromers in which the (meth)acrylate functionalities are connected to the polymer backbone via hydrolysable hydroxyethyl esters, a design that fosters degradability of the crosslinked hydrogels.

Initial experiments identified THF as a more suitable solvent for the synthesis of uncrosslinked low-molecular weight macromers than toluene (data not shown). The reaction protocol described in the "Materials and Methods" section yielded copolymers that remained dissolved in the reaction mixture without increasing its viscosity significantly. The copolymers were precipitated out in diethyl ether and a colorless water- and chloroform-soluble powder was obtained after vacuum drying at yields around 80% - 85%. The purification protocol was verified by comparing GPC, NMR and cytocompatibility analysis of TGMs purified by precipitation in diethyl ether vs. TGMs purified by membrane dialysis (MWCO: 1000 Da). Results indicated that the removal of low-molecular weight side products was equally effective with both methods. Initial studies further identified a 1:20 ratio of bifunctional PEDAS to the monofunctional acrylic comonomers to yield copolymers of reproducible molecular weight and promising hydrophilic-hydrophobic balance (data not shown). In order to establish the synthetic protocol and identify structure-property relations, terpolymers of PEDAS, NiPAAm and AAm were first synthesized and characterized. Since PEDAS contains a free hydroxyl group, such terpolymers technically already fulfill the design criteria. Copolymers that contain HEA as a fourth comonomer were later synthesized with the objective to increase the number of free nucleophilic moieties for chemical modification. All copolymers are referred to with their theoretical comonomer composition throughout this study.

Synthesis and structural characterization of thermogelling poly(PEDAS-stat-NiPAAm-stat-AAm) terpolymers

Statistical copolymers were synthesized from PEDAS, NiPAAm and AAm with the content of hydrophilic AAm varying between 0% and 30% (Table III-1).

Qualitative ^{1}H-NMR analysis of the purified polymers revealed the absence of any olefinic signals (5 - 7 ppm) from unreacted monomers (data not shown) and the presence of all characteristic signals derived from the copolymerized monomers (Fig. III-2, trace a). Aliphatic signals derived from the stearic acid chain of PEDAS were found at 0.9 ppm (-CH_3, 3H, triplet) and around 1.3 ppm (-CH_2-, 28H, broad signal). The integral of the signal between 1.25 and 1.34 ppm was set to 28 and used as internal reference to calculate comonomer composition relative to PEDAS. Further signals were derived from the N-isopropyl group in NiPAAm and found at 1.15 ppm (-NH-CH($C\mathbf{H}_3$)$_2$) and 4 ppm (-NH-C**H**(CH_3)$_2$), and the methine and methylene groups of the polyacrylate backbone together with some functionalities in PEDAS between 1.4 and 2.4 ppm. The signals at 2.9 ppm (Fig. III-2, trace a) and 2.5 ppm (trace b) were attributed to residual water. Due to interactions of the moisture with the macromer molecules in $CDCl_3$, the signal was found to vary in intensity and chemical shift dependent on macromer composition and concentration (data not shown). With increasing AAm content and correspondingly decreasing NiPAAm content (Table III-1), the relative signal intensities of the aliphatic signals at around 1.15 and 1.3 ppm accordingly shifted towards the signal at 1.3 ppm indicating the varied comonomer composition in the copolymer (Fig. III-3A). Quantitative analysis of the NMR spectra revealed that copolymers at the desired comonomer ratios could be synthesized with appropriate control (Table III-1).

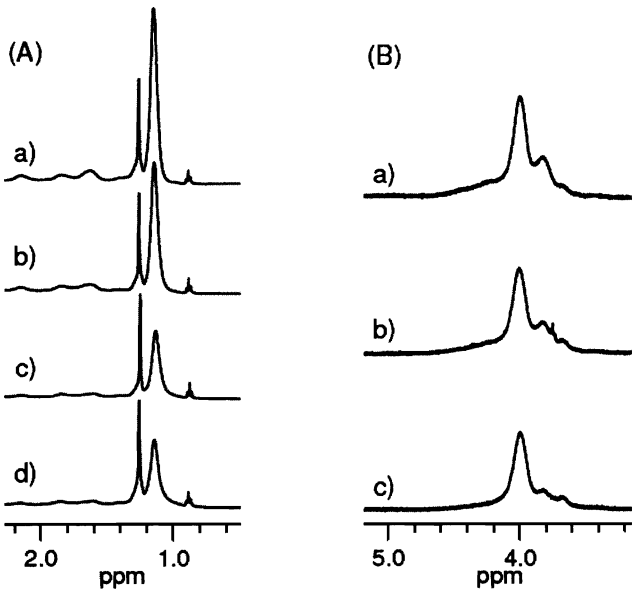

Figure III-3: Close-ups of ^{1}H-NMR spectra for different TGMs illustrating qualitative changes in signal intensities with changing comonomer ratios. (A) Poly(PEDAS$_1$-*stat*-NiPAAm$_{(20-m)}$-*stat*-AAm$_m$) with m = 0, 2, 4, 6 (a-d). (B) Poly(PEDAS$_1$-*stat*- NiPAAm$_{(20-m-n)}$-*stat*-AAm$_m$-*stat*-HEA$_n$) with m/n = 1/3.6 (a), 2/2.6 (b), and 3/1.6 (c).

With regard to the applicability of these macromers as injectable materials, control over macromer molecular weight and branching is critical, especially since PEDAS is a bifunctional monomer. The free radical polymerization protocol was optimized to allow for the synthesis of macromers that contain one to two PEDAS molecules and comprise the other comonomers at the feed ratio. In any case, the formation of branched, high molecular weight products should be avoided. Living radical polymerization techniques, such as group transfer polymerization (GTP) or reversible addition-fragmentation chain transfer (RAFT), may likely provide better control over

macromer composition and molecular weight, but the requirements of comonomer chemistry and purity (GTP) and catalyst chemistry (RAFT) are far more specific [168]. Using these techniques, a systematic screening of different comonomer compositions as presented here would involve laborious adaptation of the protocol to the different comonomer compositions. The versatility of a free radical polymerization protocol appeared advantageous for this study especially when control of macromer composition and weight can be achieved.

GPC analysis of the PEDAS-NiPAAm-AAm terpolymers with AAm contents up to 20% revealed number average molecular weights ranging between 1690 and 2250 Da (Table III-1). These values correlate well with theoretical molecular weights calculated for macromers that consist of one to two PEDAS precursors and the corresponding comonomers. The observed trend of decreasing molecular weights with increasing AAm and correspondingly decreasing NiPAAm content correlates with the difference in molecular weight between NiPAAm and AAm. Polydispersity indices between 2.3 and 2.7 were calculated. Figure III-4 shows representative chromatograms of different TGMs and precursors as obtained by GPC in chloroform. The polymer chromatograms were free of monomer signals at around 25 min, the elution time of NiPAAm monomers (Fig. III-4, trace a). PEDAS yielded a broad signal for which a PI of around 2 was determined (Fig. III-4, trace b). The copolymer chromatograms were characterized by a broad signal with a significant tail (Fig. III-4, trace c-e). As a similar shape was found for a control polymer containing ODA, a monofunctional lipophilic monomer, instead of the bifunctional PEDAS (Fig. III-4, trace c), the broad distribution was not attributed to macromer branching but to the amphiphilic properties and resulting possible interactions with the

chromatographic system. Extensive branching, indicated by a high molecular weight peak at low retention time (Fig. III-4, trace f) was however observed for poly($PEDAS_1$-*stat*-$NiPAAm_{14}$-*stat*-AAm_6), the terpolymers with the highest AAm content. Quantitative analysis consequently revealed a low Mn with a high PI of almost 7 (Table III-1). Further studies revealed that macromer molecular weight and branching increased with increasing reactant concentrations and decreasing initiator concentration (data not shown). From the above described results one can conclude that good control over macromer architecture can be achieved with the established synthesis protocol for different comonomer compositions with AAm contents of up to 20%.

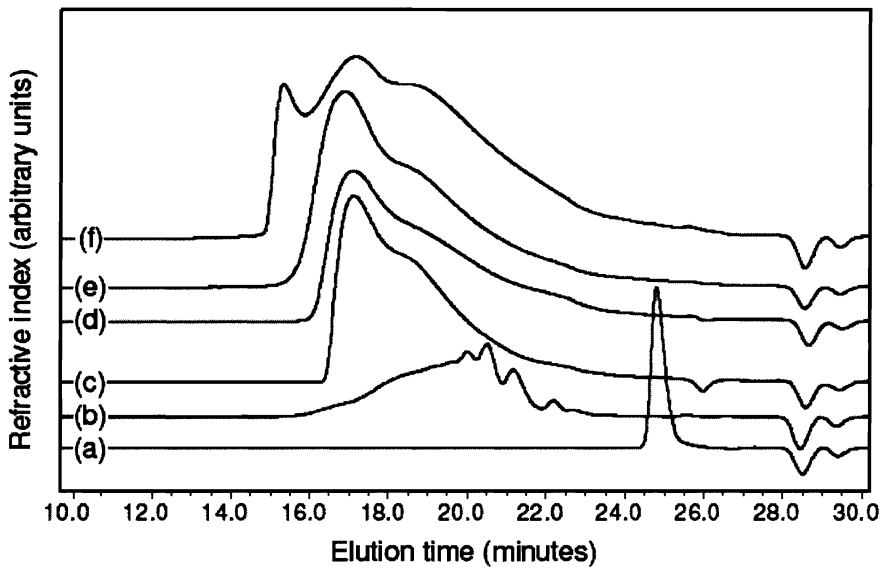

Figure III-4: GPC traces of (a) NiPAAm, (b) PEDAS, (c) poly(ODA_1-*stat*-$NiPAAm_{15.4}$-*stat*-AAm_3-*stat*-$HEA_{1.6}$) (control), (d) poly($PEDAS_1$-*stat*-$NiPAAm_{15.4}$-*stat*-AAm_3-*stat*-$HEA_{1.6}$), (e) poly($PEDAS_1$-*stat*-$NiPAAm_{16}$-*stat*-AAm_4), and (f) poly($PEDAS_1$-*stat*-$NiPAAm_{14}$-*stat*-AAm_6) (macromer that showed formation of branched networks).

Thermogelation properties of poly(PEDAS-stat-NiPAAm-stat-AAm) terpolymers

The thermogelation properties of solutions of the synthesized macromers (10% (w/v)) were analyzed by oscillation rheology. It is known that thermally induced phase separation is strongly affected by solution pH and ionic strength. Therefore, cell culture medium (α-MEM) was used as solvent during these experiments to simulate physiological and *in vitro* cell culture conditions. Figure III-5 shows a typical rheogram of a TGM, here poly($PEDAS_1$-*stat*-$NiPAAm_{15}$-*stat*-$AAm_{3.5}$-*stat*-$HEA_{1.5}$). The temperature dependent profiles observed for the complex moduli G' (storage modulus) and G'' (loss modulus), the complex viscosity $|\eta^*|$ and the phase angle δ are typical for thermogelling materials [155, 169]. At low temperatures, G'' far exceeded G', which was indicated by a phase angle $\delta >> 45°$, a property characteristic of viscous liquids (Fig. III-5). For temperatures below 25°C, the storage modulus of the displayed TGM was below the detection limit of the instrument. At temperatures below the phase transition, complex moduli and complex viscosity of the polymer solution decreased slightly with temperature, which is a typical behaviour of viscoelastic polymer solutions. Upon further heating and thermogelation (here past 26°C), G' and G'' both increased drastically with G' finally exceeding G'' ($\delta < 45°$), which indicated the formation of a viscoelastic hydrogel. The complex viscosity of the system increased by almost five orders of magnitude during this transition. Characteristic temperatures that were determined from the rheograms of different TGMs for sample comparison are the temperatures at the first inflection point of the temperature-phase angle curve (T_δ) and the inflection point of the temperature-complex viscosity curve (T_η). While T_δ represents the onset of phase transition that is associated with colloidal aggregation of the macromers and clouding of

the solution, T_η depicts the temperature at which the molecules have aggregated into a coherent network and form a hydrogel.

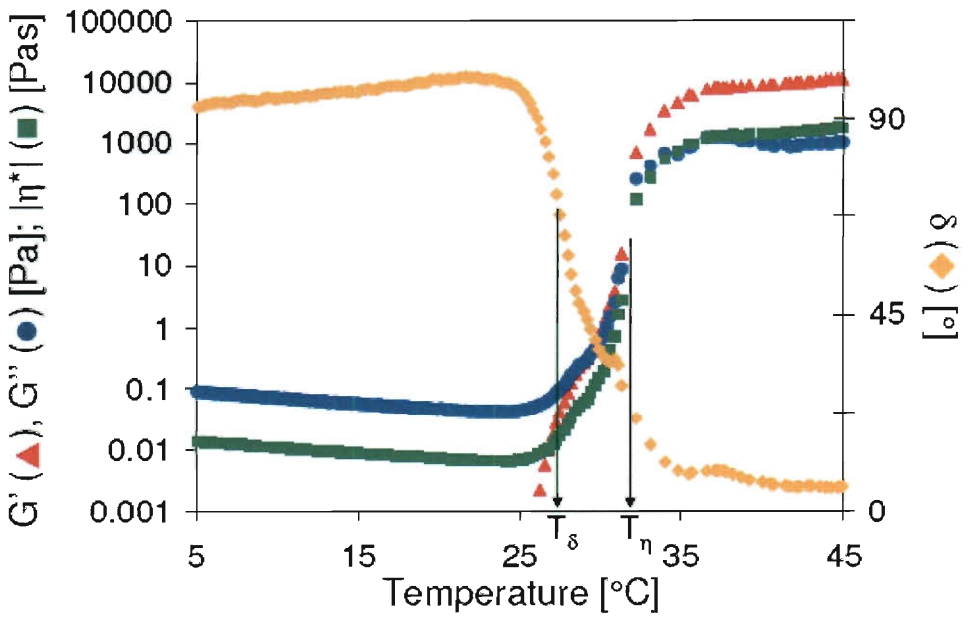

Figure III-5: Representative rheogram of poly(PEDAS$_1$-*stat*-NiPAAm$_{15}$-*stat*-AAm$_{3.5}$-*stat*-HEA$_{1.5}$) obtained during a temperature sweep between 5 and 45°C at 1 Hz. The complex moduli (G' and G'') and the complex viscosity |η*| are displayed on the left y-axis, while the right y-axis refers to the loss angle (δ). The locations of the characteristic temperatures T_δ and T_η are indicated by arrows.

The transition temperatures determined for poly(PEDAS$_1$-*stat*-NiPAAm$_{20}$) and the different PEDAS-NiPAAm-AAm terpolymers are summarized in Figure III-6A. The figure also contains the transition temperatures as obtained by DSC (T_{DSC}) for the different TGM solutions (10% (w/v) in α-MEM). The characteristic temperatures determined for pNiPAAm are displayed in Figure III-6B, I. Almost identical transition

temperatures T_δ (27.4 ± 1.2 °C) and T_η (27.4 ± 1.3 °C) were obtained for pNiPAAm by rheology. DSC analysis yielded a transition temperature of 30.7 ± 0.1 °C. The discrepancy between the different temperatures likely has methodical reasons especially since T_{DSC} is derived from a calorimetric signal and the other two temperatures are derived from viscoelastic parameters relevant for material application. Poly(PEDAS$_1$-*stat*-NiPAAm$_{20}$) was characterized by significantly lower values for T_δ (25.7 ± 0.1 °C) and T_η (26.8 ± 0.0 °C) (Fig. III-6A). T_{DSC} (23.5 ± 0.6 °C) confirmed the shift towards a lower phase transition temperature, which is caused by the hydrophobic structures in PEDAS. Increasing contents of the hydrophilic comonomer AAm in PEDAS-NiPAAm-AAm terpolymers compensated for the hydrophobic effect of PEDAS and the characteristic temperatures increased above the values of pNiPAAm. For poly(PEDAS$_1$-*stat*-NiPAAm$_{14}$-*stat*-AAm$_6$), the terpolymer with the highest AAm content investigated, transition temperatures of 34.7 ± 2.4 °C (T_δ), 43.5 ± 2.3 °C (T_η), and 36.6 ± 1.4 °C (T_{DSC}) were measured. A similar correlation between TGM composition and the different transition temperatures was found. For all TGMs a difference between T_δ and T_η was observed, which typically increased with AAm content. In comparison to pure pNiPAAm, for which identical values for T_δ and T_η were obtained, the TGMs are amphiphilic molecules and the formation of micellar aggregates is likely involved in the colloidal aggregation of the macromers during phase transition [170]. Upon thermogelation the micelles aggregate and packing interactions increase to form dense gels. As the NiPAAm residues of the amphiphilic TGMs drastically change their interactions with solvent molecules during thermogelation, the hydrophilic-hydrophobic balance of the micelle-forming macromers is also altered significantly and micelle structure affected.

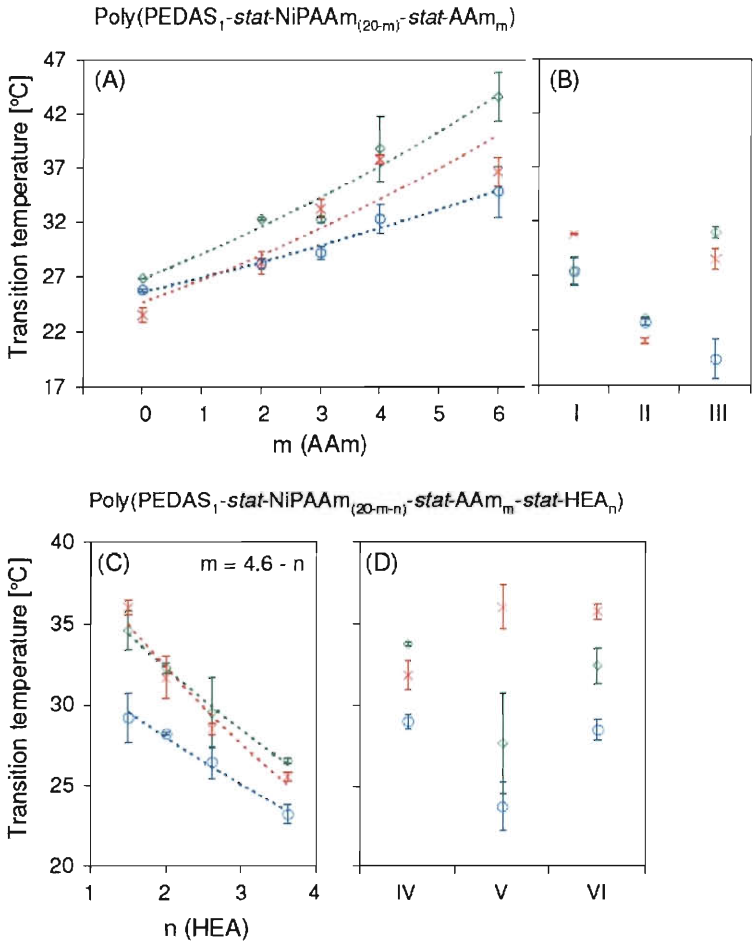

Figure III-6: Phase transition temperatures determined from rheology (T_δ:o, T_η: ◇) and differential scanning calorimetry (T_{DSC}: x) for different TGMs. (A) Co- and terpolymers composed of PEDAS, NiPAAm and different contents of AAm (m = 0-6). (B) Polymeric controls: (I) pNiPAAm, (II) poly(PEDAS$_1$-*stat*-NiPAAm$_{16}$-*stat*-HEA$_4$) and (III) poly(ODA$_1$-*stat*-NiPAAm$_{15.4}$-*stat*-AAm$_3$-*stat*-HEA$_{1.6}$). (C) Poly(PEDAS$_1$-*stat*-NiPAAm15.4-*stat*-AAm$_{(4.6-n)}$)-*stat*-HEA$_n$) with differents contents of HEA (n = 1.6, 2, 2.6, 3.6) (D) TGMs with different NiPAAm:AAm:HEA comonomer ratios, (IV) 14:3:3, (V) 13:4:3, (VI) 15:3.5:1.5.

Complex structural changes of the TGM solution are expected during thermogelation that involve micelle formation, aggregation and vesicle shrinkage upon macromer dehydration. With this transition, T_δ depicts the onset of colloidal aggregation and sol-gel transition, while T_η describes the temperature at which the macromers finally assemble into a coherent physical network and a dense gel is formed. For hydrophobic monomers (systems with low phase transition temperatures), the calorimetric transition (T_{DSC}) appears to correlate with the onset of phase transition T_δ. With increasing hydrophilicity of the macromers, T_{DSC} shifts closer towards T_η (Fig. III-6 A,C). Since the different transition temperatures depend on solution concentration, trends between T_{DSC}, T_δ and T_η might differ at different concentrations. The relatively low T_{DSC} observed for poly(PEDAS$_1$-*stat*-NiPAAm$_{14}$-*stat*-AAm$_6$) is likely attributed to the extensive branching of this macromer (Fig. III-6A, Table III-1).

Due to thermodynamic instability, pNiPAAm-based thermogels show considerable syneresis and possibly full phase separation when the temperature is increased above the phase transition temperature [155, 171]. With regard to biomedical applications, it has been shown that the extent of phase separation correlates with the difference between transition temperature, commonly the LCST, and 37°C. In order to test for the thermodynamic stability of thermogels formed by the different TGMs, solutions (10% (w/v) were incubated at a constant temperature of 37°C and the extent of syneresis was determined after 1h, 2h and 24h. The results from the 2h time point are summarized in Figure III-7. Part A depicts the gross view of the thermogels after 2h at 37°C. The residual gel mass is summarized in part B. The solutions were prepared and pipetted into glass vials at ambient temperature below the transition temperature of the

TGM solution. In a typical experiment thermogel formation occurred approximately 10 min after the vials were placed into the incubator. Immediately after gelation, the gel volume equalled the volume of the polymer solution (450 μL). After 24h, the residual gel fractions of all thermogels ranged around 10 - 15%, which was assumed to correlate with full syneresis and phase separation (data not shown). In accordance with the literature, pNiPAAm solutions (Fig. III-7, sample a) show extensive syneresis and phase separation at 37°C. Solutions of poly($PEDAS_1$-*stat*-$NiPAAm_{20}$), which gelled at a lower temperature than pNiPAAm, shrunk to a comparable extent after 2h (sample b). With increasing AAm content, improved stability was observed for PEDAS-NiPAAm-AAm terpolymers (sample c, d) with poly($PEDAS_1$-*stat*-$NiPAAm_{16}$-*stat*-AAm_4) forming stable thermogels at 37°C for 2h (sample d). Solutions of poly($PEDAS_1$-*stat*-$NiPAAm_{14}$-*stat*-AAm_6) ($T_\eta = 43.5 \pm 2.3$ °C) did not gel at 37°C; correspondingly, no gel fraction could be quantified after 2h (sample e).

These results show that amphiphilic terpolymers were synthesized with controlled molecular composition and structure. TGM structure, especially the hydrophobic-hydrophilic balance, controlled the thermally induced gelation of corresponding aqueous macromer solutions. The thermodynamic stability of the resulting thermogels correlated with transition temperature. With regard to the intended chemical modification of the macromers, initial tests revealed that the free hydroxyl group in PEDAS (Figure III-1) was not sufficiently accessible for (meth)acrylation reaction possibly due to steric hindrance (data not shown). In order to incorporate additional hydroxyl groups, HEA was introduced as comonomer and initially copolymerized with PEDAS and NiPAAm. HEA is known as a hydrophilic monomer and was therefore considered as a building block that

could provide chemically accessible hydroxyl groups in combination with a potential to balance the hydrophobicity of PEDAS and control the transition temperature of the macromers. Analogous to the synthesis of poly(PEDAS$_1$-*stat*-NiPAAm$_{16}$-*stat*-AAm$_4$), poly(PEDAS$_1$-*stat*-NiPAAm$_{16}$-*stat*-HEA$_4$) was synthesized at the desired composition and molecular weight (Table III-1). Analysis of the transition temperatures revealed values below 25°C for T_δ, T_η and T_{DSC} (Fig. III-6B, II). As a result of intra- or intermolecular hydrogen bond formation the hydroxyl group of HEA did not fully interact with water and the expected hydrophilic effect of HEA was diminished in solution. Correspondingly, extensive syneresis was observed for these thermogels (Fig. III-7, sample h). Consequently, copolymers of PEDAS, NiPAAm, AAm, and HEA were synthesized for further experiments. The molar ratio of PEDAS to NiPAAm + AAm + HEA was maintained at 1:20.

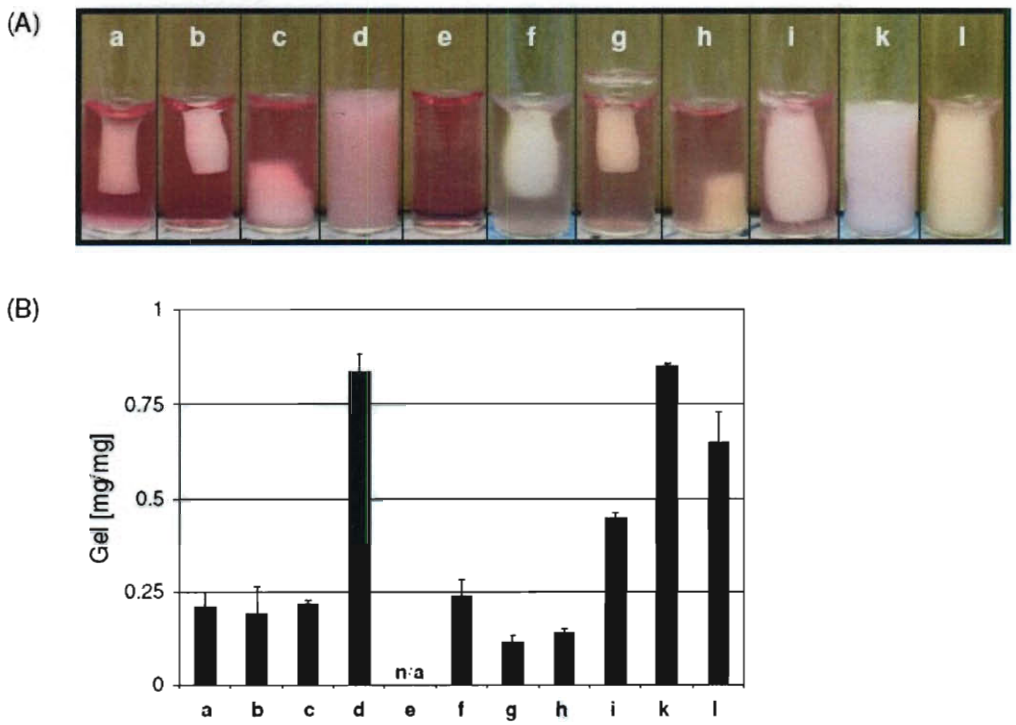

Figure III-7: Stability of thermogels of different comonomer composition at 37°C. (A) Macroscopic images of thermogels after 2 h of incubation. (B) Mass fraction of thermogels after 2 h. Columns and error bar represent means ± standard deviation for n = 3. Samples: (a) pNiPAAm; poly(PEDAS$_l$-*stat*-NiPAAm$_{(20-m)}$-*stat*-AAm$_m$) with m = 0, 3, 4, 6 (b-e); poly(PEDAS$_l$-*stat*-NiPAAm$_{(20-m-n)}$-*stat*-AAm$_m$-*stat*-HEA$_n$) with m/n = 2/2.6 (f), 1/3.6 (g), 0/4 (h), 3/3 (i), 3.5/3 (k), and 3.5/1.5 (l).

Synthesis and characterization of thermogelling poly(PEDAS-stat-NiPAAm-stat-AAm-stat-HEA) copolymers

Copolymers containing 1 mol PEDAS, 15.4 mol NiPAAm and varying ratios of AAm and HEA (poly($PEDAS_1$-*stat*-$NiPAAm_{15.4}$-*stat*-AAm_m-*stat*-HEA_n)) were synthesized at the desired composition and molecular weight distribution (Table III-1, Fig. III-4). A trend relating molecular weight and HEA content as a result of the molecular weight difference of AAm and HEA was observed. ^{1}H-NMR analysis confirmed the presence of HEA specific protons in the copolymers (l,h,m in Fig. III-2, trace b). The intensities of these signals were found to increase relative to the methine signal (4.0 ppm) of the *N*-isopropyl group of NiPAAm with increasing comonomer contents of HEA (Fig. III-3B). Figure III-4 compares the molecular weight distribution of poly($PEDAS_1$-*stat*-$NiPAAm_{15.4}$-*stat*-AAm_3-*stat*-$HEA_{1.6}$) (trace d) and poly(ODA_1-*stat*-$NiPAAm_{15.4}$-*stat*-AAm_3-*stat*-$HEA_{1.6}$) (trace c). This comparison was motivated by the concern of network formation due to the use of the bifunctional monomer PEDAS. ODA is a monofunctional monomer comprising stearic alcohol and acrylic acid making the lipophilic component comparable to the stearic acid domain in PEDAS. The results illustrate that the molecular weight distributions of the different macromers do not differ significantly which indicates that PEDAS-containing TGMs are most likely branched but not networked and still contain individual macromers of controllable molecular weight (Mn) in the range of 2000 - 3500 Da (Fig. III-4, Table III-1). Despite its bifunctionality, PEDAS is considered advantageous over ODA because the lipophilic domain of PEDAS, stearic acid, can be metabolized following ester hydrolysis in contrast to stearic alcohol. Comparison of the transition temperatures of both copolymers (Fig. III-6; B, III vs. C,

data set on far left), revealed significantly higher values for poly(PEDAS$_1$-*stat*-NiPAAm$_{15.4}$-*stat*-AAm$_3$-*stat*-HEA$_{1.6}$), which likely indicates that the hydrophilic pentaerythrityl core of PEDAS positively affects the hydrophobic-hydrophilic balance within the macromer. Within the set of poly(PEDAS$_1$-*stat*-NiPAAm$_{15.4}$-*stat*-AAm$_m$-*stat*-HEA$_n$) copolymers, the transition temperatures follow the structure-property relations established in PEDAS-NiPAAm-AAm terpolymers (Fig. C). With increasing HEA and decreasing AAm contents, the transition temperatures decrease. T_{DSC} again approaches T_δ with increasing hydrophobicity of the TGMs. In correlation with the LCSTs, the thermogel stability of poly(PEDAS$_1$-*stat*-NiPAAm$_{15.4}$-*stat*-AAm$_m$-*stat*-HEA$_n$) copolymers at 37°C decreased with increasing n/m ratio (Fig. III-7, samples f and g).

Thermogel stability of amphiphilic NiPAAm-based macromers

The TGMs were designed to contain hydrophobic domains to promote disperse interactions among the macromers and potentially increase mechanical stability of a TGM-based hydrogel. With regard to the thermogelation properties, these domains necessitated the incorporation of hydrophilic domains to adjust transition temperature and thermodynamic stability of thermally gelled TGM solutions. To test for any effects of the resulting amphiphilic design on the stability of corresponding thermogels, rheological experiments investigating the reversibility of the physical gelation were performed with pNiPAAm as control polymer (Fig. III-8). Two TGMs, poly(PEDAS$_1$-*stat*-NiPAAm$_{14}$-*stat*-AAm$_3$-*stat*-HEA$_3$) and poly(PEDAS$_1$-*stat*-NiPAAm$_{15.4}$-*stat*-AAm$_2$-*stat*-HEA$_{2.6}$), with calorimetric transition temperatures (T_{DSC}) surrounding the value determined for pNiPAAm were selected considering the structure property relation established for TGM

hydrogels. Comparison of pNiPAAm with the two TGMs that were characterized by comparable transition temperatures revealed significant differences for the gel-sol transition upon cooling below transition temperature. During the rheometric experiment, the macromers were first gelled during a controlled temperature sweep to 37°C. After an isothermal phase of 2 min, the shear stress was increased and maintained for another 2 min before the temperature was set to 15°C and changes in the complex viscosity were monitored (Fig. III-8). All systems underwent thermogelation upon heating to 37°C which was associated with an increase in complex viscosity by 3-4 orders of magnitude. The pNiPAAm solution showed the highest complex viscosity at 5°C and after 2 min at 37°C. This can likely be attributed to the higher molecular weight of the pNiPAAm (Mn of 20 - 25 kDa according to manufacturer) as compared to the TGMs. In response to the temperature decrease to 15°C, the pNiPAAm system degelled almost instantly into a solution with a complex viscosity as at the start of the experiment. Both TGM hydrogels, in contrast, maintained a significantly elevated complex viscosity for 60 min at 15°C, while the systems became translucent once the temperature dropped below the transition temperature. Macroscopic observations revealed the full reversibility of the thermogelation for the TGM gels after 2-3 days at 20°C and below (data not shown). This indicates that during thermally induced gelation of amphiphilic NiPAAm-based macromers colloids are formed, which are stabilized by additional intermolecular forces than those arising from the entropically driven aggregation of pNiPAAm domains. pNiPAAm-based amphiphiles appear advantageous over pure pNiPAAm hydrogels when increased hydrogel stability is warranted and the kinetics of the gel-sol transition is of minor importance.

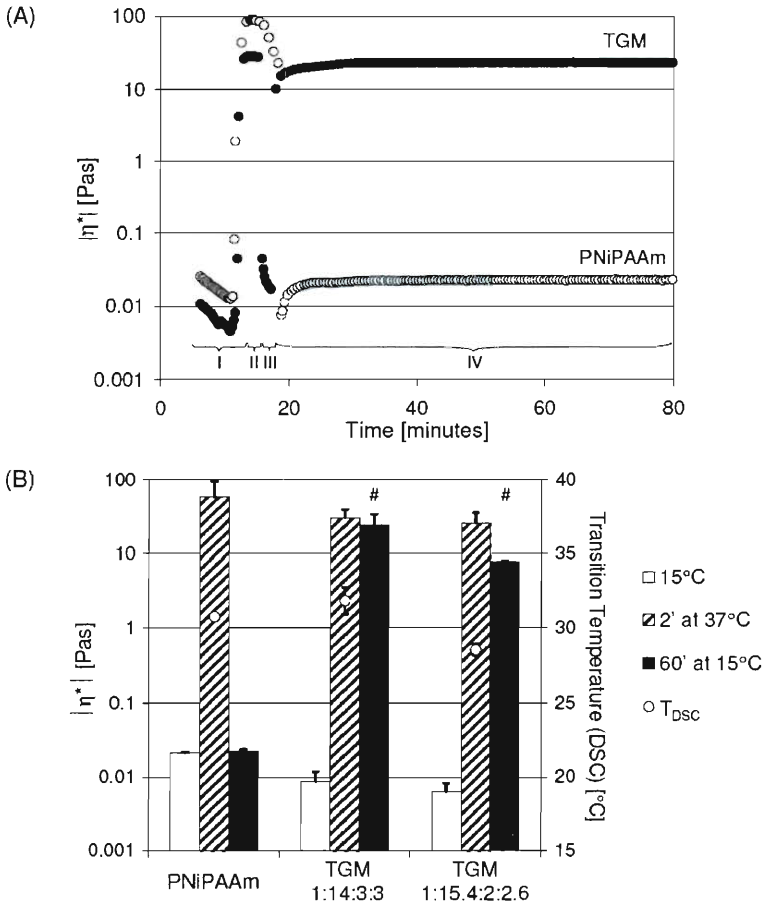

Figure III-8: (A) Representative rheograms of poly(PEDAS$_1$-*stat*-NiPAAm$_{14}$-*stat*-AAm$_3$-*stat*-HEA$_3$) (TGM) and pNiPAAm during a test for reversibility of the thermogelation. (B) Complex viscosity |η*| for pNiPAAM and two TGMs as determined at 15°C during step I, after 2 min at 37°C, and after 60' into step IV at 15°C. Transition temperatures as determined by DSC (T_{DSC}) of the different polymers are assigned to the right y-axis. Columns and error bar represent means + standard deviation for n = 3. Statistically significant differences between the complex viscosities of the TGM samples (60 min at 15°C) as compared to the corresponding value for pNiPAAm is denoted by #.

TGMs with optimized composition and gelation properties

In view of the established structure property correlations and the design objective to optimize the thermodynamic stability of the TGMs and to provide a sufficient number of hydroxyl groups available for chemical modification per macromer, TGMs with high AAm and HEA contents and reduced NiPAAm comonomer contents were synthesized and analyzed (Table III-1). Poly(PEDAS$_1$-*stat*-NiPAAm$_{14}$-*stat*-AAm$_3$-*stat*-HEA$_3$) could be synthesized at the desired composition and molecular weight. The NMR analysis of poly(PEDAS$_1$-*stat*-NiPAAm$_{13.5}$-*stat*-AAm$_{3.5}$-*stat*-HEA$_3$) revealed overly high AAm contents and low NiPAAm contents, a phenomenon also observed for poly(PEDAS$_1$-*stat*-NiPAAm$_{14}$-*stat*-AAm$_6$). These findings are attributed to likely colloid formation of these strongly amphiphilic macromers in the NMR solvent $CDCl_3$ and shielding of PEDAS and NiPAAm protons. Increased branching was observed for poly(PEDAS$_1$-*stat*-NiPAAm$_{15}$-*stat*-AAm$_{3.5}$-*stat*-HEA$_{1.5}$), which was designed to contain half of the HEA compared to poly(PEDAS$_1$-*stat*-NiPAAm$_{14}$-*stat*-AAm$_3$-*stat*-HEA$_3$) and keep the molar AAm comonomer content below 4 (relative to PEDAS). Poly(PEDAS$_1$-*stat*-NiPAAm$_{14}$-*stat*-AAm$_3$-*stat*-HEA$_3$) solutions were characterized by a T_η of 33.7 ± 0.2 °C more than 5°C above the T_η determined for pNiPAAm (Fig. III-6C, I). The stability of thermogels formed from this TGM were also significantly increased (Fig. III-7, sample i). A further increase in AAm content resulted in a TGM (poly(PEDAS$_1$-*stat*-NiPAAm$_{13.5}$-*stat*-AAm$_{3.5}$-*stat*-HEA$_3$)) that yielded even more stable thermogels (Fig. III-7, sample k). The chemical characteristics of the macromers, however, were less definite (Table III-1), which explains the disperse results obtained for T_δ, T_η and T_{DSC} (Fig. III-6D, V). Another well balanced TGM was synthesized with poly(PEDAS$_1$-*stat*-NiPAAm$_{15}$-*stat*-AAm$_{3.5}$-

stat-$HEA_{1.5}$), which was characterized by T_δ and T_η comparable to poly($PEDAS_1$-*stat*-$NiPAAm_{14}$-*stat*-AAm_3-*stat*-HEA_3) but a significantly increased T_{DSC} (35.6 ± 0.5 °C) (Fig. III-6C, VI) and formed thermogels of appropriate stability (Fig. III-7, sample l). In view of their favorable thermogelation properties, poly($PEDAS_1$-*stat*-$NiPAAm_{14}$-*stat*-AAm_3-*stat*-HEA_3) and poly($PEDAS_1$-*stat*-$NiPAAm_{15}$-*stat*-$AAm_{3.5}$-*stat*-$HEA_{1.5}$) were chemically modified to yield chemically crosslinkable TGMs (Figure III-1, step II).

Synthesis and structural characterization of chemically crosslikable TGMs

With the objective to introduce chemically crosslinkable domains into the TGMs to yield macromers that can be gelled both physically and chemically, TGMs were reacted with AcCl or MACl. Anhydrous sodium carbonate was used to scavenge any acidic by-products during the reaction and upon termination any salt was removed by filtration [172]. Triethylamine, which is a commonly used base to catalyze such (meth)acrylation reactions, could not be effectively removed from the reaction products due to the lack of a suitable extraction solvent that would precipitate the amphiphilic macromers. As described for the hydroxyl group methacrylation of other molecules [173], the molar excess of the acrylation or methacrylation agent, AcCl or MACl, controlled the extent of hydroxyl group conversion (Table III-2, Fig. III-9). Figure III-9 shows representative ^{1}H-NMR traces of poly($PEDAS_1$-*stat*-$NiPAAm_{14}$-*stat*-AAm_3-*stat*-HEA_3) as well as two acrylated and one methacrylated derivative. Characteristic changes of the proton signal indicate successful (meth)acrylation of the TGM. Upon (meth)acrylation, characteristic olefinic proton signals appear between 5.6 and 6.6 ppm representing three (TGM-Ac) or two (TGM-MA) olefinic protons per (meth)acrylic ester. In addition, a

downfield shift of the methylene protons in α-position to the newly formed (meth)acrylic ester was observed (signal at 4.3 ppm). A signal at 1.9 - 2.0 ppm representing the methyl group of the methacrylate ester group was found in the spectrum of TGM-MA. The conversion was calculated relative to the PEDAS molecules per TGM and an increased conversion was found with higher feeds of (meth)acryloyl chloride. Poly(PEDAS$_1$-*stat*-NiPAAm$_{14}$-*stat*-AAm$_3$-*stat*-HEA$_3$), the TGM with the higher HEA content per macromer, showed a higher conversion relative to PEDAS. A maximum of 1.25 acrylic groups per macromer subunit identified by one PEDAS block was achieved with an acryloyl chloride excess of 2.5 (relative to the theoretical number of hydroxyl groups per macromer subunit). This means that 1.25 out of the 4 theoretical hydroxyl groups per macromer subunit (3 in HEA and one in PEDAS) were acrylated. Additional experiments revealed that the hydroxyl group of PEDAS was not accessible for (meth)acrylation under the applied conditions (data not shown).

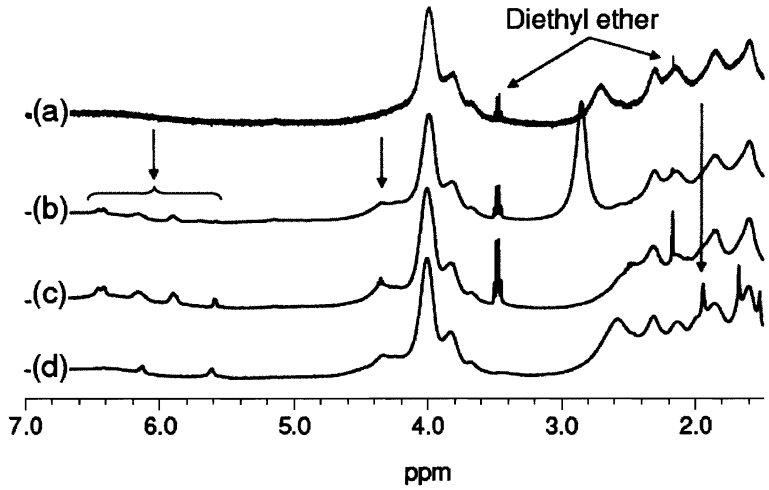

Figure III-9: Close up (1.5 - 7 ppm) of ^{1}H-NMR spectra obtained for (a) poly(PEDAS$_1$-*stat*-NiPAAm$_{14}$-*stat*-AAm$_3$-*stat*-HEA$_3$ (TGM) and (b-d) (meth)acrylated poly(PEDAS$_1$-*stat*-NiPAAm$_{14}$-*stat*-AAm$_3$-*stat*-HEA$_3$ at different molar excesses of (meth)acryloyl chloride: (b) TGM-Ac (0.75x), (c) TGM-Ac (2.5x), and (d) TGM-MA (2.5x). Proton signals derived from the (meth)acrylate groups are indicated by arrows.

Due to the lower reactivity of methacryloyl chloride, a likely consequence of steric limitations, a lower conversion was found for the methacrylated TGMs as compared to the acrylation products at corresponding molar feeds of the reactive chlorides (Table III-2). The transition temperatures of the (meth)acrylated macromers, here T_{DSC}, were found to decrease with the extent of (meth)acrylation. As hydrophilic hydroxyl functionalities are turned into considerably less hydrophilic (meth)acrylic esters, the hydrophilic-hydrophobic balance of the macromer was changed towards increased hydrophobicity and the phase transition temperature decreased. A stronger

effect of macromer derivatization on transition temperature was found for TGM-MA, which is explained by the stronger hydrophobicity of the methacrylic ester as compared to an acrylic ester.

Table III-2: Methacrylated (TGM-MA) or acrylated (TGM-Ac) macromers synthesized from two different TGMs at increasing molar ratios of the (meth)acrylation reagents (XCl) methacryloyl chloride or acryloyl chloride, respectively. Conversion of TGM hydroxyl groups into (meth)acrylate esters as determined by ^{1}H-NMR per PEDAS molecule (n_{Olefin}/n_{PEDAS}) and corresponding transition temperature of a 10% (w/v) macromer solution as determined by DSC (n = 3).

TGM (PEDAS:NiPAAm:AAm:HEA)		1:14:3:3		1:15:3.5:1.5	
Modification	**Reagent feed n_{XCl}/n_{OH}**	**^{1}H-NMR n_{Olefin}/n_{PEDAS}**	**T_{DSC} [°C]**	**^{1}H-NMR ($n_{MA/Ac}/n_{PEDAS}$)**	**T_{DSC} [°C]**
Unmodified	n/a	n/a	33.1 ± 0.4	n/a	35.6 ± 0.5
Methacrylation	1.25	0.55	13.6 ± 1.1	0.19	24.1 ± 0.6
	2.5	1.12	13.8 ± 0.5	0.57	15.2 ± 0.9
Acrylation	0.75	0.27	25.1 ± 0.6	0.15	31.2 ± 0.2
	1.25	1.01	22.3 ± 1.2	0.64	24.6 ± 0.3
	2.5	1.25	19.6 ± 0.7	0.98	20.8 ± 0.9

Gelation properties of chemically crosslinkable TGMs

Results of rheological experiments performed with solutions of the (meth)acrylated TGMs (10% (w/v)) with and without the presence of the thermal initiator system APS/TEMED (25mM each) are summarized in Figure III-10.

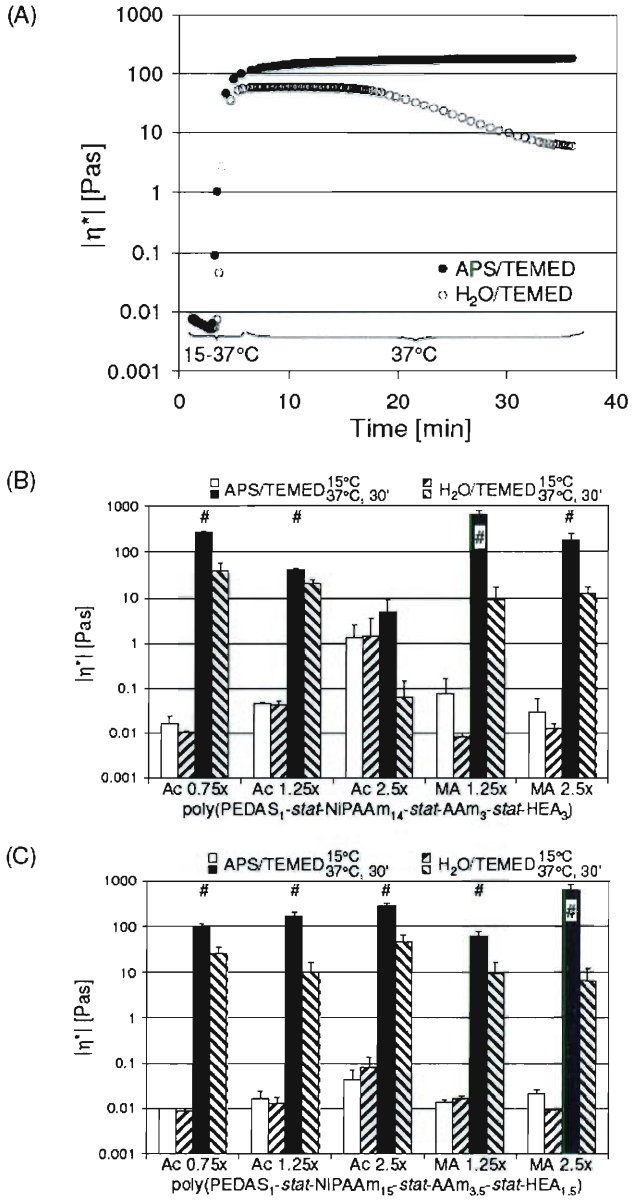

Figure III-10: Rheological characterization of solutions of different (meth)acrylated TGMs with (APS/TEMED) and without (H_2O/TEMED) chemical initiation. (A) Representative rheograms. (B) and (C) show the complex viscosity $|\eta^*|$ at 15°C and after 30' at 37°C for two macromers with various modifications. # denotes statistical significance between initiated and non-initiated samples after 30 min at 37°C.

Redox initiator system and concentration have been shown suitable and sufficiently biocompatible for direct cell encapsulation with *in situ* crosslinked hydrogels [31, 142]. All (meth)acrylated TGMs except acrylated (Ac 2.5x) poly(PEDAS$_1$-*stat*-NiPAAm$_{14}$-*stat*-AAm$_3$-*stat*-HEA$_3$) showed thermogelation during the initial temperature sweep to 37°C, which was associated with a significant increase in complex viscosity for samples with (APS/TEMED) and without (H_2O/TEMED) chemical initiation (Fig. III-10A,B). Acrylated (2.5x) poly(PEDAS$_1$-*stat*-NiPAAm$_{14}$-*stat*-AAm$_3$-*stat*-HEA$_3$), which showed the highest degree of acrylation, had likely partially crosslinked during preparation of rheological samples. The high complex viscosity values determined for this sample at the beginning of the rheological experiment confirmed this assumption. For the other samples, low complex viscosities below 0.1 Pa•s were determined for the solutions at 15°C and no significant differences were found between the APS containing samples and the control samples (H_2O/TEMED) at 15°C (Fig. III-10B,C). At 37°C, higher complex viscosity values were typically determined for initiated samples (APS/TEMED) compared to the non-initiated controls (Fig. III-10A). During the subsequent time sweep at 37°C, the complex viscosity was monitored for 30 min at 37°C. While the APS/TEMED groups typically maintained the values for complex viscosity during this time, decreasing complex viscosity values due to the thermodynamic instability of the physical gels were recorded for the H_2O/TEMED groups (Fig. III-10A). This result indicates thermally initiated crosslinking of the (meth)acrylated TGMs in the presence of APS/TEMED during the temperature sweep within a few minutes. Based on these findings, that show that physical and chemical crosslinking occurred almost simultaneously, the tested initiator concentration appears high. If slower crosslinking

kinetics are desired to achieve successive thermogelation and chemical crosslinking, a lower initiator concentration would be recommended. Comparison of the complex viscosities after 30 min at 37°C revealed a significant difference between the crosslinked macromers and the physically gelled systems. The viscosities determined for the highly acrylated poly(PEDAS$_1$-*stat*-NiPAAm$_{15}$-*stat*-AAm$_{3.5}$-*stat*-HEA$_{1.5}$) were comparable to those achieved for poly(PEDAS$_1$-*stat*-NiPAAm$_{14}$-*stat*-AAm$_3$-*stat*-HEA$_3$) acrylated using a low AcCl feed (0.75x). For this polymer higher acrylation rates could be achieved with AcCl feeds of 1.25x and 2.5x (Table III-2), but the viscosity of gels crosslinked from these macromers was decreased likely due to extensive phase separation of these hydrophobic macromers at 37°C (Fig. III-10B). In general, high viscosities were reached by crosslinking the methacrylated macromers but their low transition temperatures significantly impair polymer processing with regard to biomedical applications. Macroscopically, the APS/TEMED systems remained as a coherent hydrogel film on the geometry upon disassembly of the rheometer, while the non-initiated samples resembled a highly viscous liquid (data not shown). The crosslinking density and (meth)acrylate conversion of the crosslinked hydrogels could be determined by total hydrolysis of the gels and subsequent chromatographic analysis [174]. For all experiments, macromer solutions with a concentration of 10% (w/v) have been used. This concentration is comparably low with regard to other injectable hydrogels based on synthetic polymers such as poly(ethylene glycol), which typically range from 20 - 25% [31, 175, 176]. The use of macromer concentrations higher than 10% is expected to yield TGM hydrogels with increased crosslinking densities.

Conclusions

Amphiphilic TGMs with controlled polymer architecture and low molecular weight (~2 - 3.5 kDa) were synthesized from PEDAS, NiPAAm, AAm, and HEA at different compositions and selected macromers were subsequently (meth)acrylated to yield chemically crosslinkable thermogelling materials for biomedical applications. Structure-property correlations for non-modified TGMs were established and the hydrophilic-hydrophobic balance was characterized as an important design criterion to adjust the gelation temperature of TGM solutions and thermodynamic stability of the resulting thermogels. The amphiphilic design was shown to support intermolecular interactions, a property which could improve the mechanical stability of crosslinked TGM-based gels. (Meth)acrylated TGMs were synthesized and the combination of thermogelation and thermally induced chemical crosslinking was shown to improve hydrogel stability. The experiments further suggest that degree of acrylation and hydrophilic-hydrophobic balance of the macromers have to be well-adjusted to yield hydrogels of optimal stability. The synthesis of chemically crosslinkable, thermogelling, and potentially biodegradable macromers was realized and promising macromers for the design of injectable drug and/or cell delivery systems with improved properties and stability are presented.

CHAPTER IV

CYTOCOMPATIBILITY EVALUATION OF THE MACROMERS [▲]

Abstract

The cytocompatibility of amphiphilic, thermoresponsive and chemically crosslinkable macromers was examined *in vitro*. Macromers synthesized from pentaerythritol diacrylate monostearate, *N*–isopropylacrylamide, acrylamide and hydroxyethyl acrylate in different molar ratios and with varying molecular weights and lower critical solution temperatures were evaluated for cytocompatibility with rat fibroblasts. Cell viabilities of over 60% for all and over 80% for most formulations were observed after 24-h incubation with macromers with molecular weights in the range of approximately 1500 to 3000 Da. The chemical modification of the macromers with a (meth)acrylate group was shown to have a time- and dose-dependent effect on cell viability. Uncrosslinked macromers with lower degrees of (meth)acrylation allowed for cell viability of over 60% for up to 6 h. (Meth)acrylated macromers with lower critical solution temperature (LCST) closer to physiological temperature allowed for higher cell viabilities as opposed to those with lower LCST. The data suggest that when the (meth)acrylated macromers are assembled into a physical gel, their cytotoxicity is

[▲] This chapter has been published as follows: L. Klouda, M.C. Hacker, J.D. Kretlow and A.G. Mikos, Cytocompatibility evaluation of amphiphilic, thermally responsive and chemically crosslinkable macromers for in situ forming hydrogels, Biomaterials 30 (2009), 4558-4566

diminished. After gel phase separation, cytotoxicity increased. This study gives information on the parameters that enable viable cell encapsulation for *in situ* forming hydrogel systems.

Introduction

Injectable, *in situ* forming materials represent an attractive option for cellular delivery in tissue engineering. Hydrogels in particular are excellent extracellular matrix equivalents due to their highly hydrated nature [65] and can be delivered in liquid form and then solidify *in situ*. It is highly important that the solidification takes place in a clinically relevant time frame so that the material is localized at the point of interest. The solidification mechanism should be selected as not to cause necrosis to surrounding tissue by excessive heat formation and to be tolerated by encapsulated cells and/or any potentially sensitive molecules that are encapsulated for delivery. Moreover, fast solidification allows for homogeneous cell dispersion within the hydrogel matrix [137, 177-179]. Thermally responsive hydrogels, materials that solidify upon temperature change, form *in situ* in a mild and fast manner, but they often possess insufficient mechanical properties and stability [148]. To circumvent this problem, thermogelling polymers have been modified by the addition of reactive groups that allow for covalent crosslinking. These polymers exhibit physical gelation triggered by temperature increase, followed by an irreversible chemical crosslinking after a Michael-type addition [124, 159, 160] or a photoinitiated polymerization reaction [180].

Our group has recently proposed a type of thermally responsive, chemically crosslinkable macromer for the fabrication of *in situ* forming hydrogels based on *N*-isopropylacrylamide [181]. These macromers employ a hydrophobic core molecule that increases cohesive interactions of polymeric chains, augmenting the mechanical stability of the resulting hydrogel. The addition of a methacrylate or acrylate group enables chemical crosslinking with the use of a biocompatible, water-soluble thermal initiator system. The macromers are designed to exhibit a rapid thermal gelation at temperatures slightly below physiological temperature, followed by a slower chemical crosslinking *in situ*. The advantage of this approach is that fast solidification is achieved in a mild process through thermal gelation, with the subsequent slow chemical crosslinking not requiring high amounts of initiator. The rate of the chemical crosslinking reaction is dependent on the amount of initiator used, and it has been shown that thermal initiator systems are less cytocompatible above a certain concentration [142, 143, 182].

The macromers are synthesized from pentaerythritol diacrylate monostearate, a bifunctional monomer containing a natural fatty acid as hydrophobic chain, *N*–isopropylacrylamide, which provides thermoresponsive properties, acrylamide, a hydrophilic monomer, and hydroxyethyl acrylate, a hydrophilic monomer which provides hydroxyl groups for further chemical modification [181]. The lower critical solution temperature (LCST) of macromer solutions and the resultant gel stability are shown to be a function of the comonomer ratios in the composition and the amphiphilicity of the macromers. As a further step, the modification of the macromers with the addition of a (meth)acrylate group allows for covalent crosslinking of gels with higher stability as compared to physically gelled, uncrosslinked controls.

The scope of this study is to evaluate the *in vitro* cytocompatibility of this type of macromer. Specifically, properties of unmodified macromers such as the molecular weight, the composition and the transition temperature are assessed for their effect on cytocompatibility. After chemical modification, (meth)acrylated macromers are evaluated to determine the optimal variables for viable cell delivery. The degree of modification, the concentration and the effects of acrylation versus methacrylation on cell viability are examined. Furthermore, cell viability is examined at intervals over 24 h in order to determine the length of exposure to (meth)acrylated macromers tolerable by cells.

Materials and Methods

Unmodified thermogelling macromers

Amphiphilic, water-soluble thermogelling macromers (TGMs) were synthesized from pentaerythritol monostearate diacrylate (PEDAS), *N*-isopropylacrylamide (NiPAAm) and varying contents of acrylamide (AAm) and 2-hydroxyethyl acrylate (HEA) via a free radical polymerization reaction as previously described [181]. The macromers were subsequently purified by precipitation in diethyl ether and were characterized by gel permeation chromatography (GPC), proton nuclear magnetic resonance spectroscopy (^{1}H-NMR), rheology and differential scanning calorimetry (DSC) [181]. The structure of the TGMs is illustrated in Figure IV-1. Table IV-1 summarizes the composition of the macromers evaluated in the study, denoted by their molar feed composition, and their respective properties. The number-average molecular

weights ($M_{n)}$ and polydispersity indices (PI) were obtained by GPC for n=3. The lower critical solution temperature (T_η) had been previously determined rheologically as the inflection point of the temperature-complex viscosity curve (n=3).

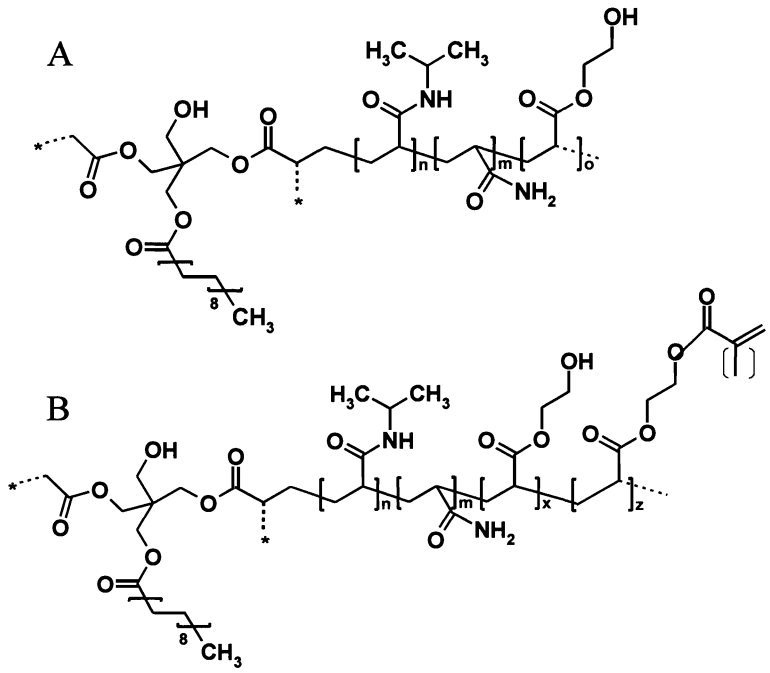

Figure IV-1: Structure of thermogelling macromers (A) before and (B) after modification with the addition of a (meth)acrylate group. The asterisk indicates possible branching sites. The indices m,n,o could equal zero in some formulations. The sum of the modified (z) and unmodified (x) hydroxyl groups equals the initial hydroxyl group number prior to (meth)acrylation (x+z=o).

Table IV-1: Molecular composition, molecular weight characteristics and transition temperature of unmodified thermogelling macromers [a]

Molecular weight group

Molar Composition	M_n [Da]	PI	T_η [°C]
PEDAS/NiPAAm/AAm/HEA			
1/15.4/2.6/2	1750±370	3.4±0.6	31.6±0.3
1/15.4/2.6/2	2300±140	2.9±0.3	32.7±0.8
1/15.4/2.6/2	2440±420	3.0±0.8	32.6±0.2
1/15.4/2.6/2	2830±170	3.6±0.5	31.5±1.2

Composition group

Molar Composition	Acrylic Monomer Ratios (%HEA/%AAm)	M_n [Da]	PI	T_η [°C]
PEDAS/NiPAAm/AAm/HEA				
1/16/0/4	20/0	3050±140	2.9±0.2	23.2±0.1
1/15.4/1/3.6	18/5	3810±260	3.0±0.3	26.5±0.1
1/15.4/2.6/2	10/13	1750±370	3.4±0.6	31.6±0.3
1/14/3/3	15/15	2700±120	2.7±0.1	33.7±0.2
1/16/4/0	0/20	1700±80	2.7±0.1	38.7±3.0

LCST group

Molar Composition	M_n [Da]	PI	T_η [°C]
PEDAS/NiPAAm/AAm/HEA			
1/20/0/0	2560±250	2.7±0.1	27.2±0.2
1/18.5/1.5/0	2450±280	2.6±0.2	30.6±0.4
1/16/4/0	1700±80	2.7±0.1	38.7±3.0
1/16/4/0	1370±100 [b]	2.9±0.1 [b]	40.8±1.4
1/14/6/0	1470±250	6.9±2.1	43.5±2.3

[a] Molecular composition describes the molar feed ratio of monomers as used for polymerization. Molecular weight characteristics were obtained by gel permeation chromatography. The transition temperature T_η was determined from rheological measurements of 10% (w/v) macromer solutions as the inflection point of the temperature-complex viscosity curve. Values represent means ± standard deviation for a sample size of n=3.[b] The average and range for this formulation were determined for n=2. Table is adapted from [181] with permission.

Cell culture

A rat fibroblast cell line (ATCC, CRL-1764) was cultured on T-75 flasks using Dulbecco's modified Eagle medium (DMEM; Gibco Life, Grand Island, NY) supplemented with 10% (v/v) fetal bovine serum (FBS; Cambrex BioScience, Walkersville, MD) and 1% (v/v) antibiotics containing penicillin, streptomycin and amphotericin (Gibco Life). Cells were cultured in a humidified incubator at 37 °C and 5% CO_2. Cells of passage numbers 7-9 were used in this study.

Cytocompatibility assays of unmodified thermogelling macromers

Leachables assay

Solutions of thermogelling macromers were prepared at a 10% (w/v) concentration in cell culture media (DMEM, supplemented with antibiotics) without the addition of serum. The solutions were left on a shaker table overnight to dissolve. In the case of macromer solutions with LCST below room temperature, the solutions were left to dissolve at a temperature of 4°C. After dissolution, macromer solutions were incubated at 37°C for 24 h. During this time interval, the solutions first gel and subsequently phase-separate and collapse. After 24 h in the incubator, the supernatant of the macromer solutions was aspirated, sterile-filtered through a Nalgene 0.2 μm filter (Nalge, Rochester, NY) and diluted 10 times in cell culture media. Cells were seeded on a 96-well plate at a density of 28,300 cells/cm^2 using a working volume of 100 μL cell suspension per well. The cells were incubated for 24 hours to achieve 80-90% confluence and were then exposed to 100 μL of the solution supernatant. Two experimental groups

were used, one without and one with 10-fold dilution (n=5). Following 24 h of incubation, the macromer-conditioned media were removed, and the cells were rinsed three times with phosphate-buffered saline (PBS, Gibco), followed by the addition of calcein AM and ethidium homodimer-1 in 2 μM and 4 μM concentrations in PBS, respectively (Live/Dead viability/cytoxicity kit, Molecular Probes, Eugene, OR). The cells were incubated with the Live/Dead reagents for 30 min in the dark at room temperature. Cell viability was quantified using a fluorescence plate reader (Biotek Instrument FLx800, Winooski, VT) equipped with filter sets of 485/528 nm (excitation/emission) for calcein AM (live cells) and 528/620 nm (excitation/emission) for EthD-1 (dead cells). Untreated cells that were cultured with primary media only served as the positive (live) control, whereas cells exposed to 70% ethanol for 15 min served as the negative (dead) control. The fluorescence of the cell populations was recorded and the fractions of live and dead cells were calculated relatively to the controls as previously described [142]. Following quantification, images of the cells were obtained with a fluorescence microscope (LSM 510 META, Carl Zeiss, Germany).

Direct contact assay

The macromers were vacuum-dried and sterilized under UV irradiation for 3 h. Macromer solutions were prepared in 10% (w/v) concentration in DMEM without FBS as described above. Cells were seeded on 48-well plates at a seeding density of 28,300 cells/ cm^2 with a working volume of 500 μL cell suspension per well. After 24-h incubation, the media were aspirated and 150 μL of macromer solution was added to the cells (n=4-5). This quantity was calculated so that after gelation, a thin gel film would form above the cells. After 30-minute incubation at 37 °C to ensure gel formation, 300 μL DMEM

without FBS was carefully added on top of the gel and the cells were incubated with the macromers for 24 h. Following this incubation period, the gel pellet was carefully removed with tweezers at room temperature, and cells were rinsed three times with PBS before adding the Live/Dead reagents and evaluating cell viability as described above.

Modified (acrylated and methacrylated) thermogelling macromers

In order to add chemically crosslinkable domains, the purified macromers were modified with the addition of an acrylate or methacrylate group through a reaction between the hydroxyl group of 2-hydroxyethyl acrylate (HEA) and (meth)acryloyl chloride. The hydroxyl group on PEDAS was not modified during this reaction. The reaction, purification and characterization processes were performed as previously described by Hacker et al. [181]. The structure of modified macromers can be seen in Figure IV-1. Macromers with varying acrylate or methacrylate group contents were synthesized by feeding different volumes of acryloyl chloride or methacryloyl chloride respectively. Due to the lower reactivity of methacryloyl chloride, different hydroxyl conversions were observed in comparison to formulations that were supplied with an equivalent amount of acryloyl chloride. Table IV-2 denotes the composition of the modified TGMs and the conversion of the hydroxyls to (meth)acrylate groups as determined by ^{1}H-NMR. The thermal transition temperatures are also included in Table IV-2, as the substitution of the hydroxyl group of HEA by the more hydrophobic (meth)acrylate moieties has an effect on the lower critical solution temperature of these macromers. LCST was previously obtained by differential scanning calorimetry for n=3.

Table IV-2: Acrylated and methacrylated thermogelling macromers with varying degrees of modification and their transition temperatures [c]

Molar Composition: PEDAS/NiPAAm/AAm/HEA = 1/15/3.5/1.5

Modification	**% of hydroxyls modified**	**T_{DSC} [°C]**
No modification	0	35.6 ± 0.5
Acrylation	8	31.2 ± 0.2
Acrylation	32	24.6 ± 0.3
Acrylation	49	20.8 ± 0.9
Methacrylation	10	24.1 ± 0.6
Methacrylation	29	15.2 ± 0.9

[c] The degree of hydroxyl group conversion was determined by ^{1}H-NMR. The transition temperature T_{DSC} was obtained by differential scanning calorimetry (DSC) for 10% (w/v) macromer solutions. Values represent means ± standard deviation for a sample size of n=3. Table is adapted from [181] with permission.

Cytocompatibility of modified (acrylated and methacrylated) thermogelling macromers

The macromers were vacuum-dried and sterilized under UV irradiation for 3 h. Macromer solutions were prepared in 10, 1 and 0.1% (w/v) concentrations in DMEM without FBS as described above, which will be denoted throughout the text also as 100, 10 and 1 mg/mL respectively. Cells were seeded on 96-well plates at a seeding density of 28,300 cells/cm^2. After 24-h incubation, the media were aspirated. For the 1 and 0.1% solutions, 100 µL of macromer solution was added to the cells. These concentrations

showed minimal gel formation at 37°C and therefore the addition of media for nutrient supply was not required. For the 10% solutions, 40 μL of macromer solution was applied, followed by 30-min incubation at 37°C to ensure gel formation, and 60 μL DMEM without FBS was carefully added on top of the gel. For all groups, a sample size of five was used (n=5). Cell viability was evaluated after 2, 6 and 24-hour incubation using the Live/Dead assay as described above.

Osmolality measurements

The osmolality of the solutions was measured with an Osmette automatic osmometer (Precision Systems, Natick, MA). In order to create a standard curve for cell viability versus osmolality of solution, the osmolalities of dextran (average molecular weight 68.8 kDa, Sigma, St. Louis, MO) solutions in concentrations from 0 to 30% (w/v) in DMEM were measured. Cells were then incubated with dextran solutions in that concentration range for 24 h, and their viability was recorded. Dextran was chosen because it is a known biocompatible polysaccharide and thus in case any toxic effects were observed, they would be due to changes in osmolality of the solution and not molecular composition.

The osmolality of the 10% (w/v) macromer solutions as used in the study was measured. Moreover, the osmolality of the supernatant solutions was measured. The supernatant was obtained after incubating the macromer solutions for 24 h at 37°C and following gel phase separation in order to simulate the properties of the solutions to which cells are exposed during the direct contact assay.

Statistical analysis

Statistical analysis of the data was performed with a single-factor analysis of variance (ANOVA) with a 95% confidence interval ($p<0.05$). In the case of statistically significant differences, Tukey's post hoc test was conducted. Data are expressed as mean ± standard deviation.

Results

Effect of molecular weight on unmodified macromer cytocompatibility

Viability of over 80% was observed for cells incubated with the supernatant of hydrogels composed of macromers with number-average weights ranging from 1750 to 2830 Da and polydispersity indices from 2.9 to 3.6 (Figure IV-2A). In this experimental group, no statistically significant differences were found between undiluted and 10-fold diluted samples. For the direct contact assay, viabilities of above 80% were found for the lower molecular weight groups (Figure IV-2B). The higher molecular weight group showed cell viability of 69±3 %.

Effect of composition on unmodified macromer cytocompatibility

Cells incubated with hydrogel supernatant showed high viabilities (above 75%) for all but one formulation, with a decrease in live cells with increasing acrylamide content in the composition (Figure IV-3A). The formulation with the highest acrylamide content in the composition (20%) and no 2-hydroxyethyl acrylate showed lower viability

values of 55±2%. No statistically significant difference was noted between undiluted and 10-fold diluted supernatant. When cells were exposed to the thermogelling macromers in a direct contact assay, cell survival was above 80% (Figure IV-3B).

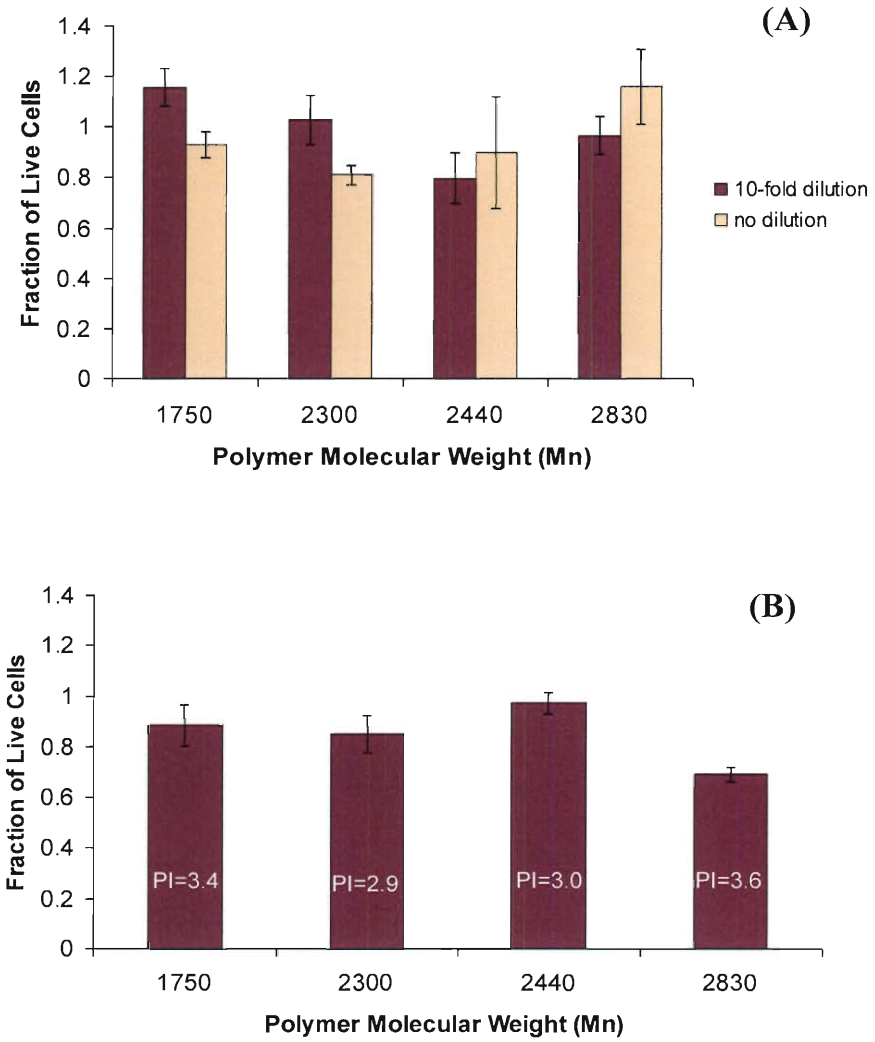

Figure IV-2: Cell viability after 24-h incubation with macromers of different number-average molecular weights and polydispersity indices (PI). A) Leachables assay: incubation with hydrogel supernatant B) Direct contact assay: incubation with hydrogel. Error bars represent standard deviation; n= 3-5.

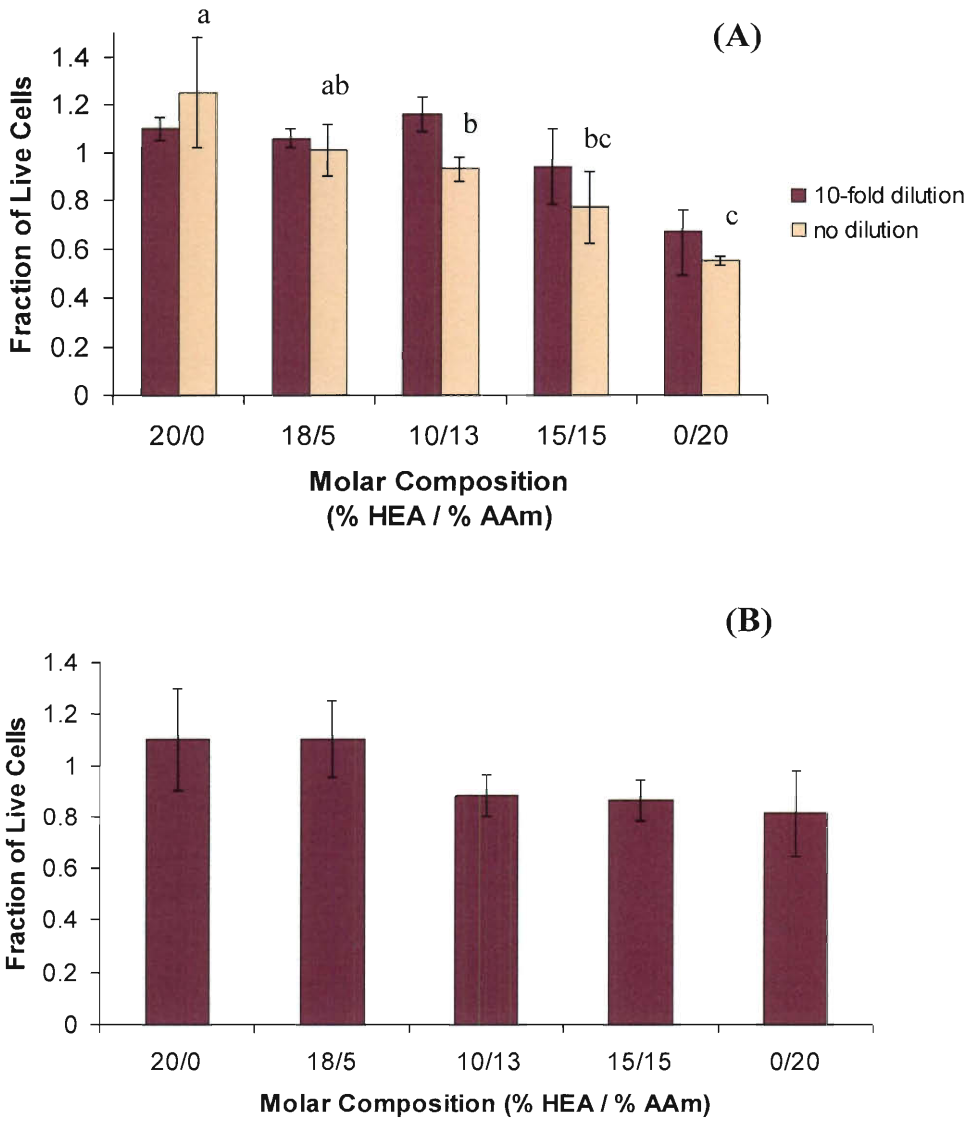

Figure IV-3: Cell viability after 24-h incubation with macromers of different molecular ratios of HEA and AAm. A) Leachables assay and B) Direct contact assay. Error bars represent standard deviation; n= 3-5. Characters on experimental groups indicate statistically significant differences when groups are not marked with the same letter ($p<0.05$). For clarity purposes, in figure (A) differences are marked for undiluted group only.

Effect of LCST on unmodified macromer cytocompatibility

Among the formulations tested, lower cell viability was observed for the formulations with transition temperatures of 38.7 and 40.8 °C, both in the leachables (55±2% and 61±5% respectively) as well as in the direct contact assay (81±19% and 60±22%) (Figure IV-4). Macromer solutions with lower or higher transition temperatures than the aforementioned showed viabilities of 70% or more for their leachable components and the direct contact assay. Characteristic fluorescence microscopy images of the cells after incubation with these macromers can be seen in Figure IV-5. High densities of live cells (stained green) with morphology similar to the positive control were observed for most formulations, and no obvious damage to cells that were in direct contact with the hydrogel was noted. The composition with an LCST of 40.8 °C (molecular composition $PEDAS_1NiPAAm_{16}AAm_4$) showed an increased number of dead cells (stained red).

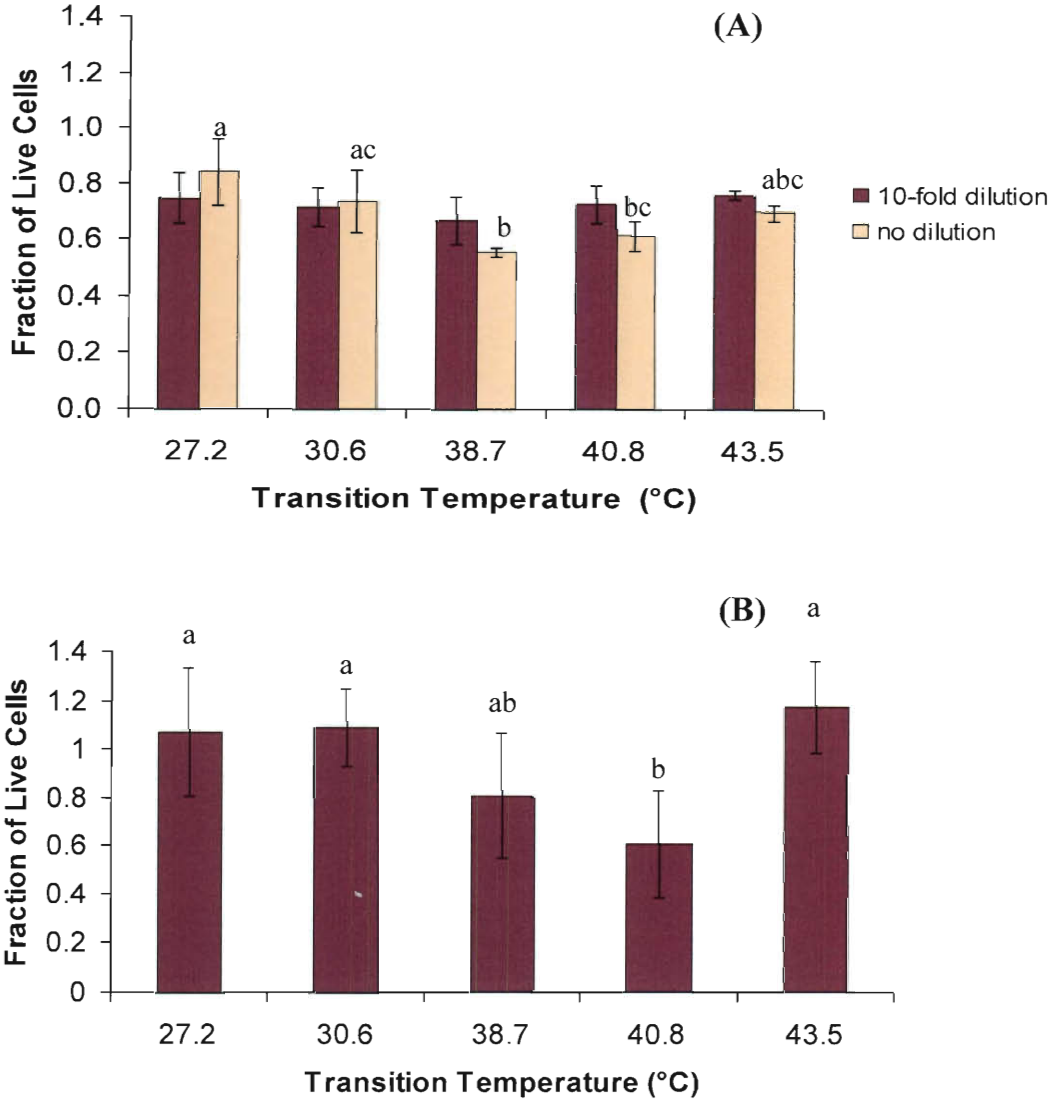

Figure IV-4: Cell viability after 24-h incubation with macromers of different transition temperatures (T_n). A) Leachables assay: incubation with hydrogel supernatant B) Direct contact assay: incubation with hydrogel. Error bars represent standard deviation; n= 5. Experimental groups denoted by different letters show statistically significant differences ($p<0.05$). For clarity purposes, in figure (A) differences are marked for undiluted group only.

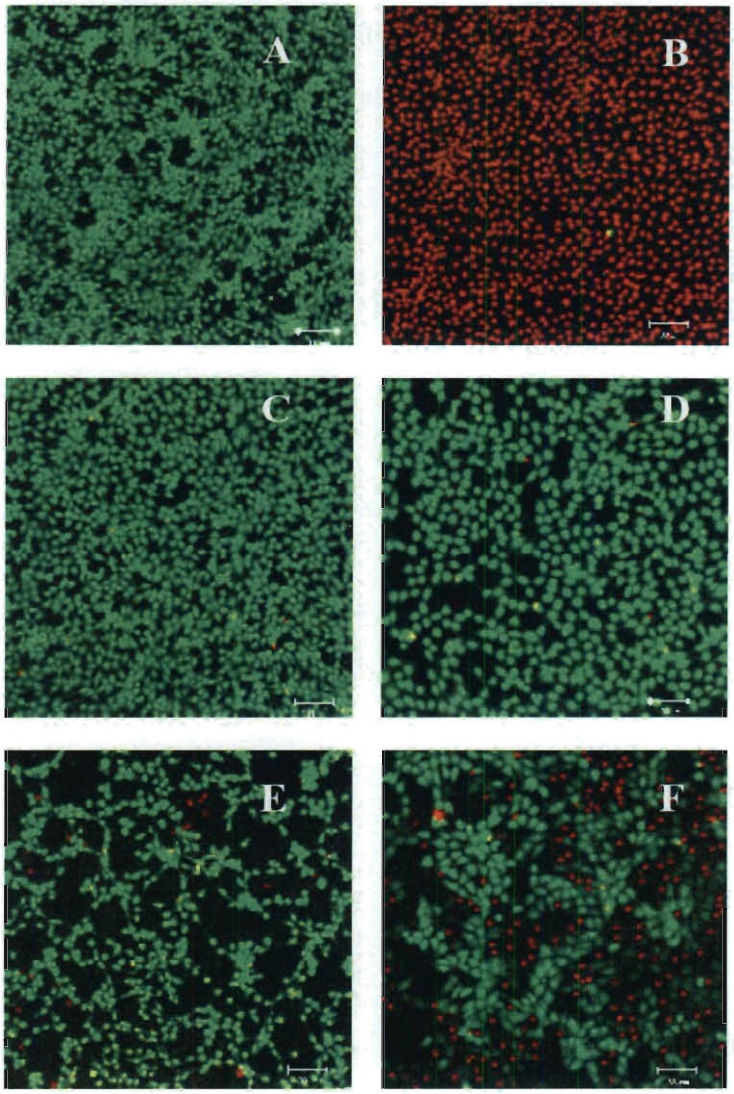

Figure IV-5: Fluorescence microscopy images of fibroblasts after 24-h exposure to hydrogel leachables or in direct contact with hydrogel and treatment with Live/Dead reagent. (A) positive control, (B) negative control, (C) treatment with a formulation composed of $PEDAS_1NiPAAm_{20}$ in leachables assay (C) and direct contact (D), treatment with a formulation composed of $PEDAS_1NiPAAm_{16}AAm_4$ in polymer-conditioned media (E) and direct contact (F). Scale bars indicate 100 μm.

Effect of macromer solution osmolality on cytocompatibility

Cell viability showed a decreasing trend after 24-h incubation with increasing osmolalities of dextran solutions in various concentrations; differences, however, were not statistically significant (Figure IV-6). For a solution osmolality of 451 mOsm/kg, cell viability was 85±7%. Thermogelling macromer solutions in 1% (w/v) concentration in cell culture media showed similar osmolalities to that of DMEM (330 mOsm/kg). Solutions of 10% (w/v) concentration had osmolalities on the order of 406-462 mOsm/kg. The supernatant of gels after 24-h incubation at 37 °C and full phase separation showed even lower values (340-408 mOsm/kg).

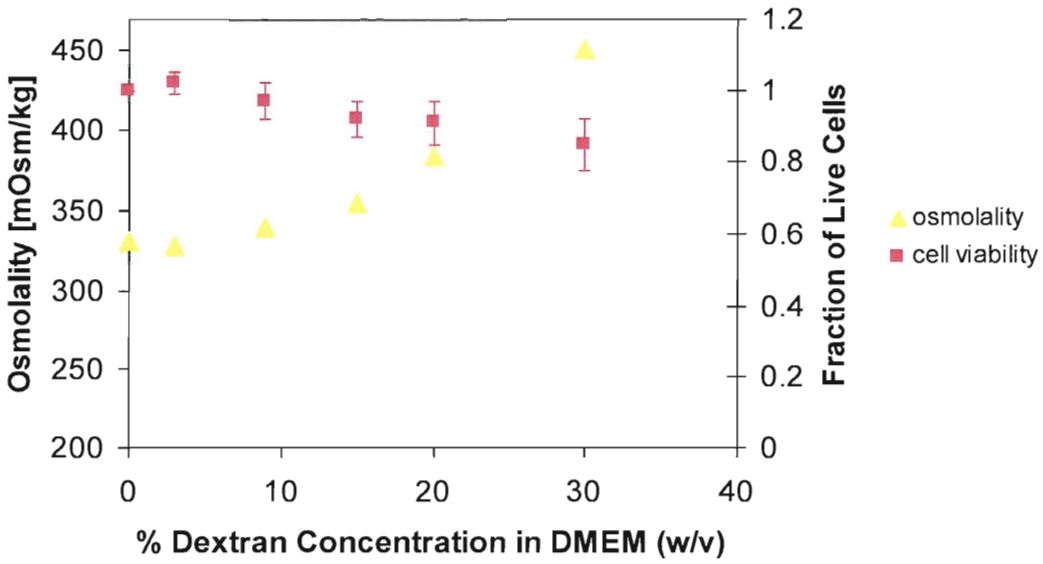

Figure IV-6: Osmolality of dextran solutions of different concentrations and cell viability values after 24-h incubation with these solutions. Differences in cytocompatibility are not statistically significant ($p<0.05$).

Cytocompatibility of (meth)acrylated thermogelling macromers

Effect of macromer concentration

At the 2 h time interval, most formulations had similar cell viabilities in 1, 10 and 100 mg/mL concentrations or showed trends of decreasing viability (Figure IV-7). A formulation with a 32% degree of acrylation showed values of 0.95±0.09, 0.71±0.08 and 0.68±0.10 at 1, 10 and 100 mg/mL respectively. A formulation with a 49% acrylation had cell viabilities of 1.23±0.06, 0.99±0.05 and 0.12±0.01 at the above concentrations. The effect of concentration was even more pronounced with decreasing trends in viability at the 6- and 24-h intervals. At 24 h, the cell viabilities for the 32% acrylated formulation decreased from 0.75±0.02 at the 1 mg/mL concentration to 0.16±0.05 at 100 mg/mL.

Effect of time

In addition to the aforementioned results, the effect of incubation time on cell viability can be seen in Figure IV-8 for a concentration of 100 mg/mL. An unmodified composition showed a statistically significant decrease in viability at 6 h. The fraction of live cells at 24 h was 0.61±0.05, which did not change from the viability at 6 h. For all acrylated formulations, a statistically significant decrease in viability was observed after 24 h. At 6 h, the compositions with lower degrees of acrylation showed cell viabilities of 60% and higher. A composition with low methacrylation also showed a statistically significant decrease in cytocompatibility at 24 h, whereas the macromers with higher methacrylation exhibited high toxicity as soon as 6 h after incubation.

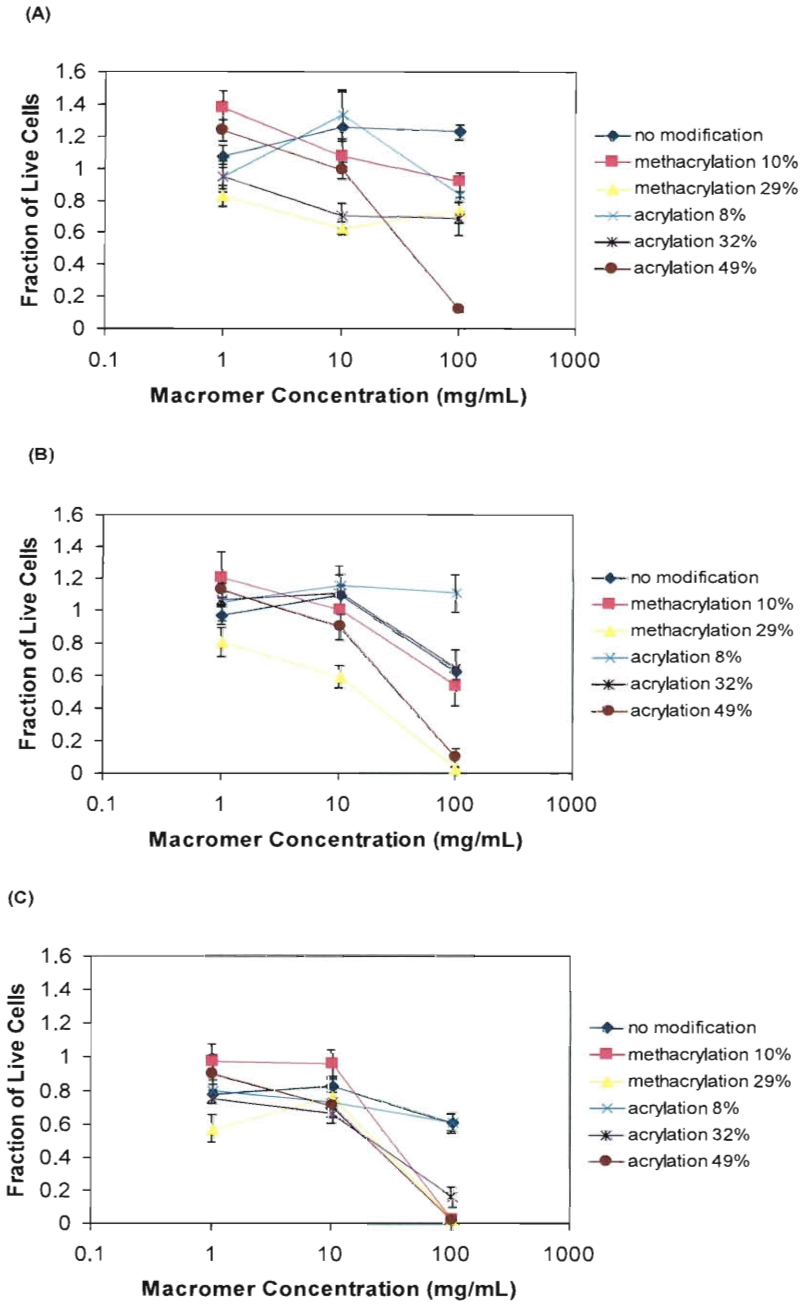

Figure IV-7: Cell viability after (A) 2-h, (B) 6-h and (C) 24-h incubation with various concentrations of (meth)acrylated macromers with a theoretical composition of $PEDAS_1$-$NiPAAm_{15}$-$AAm_{3.5}$-$HEA_{1.5}$. Error bars represent standard deviation for n=3-5.

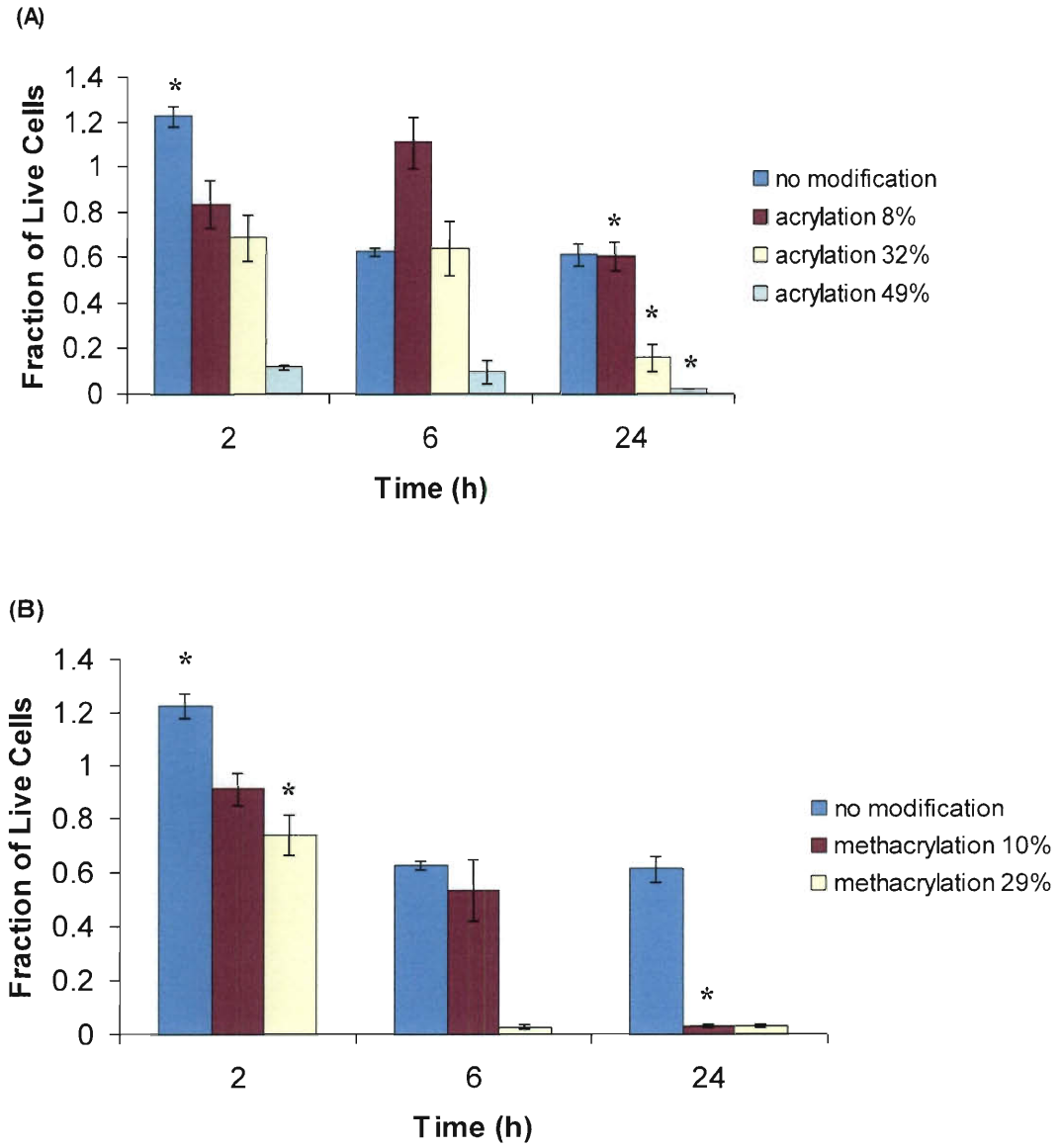

Figure IV-8: Cell viability over time after exposure to 100 mg/mL solutions of (A) acrylated and (B) methacrylated macromers, with an unmodified composition as a control. Error bars represent standard deviation for n=3-5. Statistically significant differences over time within one composition group are marked with an asterisk ($p<0.05$).

Effect of modification

The macromers were rendered less cytocompatible with increasing degrees of modification. Figure IV-9 depicts cell viability after 24-h incubation with 100 mg/mL macromer solutions. Unmodified macromers showed a viability of 61±5%, which was very similar for macromers with 8% acrylation. For macromers with higher acrylation degrees of 32% and 49%, only 16±6% and 2±1% of the cells respectively were viable after 24 h. Methacrylation seemed to be less tolerable by the cells from these results. After 24-h incubation, cell viability was only 3±1% for both formulations, which had methacrylation degrees of 10% and 29%, respectively.

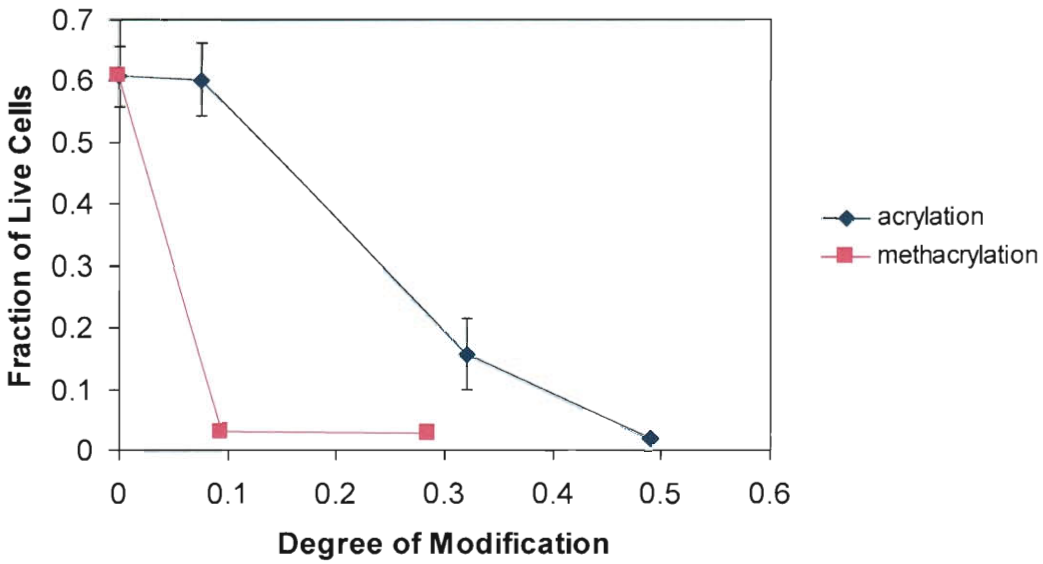

Figure IV-9: Cell viability after 24-h incubation with 100 mg/mL solutions of acrylated and methacrylated macromers with different degrees of modification. Modification is expressed as the fraction of hydroxyl moieties substituted by (meth)acrylate groups. Error bars represent standard deviation for n=3-5.

Discussion

The effects of molecular weight, monomer ratios in the composition and solution thermal transition temperature were the parameters investigated for their effect on macromer cytocompatibility. A second set of studies examines the cytocompatibility of the macromers after the addition of a reactive (meth)acrylate group over time and for different compositions and concentrations. Although these macromers can be physically gelled and chemically crosslinked, all experiments were performed with the non-crosslinked macromers to evaluate toxicity of the reactive groups and macromer composition, mainly hydrophilic-hydrophobic balance.

Cytocompatibility of unmodified thermogelling macromers

Macromer molecular weight is a factor that influences the compatibility of hydrogels with cells. Low-molecular weight oligomers are often associated with toxicity issues in hydrogels [65]. Generally, hydrogels for cell encapsulation are fabricated with macromers of molecular weights above 3000 Da [183], as they otherwise may enter the cell. No adverse effects of thermogelling macromers with the same composition but various molecular weights, ranging from 1750 to 2830 Da, were observed on cell viability. Cell viability was over 80% for most formulations, both in the leachables as well as in the direct contact assay.

As for the macromer composition, it had been shown [181] that increasing acrylamide contents correlates with higher transition temperatures of the macromer solutions (Table IV-1). Therefore, whether the decreasing cytocompatibility observed

with increasing acrylamide in the formulation was an effect of LCST rather than composition had to be evaluated. Macromers with transition temperatures higher than the incubation temperature stay in solution or show minimal gel formation as opposed to those with transition temperatures close to physiological temperature which gel rapidly at 37 °C. The experimental data showed a decrease in cell viability for the macromer solutions with transition temperatures close to physiological. Interestingly, a macromer solution with a transition temperature of 43.5 °C, which did not gel after 24-h incubation at 37 °C, allowed for cell viability of over 70%, whereas solutions with transition temperatures significantly lower than physiological temperature showed similar cell survival values. The differences in the relative amphiphilicity may explain these observations. The lower critical phase separation phenomenon is imparted by hydrophobic interactions between macromolecular chains [184]. For macromers with an LCST below the incubation temperature of 37°C, associations between polymer chains were more pronounced, leading to gel formation. On the other hand, an increase in the hydrophilicity of the macromers facilitated polymer-water interactions, not allowing gel formation at this temperature. This hydrophilic structure, as suggested by the viability data, caused minimal interactions with the cells. The macromers with transition temperatures around physiological temperature exhibited such a hydrophilic/hydrophobic balance at 37°C that might have caused increasing interactions with the cell membrane and could explain the lower cell viability values observed.

Another possible source of toxicity evaluated, solution osmolality, does not seem to be a contributing factor in these studies. Cells would be first exposed to the macromer solution until the gelation takes place and later to the supernatant solution after gel

syneresis. Even though high osmotic stress has been shown to suppress growth [185] and induce apoptosis [186] in mammalian cells, the osmolality of solutions was within the range tolerable by cells as suggested the dextran osmolality-cell viability curve (Figure IV-6). This is in accordance with the observations of Zhu et al.[187], where viable density of CHO cells showed an 8% decrease for a solution osmolality of 460-500 mOsm/kg.

Cytocompatibility of modified thermogelling macromers

Some of the macromer solutions were too viscous for sterilization by filtration. Therefore, the macromers were dried in a vacuum oven and sterilized under UV irradiation for 3 h. The presence of the olefinic protons was confirmed by ^{1}H-NMR, indicating that after UV irradiation the structure of the (meth)acrylated macromers was preserved (data not shown). The macromers selected for (meth)acrylation were chosen based on their amphiphilic character and lower critical solution properties, and their molecular composition prior to modification was found to be cytocompatible. The parameters tested in this study were concentration, time, degree of modification and modification type (acrylation or methacrylation) on their effect on cytocompatibility. It is valuable to obtain correlations between cell viability, concentration and chemical structure of the macromers as a function of time if the hydrogel is used for cell encapsulation, as cells will be in direct contact with the macromer chains until the crosslinking of the hydrogel is completed [143].

Exposure to (meth)acrylated macromers was shown to have a dose-dependent effect on cell viability (Figure IV-7). This effect was more pronounced with higher

modification and after longer exposure. The cytotoxicity of hydrogel-forming macromers is often reported in concentrations of up to 1 mg/mL in cell culture media [188, 189]. We have opted to evaluate higher concentrations relevant for hydrogel fabrication. In this study, when the direct contact assay was performed, cell culture medium was added on top of the hydrogel layer after its solidification. In the course of the 24-h incubation, the hydrogel was phase-separated, which means that the addition of medium diluted down the supernatant solution. This step was however required to ensure nutrient delivery to the cells. Solutions of lower concentrations did not show significant gel formation, and no additional media were added. The cytotoxicity of the macromers showed also a time-dependent behavior (Figure IV-8). Acrylated macromers all showed statistically significant higher cytotoxicity at the 24 h time interval compared to 2 and 6-h exposure. The same correlation was observed for the methacrylated macromers with lower modification. Macromers with a higher degree of methacrylation showed significantly higher toxicity already after 6-h incubation compared to 2 h. This study seems to be a good indicator for determining the kinetics of the crosslinking reaction by establishing the tolerable time of exposure of cells to the (meth)acrylated macromers. It represents the worst-case scenario, since within the time frame examined, chains would have already started to crosslink with the addition of an initiator system. After crosslinking is completed, the detrimental effects of the (meth)acrylate end groups should be eliminated. The presence of reactive end groups, such as the (meth)acrylate groups, contributes to the toxicity of materials. Increasing degrees of modification drastically reduce cell viability, as can be seen in Figure IV-9.

To the best of our knowledge, there are only a few studies that investigate the cytocompatibility of (meth)acrylated, uncrosslinked macromers. Crosslinking molecules such as poly(ethylene glycol) diacrylate (PEG-DA-575 Da) [143] and hydrophobic propylene fumarate diacrylate [190] were found to be very toxic on cells, whereas higher molecular weight macromers such as dextran derivatized with methacrylate- and hydroxyethyl methacrylate groups [191] and PEG-DA (molecular weight 3.4 kDa) [143] showed more cytocompatible results. Many studies have been carried out to elucidate the cytotoxic effects of acrylic and methacrylic monomers. In general, acrylic monomers have been reported to be more toxic than their methacrylic analogues [192, 193]. Some researchers suggested that toxicity correlates with monomer lipophilicity, and that cytotoxic effects of (meth)acrylates are exerted through reacting with and disrupting the lipid bilayer in cell membranes [194, 195]. Other researchers identified a mechanism involving the covalent binding of electrophilic reactive (meth)acrylates to cellular targets such as thiol groups on proteins through a Michael-type reaction [196, 197]. In the present case, we found acrylated macromers to be more cytotoxic than methacrylated ones after 2-h incubation, but after 24 hours, this phenomenon seemed to have reversed. Figure IV-10 shows the fraction of live cells at 2 and 24 hours as a function of transition temperature of the macromer solutions. Our previous studies [181] showed that the hydrogel stability at 37°C is proportional to the LCST of the macromer solutions, and hydrogels fabricated of macromers with low LCST tend to phase-separate and precipitate faster. This offers an explanation for the higher toxicity observed for methacrylates as compared to acrylates with the same degree of modification after 24-h incubation. At 2 hours, the gels are still stable, but the precipitation over the 24-h time interval happens sooner for

macromers with lower transition temperatures, as in the case of methacrylates. This effect prolongs the period in which non-gelled, (meth)acrylated, reactive macromer chains interact directly with structures of the cells, such as membranes, as opposed to chains that are fully assembled into a gel, thus enhancing their toxic action over 24 hours. The results suggest that when (meth)acrylates form a gel, their cytotoxic effects are diminished. Macromer toxicity seems to be associated with their soluble form, or in this specific case, precipitated, and not when the macromolecular chains are assembled in a physical network.

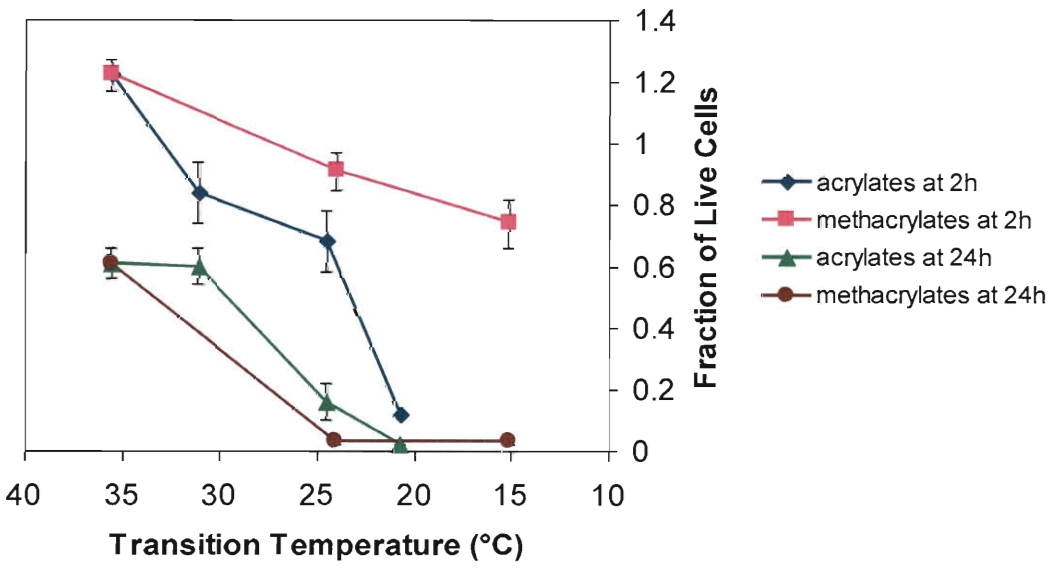

Figure IV-10: Cell viability after 2 and 24-h incubation with 100 mg/mL solutions of acrylated and methacrylated macromers as a function of their thermal transition temperature. Error bars represent standard deviation for n=3-5.

Conclusions

This study demonstrated the good cytocompatibility properties of thermally responsive, chemically crosslinkable macromers. It was found that unmodified macromers with number-average molecular weights in the range of approximately 1500 to 3000 Da with varying molecular compositions allowed for high cell viability over a 24-h time interval. The chemical modification with an acrylate or methacrylate group enables the chemical crosslinking of the macromers. We investigated the effect of the (meth)acrylate derivatization on the toxicity of uncrosslinked macromers and determined that a 6-h time frame for crosslinking completion would allow for viable cell encapsulation. Increased degrees of modification were shown to decrease the thermal transition temperature as well as the cytocompatibility of the macromers. Formulations with the parameters established in this study will be used towards the fabrication of injectable, thermoresponsive, *in situ* forming hydrogel systems for cell and drug delivery.

CHAPTER V

HYDROGEL FABRICATION, CHARACTERIZATION AND MESENCHYMAL STEM CELL ENCAPSULATION ✧

Abstract

Hydrogels that solidify in response to a dual, physical and chemical, mechanism upon temperature increase were fabricated and characterized. The hydrogels were based on *N*-isopropylacrylamide, which renders them thermoresponsive, and contained covalently crosslinkable moieties in the macromers. The effects of the macromer end group, namely acrylate or methacrylate, and the fabrication conditions were investigated on the degradative and swelling properties of the hydrogels. The hydrogels exhibited higher swelling below their lower critical solution temperature (LCST). When immersed in cell culture media at physiological temperature, which was above their LCST, hydrogels showed constant swelling and no degradation over eight weeks, with methacrylated hydrogels having higher swelling than their acrylated analogs. In addition, hydrogels immersed in cell culture media under the same conditions showed lower swelling as compared to phosphate buffered saline. The interplay between chemical crosslinking and thermally induced phase separation affected the swelling characteristics

---

✧ This chapter was submitted for publication to Acta Biomaterialia as: L. Klouda, K.R. Perkins, B.M. Watson, M.C. Hacker, S.J. Bryant, R.M. Raphael, F.K. Kasper and A.G. Mikos, Thermoresponsive, *in situ* crosslinkable hydrogels based on *N*-isopropylacrylamide: Fabrication, characterization and mesenchymal stem cell encapsulation.

of hydrogels in different media. Mesenchymal stem cells encapsulated in the hydrogels *in vitro* were viable over three weeks and markers of osteogenic differentiation were detected when the cells were cultured with osteogenic supplements. Hydrogel mineralization in the absence of cells was observed in cell culture medium with the addition of fetal bovine serum and β-glycerol phosphate. The results suggest that these hydrogels may be suitable as carriers for cell delivery in tissue engineering.

Introduction

Thermally responsive hydrogels have attracted much research interest over the past years for their use in biomedical applications [73, 74, 148]. They have been reported in drug delivery [198, 199], cell sheet tissue engineering [200], biosensors [201], myocardial injection therapy [202] and cell delivery [155, 180, 203]. Thermoresponsive systems use temperature as a stimulus to allow for solidification and changes in swelling. This is beneficial for the above mentioned functions, as the temperature change from ambient to physiological can be employed. Advantages of thermoresponsive hydrogels include a fast gelation once the transition temperature is reached, and a mild solidification process without the need for a chemical initiator system. Many natural and synthetic polymers exhibit thermoresponsive hydrogel characteristics, and among those, polymers based on poly(*N*-isopropylacrylamide) (pNiPAAm) belong to some of the most widely investigated systems. The homopolymer pNiPAAm has a transition temperature around 32°C, which can be tuned when copolymerized with more hydrophilic or hydrophobic monomers [69] and allows for a transition temperature that can be close to physiological. A problem

associated with linear pNiPAAm is the extensive collapse of the gel at 37°C. One strategy to improve the stability and mechanical properties of pNiPAAm-based hydrogels is the modification of the polymer with functional groups that enable covalent crosslinking. Systems that gel with temperature increase to physiological and can form chemical crosslinks upon a Michael-addition reaction have been recently proposed [159, 160, 204, 205].

Our group has previously reported the synthesis and characterization of macromers for the fabrication of hydrogels that can form *in situ* with two independent, physical and chemical, solidification mechanisms [181]. The thermoresponsive properties of the macromers are imparted by *N*–isopropylacrylamide, and additional comonomers include pentaerythritol diacrylate monostearate, acrylamide and hydroxyethyl acrylate. The latter monomer contains hydroxyl groups that can be modified towards acrylate or methacrylate moieties. These moieties can be covalently crosslinked with the addition of a water-soluble, thermal free-radical initiator system. Increased stability and higher viscosity values could be achieved when the hydrogels were physically and chemically gelled as opposed to only thermally gelled controls. The *in vitro* cytocompatibility of the macromers has been previously evaluated with favorable results. Parameters, such as crosslinking time, that allow for high viability of encapsulated cells during hydrogel formation have been established [206].

The objective of the present study is the fabrication and characterization of thermally responsive and chemically crosslinkable hydrogels that form upon temperature increase to physiological. The ultimate goal of this work is the application of hydrogels for cell delivery in craniofacial bone tissue engineering. The potential of these hydrogels

towards this aim in terms of hydrogel properties, cell encapsulation and mineralization are investigated. More specifically, we examine the effect of macromer end group (acrylate or methacrylate) on the swelling and degradation of the hydrogels. The resulting effects of these properties on encapsulated mesenchymal stem cell viability and osteogenic differentiation are evaluated.

Materials and Methods

Macromer synthesis and characterization

Thermally gelling macromers were synthesized from pentaerythritol diacrylate monostearate (PEDAS), *N*-isopropylacrylamide (NiPAAm), acrylamide (AAm) and 2-hydroxyethyl acrylate (HEA) in a 1:14:3:3 molar ratio via free-radical polymerization reaction as previously described [181]. Subsequently, the free hydroxyls of the HEA were modified with an acrylate or methacrylate group through a reaction with acryloyl or methacryloyl chloride, respectively, and characterization followed with established methods [181]. Formulations that contained 1.3 acrylate or methacrylate groups per chain as determined by ^{1}H-NMR were used for these studies unless otherwise noted.

Hydrogel fabrication

Methacrylated macromer solutions were prepared in phosphate buffered saline (PBS, pH=7.4, Gibco Life, Grand Island, NY) in a concentration of 10% (w/v). Ammonium persulfate (APS) and *N,N,N',N'*-tetramethylethylenediamine (TEMED) (Sigma-Aldrich, St. Louis, MO) were used as free-radical initiators for the chemical

crosslinking of the macromers. Stock solutions of the initiator system in double distilled (dd) water were added to the macromer solution in different concentrations resulting in final APS/TEMED concentrations of 10, 15 and 20 mM. The mixture was gently agitated and quickly pipeted into Teflon molds (6 mm in diameter, 3 mm in height). The hydrogels were then formed at 37°C inside a cell culture incubator over 10, 20 or 30 min. After fabrication, hydrogels were blotted dry, weighed (W_f) and placed in dd water at 37°C for one day. Gels were removed from the water, carefully blotted and the wet mass was obtained (W_s). The hydrogels were dried overnight in a lyophilizer and weighed (W_d). Sol fraction is calculated as (W_f - W_d)/ W_f. Swelling ratio is calculated as (W_s – W_d)/ W_d.

Hydrogel swelling below and above the LCST

Hydrogels were fabricated using APS/TEMED in a 20 mM concentration and 30-min incubation at 37°C. Hydrogels were weighed after fabrication, swollen in dd water at 4°C for 20h, blotted and weighed. Subsequently, they were immersed in dd water at 37°C for 20h. The wet mass was obtained after careful blotting and gels were finally dried and weighed. Swelling ratio was calculated as outlined above.

Hydrogel degradation and swelling in cell culture medium and PBS

Hydrogel samples were prepared as described below for cell encapsulation but with the addition of PBS instead of cell suspension. The gels were immersed in complete osteogenic media or PBS in an incubator at 37°C over 8 weeks. Samples were removed at

1h, 1, 7, 14, 21, 28 and 56d and sol fraction and swelling ratio were calculated. Additionally, samples immersed in media were prepared and saved as controls for the biochemical assays as follows below.

Rat mesenchymal stem cell (MSC) isolation and preculture

Cells were harvested from the marrow of the femora and tibiae of male 6-8 week old Fischer 344 rats (Charles River Laboratories, Wilmington, MA) as previously described [207]. The protocol followed in these studies was approved by the Rice University Institutional Animal Care and Use Committee. The cells were cultured in minimum essential medium Eagle-alpha modification (Sigma) supplemented with 10% v/v fetal bovine serum (FBS, Cambrex BioScience, Charles City, IA), 10mM β-glycerol-2-phosphate, 50 μg/mL ascorbic acid, 50 μg/mL gentamicin, 100 μg/mL ampicillin and 1.25 μg/mL fungizone (Sigma). The medium was changed after 24h to remove non-adherent cells and every 2-3 days thereafter until confluence was reached.

Cell encapsulation and culture

Vacuum-dried macromers were sterilized with UV irradiation for 3h [206]. 10% w/v solutions were prepared in sterile PBS and stock solutions of APS and TEMED in dd water were sterile-filtered. Complete osteogenic medium was prepared as the medium used for MSC preculture but with the addition of 10 nM dexamethasone, an osteogenic supplement. Prior to encapsulation, cells were counted in a hemocytometer with trypan blue to confirm cell viability. Macromer solutions were mixed with APS and TEMED

(final concentration 20 mM) on ice. Subsequently, cells were added in a final concentration of 10 million cells/mL, the mixture was gently shaken and pipeted into sterile Teflon molds. After 30min in an incubator, the gels were transferred to 12-well plates and 2.5 mL complete osteogenic medium was added. The medium was changed after 1h to remove hydrogel leachables and every 2-3 days during the culture duration. After 1h, 1, 7, 14 and 21d of culture, hydrogels were removed from the medium and immersed in PBS at 37°C for 30 min, then carefully blotted and weighed. Samples were prepared for biochemical assays (n=3-5), confocal fluorescence microscopy (n=3) and histology (n=2).

Biochemical assays

Samples reserved for biochemical assays were homogenized with a pellet grinder in 0.5 mL of sterile dd water and stored at -20°C. Prior to analyses, samples underwent three freeze-thaw-sonication cycles, with sonication performed on ice for 30 min.

The hydrogel homogenates were analyzed for DNA content, alkaline phosphatase (ALP) activity, collagen and calcium content. The assays are described in more detail elsewhere [207-209]. Prior to DNA and ALP analyses, samples were centrifuged at 4000 rpm for 5 min. Double-stranded DNA content was evaluated using the PicoGreen assay (Invitrogen, Eugene, OR) according to the manufacturer's instructions. Alkaline phosphatase (ALP) activity was evaluated with phosphatase substrate capsules in an alkaline buffer solution compared to serial dilutions of p-nitrophenol standards (all from Sigma) and absorbance was measured. After the DNA and ALP assays were performed, a volume of proteinase K solution equal to the remaining volume of the hydrogel

homogenates was added and samples were incubated at 56°C for 16h. The proteinase K solution was made of 1 mg/mL proteinase K, 0.01 mg/mL pepstatin A and 0.185 mg/mL iodoacetamide in a tris-EDTA buffer (6.055 mg/mL tris(hydroxymethylaminomethane) and 0.372 mg/mL EDTA, pH=7.6). An aliquot of the digested sample was analyzed for hydroxyproline content as a measure of total collagen as previously described [210]. For calcium analysis, a solution of acetic acid was added to the homogenates resulting in a final concentration of 0.5 N and samples were placed on a shaker at 120 rpm overnight to dissolve deposited salts. The assay was performed with a commercially available kit (Genzyme Diagnostics, Cambridge, MA) according to the manufacturer's instructions. For all assays, blank hydrogels from the same time points were used as controls to subtract the fluorescence or absorbance of the material from the sample readings.

Confocal fluorescence microscopy

Sections of 0.7 mm thickness were cut from the hydrogels in the transverse direction and incubated with 2 μM calcein AM and 4 μM ethidium homodimer-1 according to the manufacturer's instructions (Live/Dead viability/cytoxicity kit, Invitrogen, Eugene, OR). As a dead control, hydrogel sections were treated with 70% ethanol for 10 min prior to staining with Live/Dead. Cell-free hydrogels were used as additional controls. Cellular viability and distribution were evaluated with a confocal fluorescence microscope (LSM 510 META, Carl Zeiss, Germany) using a 10x objective. Argon and helium-neon lasers were used for excitation at 488 and 543 nm, respectively, and emission filters at 505-526 and 612-644 nm were employed.

Histology

Hydrogels were embedded in freezing medium (Histo-Prep, Fisher Scientific, Fair Lawn, NJ) and frozen at -20°C. As controls, blank hydrogels were processed and stained in the same manner. Frozen longitudinal sections of 8 μm thickness were cut with a cryostat (Leica CM3050S). Sections were fixed in 10% formalin (Formalde-Fresh, Fisher), stained with Mayer hematoxylin and counterstained with Eosin-Y (Sigma). A second set of sections was stained with von Kossa reagent. Samples were immersed in 1% silver nitrate solution (Sigma) under a UV lamp at 365 nm for 30 min to visualize mineralization and counterstained with Eosin-Y. Sections were imaged with a light microscope (Eclipse E600, Nikon) and camera (3CCD Color Video Camera, Sony).

Cell-free hydrogel mineralization

Hydrogels were fabricated as outlined above and were soaked in complete osteogenic medium, osteogenic medium but without the addition of FBS, or simulated body fluid (SBF) which was prepared according to Kokubo and Takadama [211]. Samples were incubated for 7, 14, 21 and 28d at 37°C, with medium changes every 2-3 days. A set of hydrogels was saved after fabrication and not immersed in any medium, serving as control. At time points, hydrogels were rinsed by immersing in dd water at 37°C for 30 min. Gels were lyophilized, weighed, homogenized in 0.5 N acetic acid and analyzed for calcium as described above.

Statistical analysis

Data from the studies were analyzed using single-factor analysis of variance (ANOVA) with a 95% confidence interval and Tukey's post hoc test. The global effects of the conditions in the swelling study in medium and PBS were evaluated with a two-factor ANOVA and a 95% confidence interval. Data are reported as mean ± standard deviation. In the case of a sample size of n=2, data denote average ± range.

Results

Effect of initiator concentration and fabrication interval on hydrogel swelling

Higher initiator concentrations and fabrication intervals resulted in increased hydrogel swelling (Figure V-1). The hydrogels fabricated with 20mM APS/TEMED and incubated for 30 min at 37°C showed the highest swelling ratio than all other groups (5.9 ±0.4).

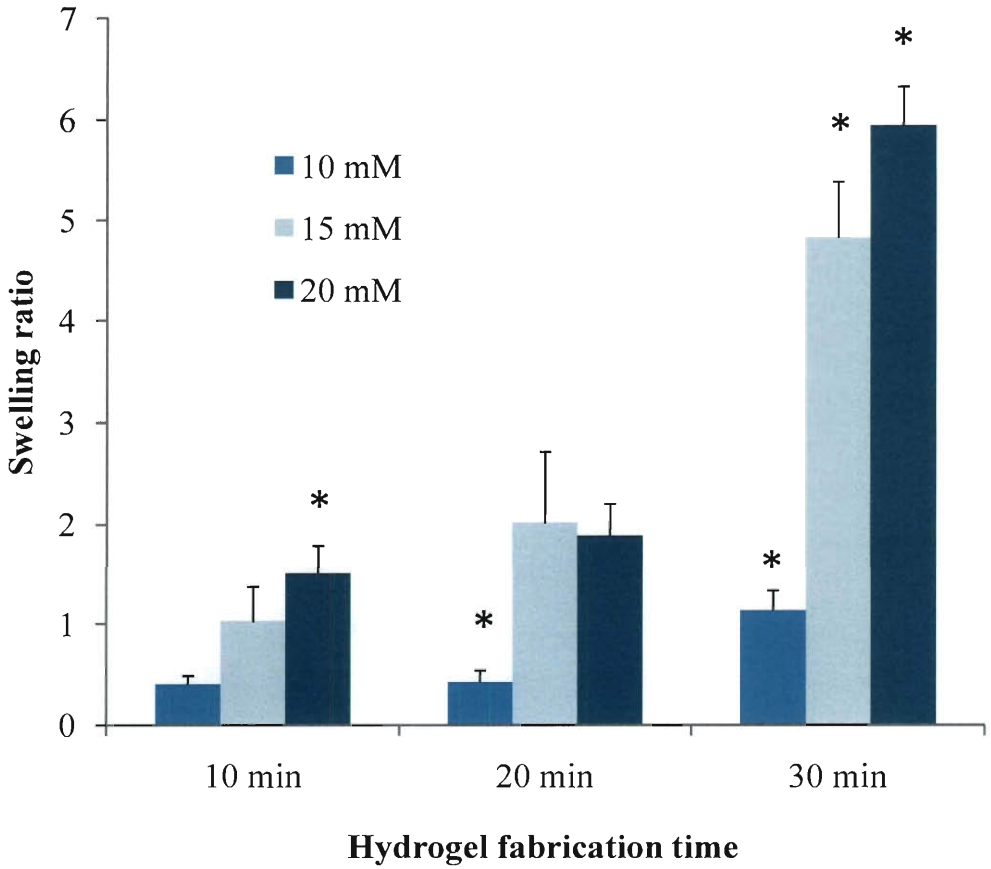

Figure V-1: Swelling behavior of hydrogels with methacrylate end groups fabricated with different concentrations of APS/TEMED initiator system (10-20 mM) and 10-30 min fabrication intervals at 37°C. Hydrogels were swollen in double distilled water for 24h. Data are reported as mean ± standard deviation for a sample size of n=3-4. Asterisk denotes statistical significance between groups from the same fabrication interval ($p<0.05$).

Hydrogel swelling below and above the LCST

The lower critical transition temperature (LCST) of the acrylated formulation was 26.5±0.5°C and the methacrylated formulation 12.7±0.4°C as determined rheologically [206]. The hydrogels swelled significantly when placed in water at 4°C after fabrication (Figure V-2). The acrylated hydrogels showed a swelling ratio of 17.8±0.9 whereas the methacrylated hydrogels had a ratio of 13.1±1.1. When the hydrogels were incubated in water at 37°C, the extent of swelling decreased, with the methacrylated hydrogels exhibiting significantly higher swelling than their acrylated analogs (6.1±0.6 and 3.9±0.2 respectively).

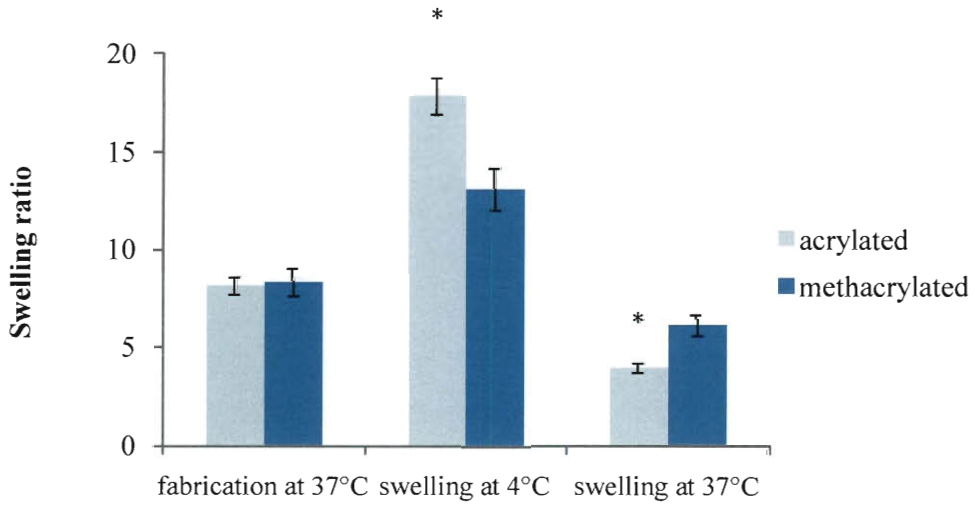

Figure V-2: Swelling behavior of hydrogels with acrylate (n=4) and methacrylate (n=5) end groups at different temperatures. Hydrogels were weighed after fabrication, swollen in double-distilled (dd) water at 4° C (below their LCST) for 20h, weighed and swollen in dd water at 37°C (above their LCST) for 20h. Data are reported as mean ± standard deviation. Asterisk denotes statistically significant differences in swelling between formulations at each temperature ($p<0.05$).

Hydrogel degradation and swelling in cell culture medium and PBS

Osteogenic cell culture medium: The swelling ratio of the acrylated hydrogels at 1h was significantly higher than at 21 and 56 days (Figure V-3). For the methacrylated hydrogels, no significant changes were observed. As for the sol fraction, no increase that would indicate mass loss was noted. On the contrary, the sol fraction of the methacrylated hydrogels at 56d was significantly lower than that measured at the time points up to 14d (Figure V-4).

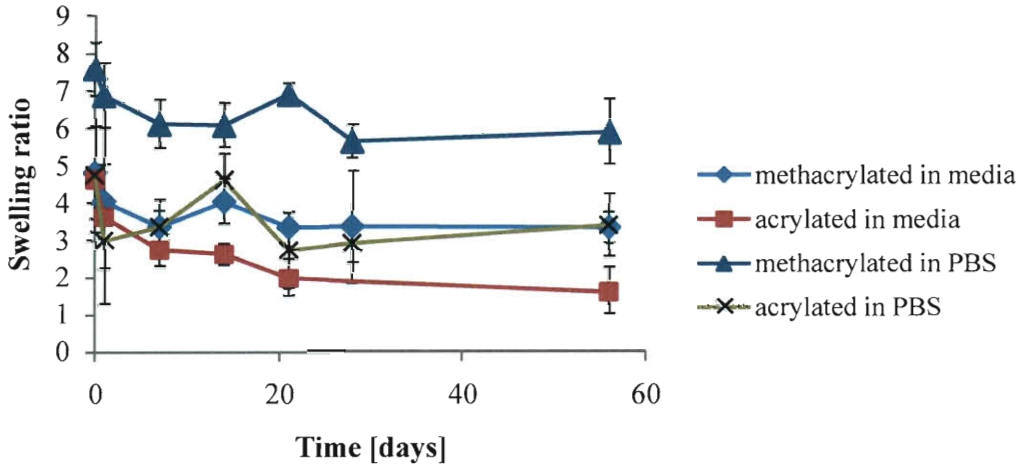

Figure V-3: Swelling behavior of hydrogels incubated in cell culture media or PBS at 37°C over 8 weeks (n=2-5). Data are reported as mean ± standard deviation or as average ± range in the case of n=2 (n=2 was obtained for acrylated gels in PBS at 1h and methacrylated gels in media at 28d). After equilibrium was reached at 1d, there were no significant differences in swelling between time points within each formulation. Acrylated hydrogels showed statistically significantly ($p<0.05$) lower swelling than their methacrylated analogs at all time points when incubated in PBS, whereas this effect was observed after 14d in media. Both acrylated and methacrylated hydrogels showed significantly ($p<0.05$) lower swelling in cell culture media compared to PBS.

PBS: After 1h, no significant differences in swelling were found for the acrylated hydrogels. The swelling at 1h was higher also for the methacrylated formulation as compared to the 28d time point. Acrylated hydrogels swelled less than the methacrylated counterparts at all time points. The sol fraction remained constant for both formulations over the course of 8 weeks.

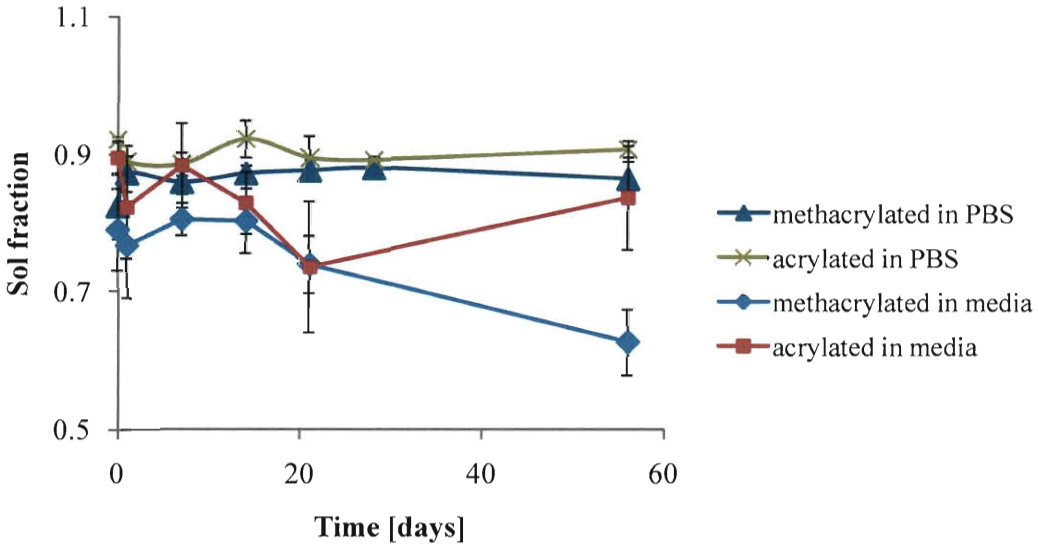

Figure V-4: Sol fraction of hydrogels incubated in cell culture media or PBS at 37° C over 8 weeks (n=2-5). Data are reported as mean ± standard deviation or as average ± range in the case of n=2 (n=2 was obtained for acrylated gels in PBS at 1h and methacrylated gels in media at 28d). A statistically significant ($p<0.05$) decrease in sol fraction was observed for the methacrylated hydrogels cultured in media, whereas no differences were noted for all other groups.

Overall, the global effect of the incubation medium was statistically significant for both acrylated and methacrylated formulations, which each exhibited lower swelling in osteogenic cell cultured medium compared to PBS.

MSC encapsulation in hydrogels

The biochemical assays revealed a drop in DNA content after the first week for both formulations (Supplemental Figure V-I). Hematoxylin and eosin stained sections showed uniform cellular distribution throughout the hydrogels as seen at sections taken from the edge as well as from the center of the gels (Figure V-5). Cell viability was confirmed with Live/Dead staining and confocal microscopy. Live cells could be observed throughout the hydrogel over the whole period of culture (Figure V-6). Due to the strong autofluorescence of the hydrogels at the wavelength used for the ethidium homodimer-1 dye, imaging of the dead cells was not possible. Alkaline phosphatase was detected after 1h in culture, peaked at 1d for both formulations and decreased at later time points (Supplemental Figure V-II). The hydroxyproline assay did not show any collagen production for either formulation over the duration of the study. As for mineralization, calcium accumulation could be found for the cell-encapsulating hydrogels by day 7 (Figure V-7). By day 21, however, cell-free hydrogels had also accumulated calcium at the same amount as the cell-laden hydrogels. Von Kossa staining confirmed the presence of calcium salts throughout the cell-laden hydrogels at 21d (supplemental Figure V-III).

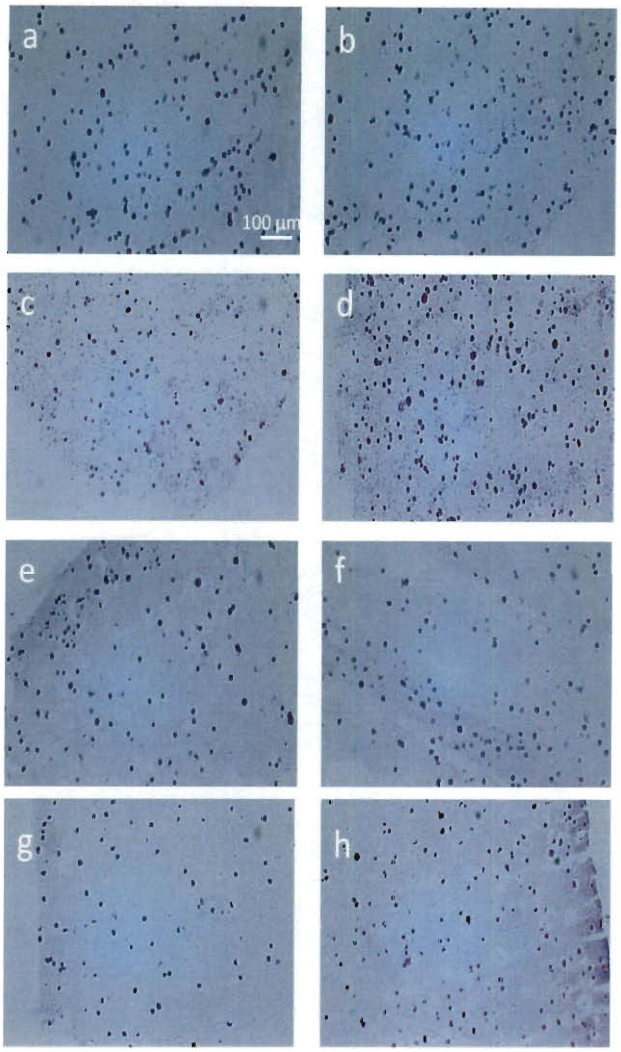

Figure V-5: Hematoxylin and eosin stained longitudinal sections from the edge (left column, images a, c, e and g) and the center of MSC-laden hydrogels (right column, images b, d, f and h). Images a-d correspond to acrylated hydrogels after 1 (a-b) and 21 (c-d) days of culture. Images e-h correspond to methacrylated hydrogels after 1 (e-f) and 21 (g-h) days of culture. Cellular distribution could be observed throughout the hydrogels at both time points. Scale bar indicates 100 µm.

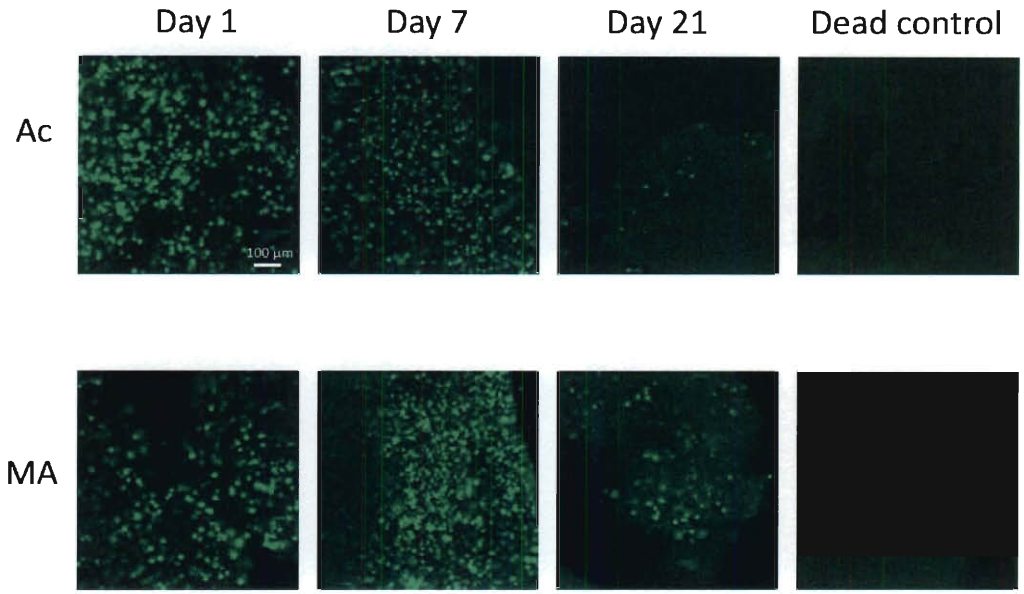

Figure V-6: Fluorescence microscopy images of sections taken from the center of the hydrogels (thickness=0.7 mm) stained with Live/Dead reagent at various time points. Live cells fluoresce green. Strong autofluorescence of the hydrogels at the wavelengths used for the dead dye component was observed and the images are therefore not shown. Included is a dead control treated with 70% ethanol for 10 min in which no live cells are observed. Acrylated hydrogels are denoted as Ac, whereas MA denotes methacrylated hydrogels. Scale bar indicates 100 μm.

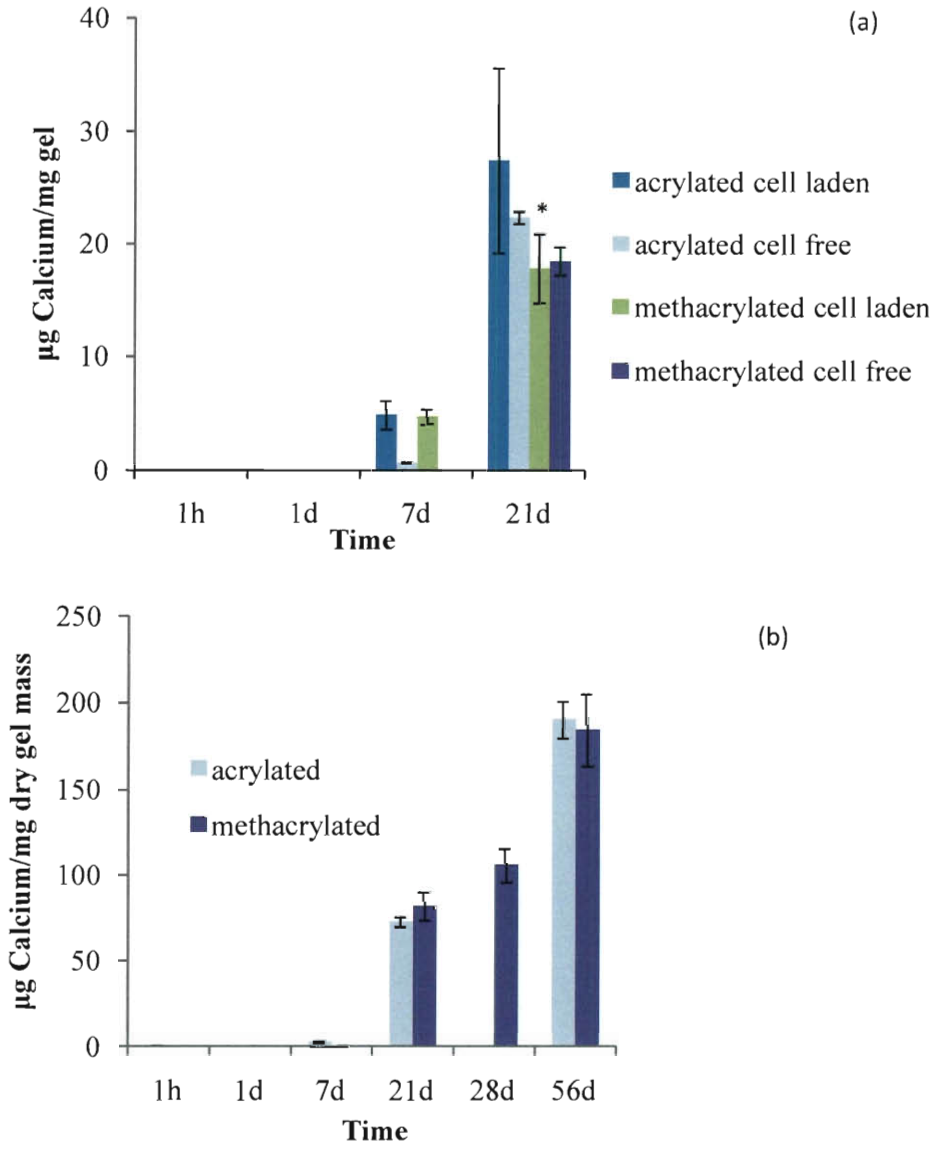

Figure V-7: Calcium content of hydrogels after culture in osteogenic media (n=3-5). (a) Calcium content per mg of "wet" hydrogel for mesenchymal stem cell-laden and cell-free hydrogels. (b) Calcium content per dry mass for cell-free hydrogels over 8 weeks. Due to experimental difficulties, the assay could not be performed on acrylated hydrogels on d28. Data are reported as mean ± standard deviation. Statistical significance between cell-free formulations at time points is marked with an asterisk ($p<0.05$).

Cell-free hydrogel mineralization in different media

Analysis for calcium showed significant accumulation in samples incubated with complete osteogenic medium over four weeks (Figure V-8). Hydrogels immersed in osteogenic medium without FBS as well as simulated body fluid did not yield mineralization. Scanning electron microscopy (SEM) coupled with an energy dispersive spectrometer (EDS) detector confirmed the presence of calcium and phosphorus in the hydrogels incubated with the FBS-containing medium over 28d but not in the two other groups (Supplemental figure V-IV).

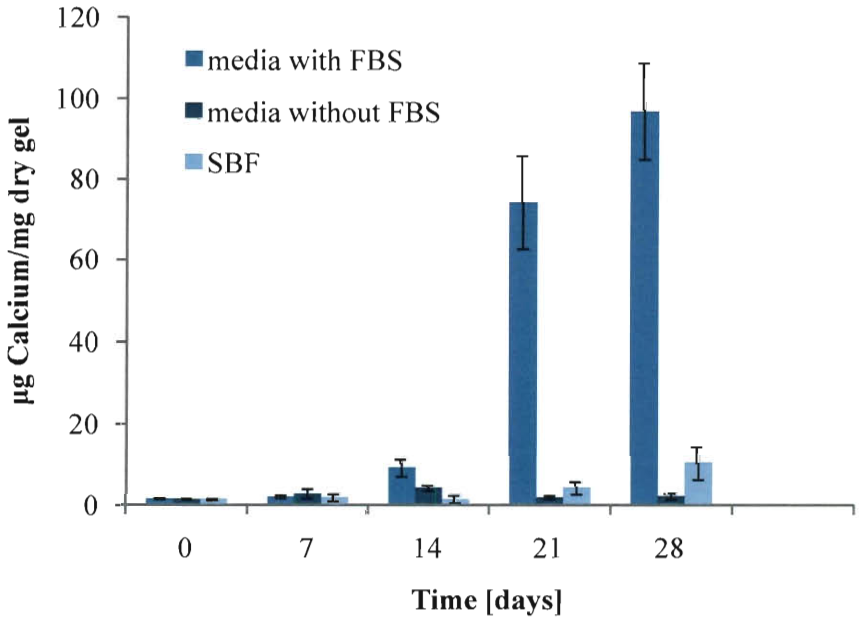

Figure V-8: Calcium content of cell-free hydrogels immersed in complete osteogenic media, osteogenic media without fetal bovine serum (FBS) and simulated body fluid (SBF) at 37° C over 4 weeks (n=4-6). Data are reported as mean ± standard deviation.

Discussion

The fabrication of hydrogels via a dual gelation mechanism was the objective of this study. The macromers used as building blocks for the hydrogels were designed to employ a thermoresponsive domain and chemically crosslinkable (meth)acrylate end groups. The effect of the macromer structure (acrylate or methacrylate functional groups) on the properties of the resulting hydrogels was investigated. The swelling and degradation characteristics of the hydrogels were evaluated and these properties were examined with respect to mesenchymal stem cell viability and osteogenic potential upon encapsulation.

Hydrogel swelling and degradation

Hydrogel systems based on *N*-isopropylacrylamide show a temperature-responsive swelling behavior. Among other factors, the swelling of these hydrogels is dependent on the hydrophilicity of the building blocks [155, 181], the temperature [155, 159, 160] and the pH [102, 202, 212] of the medium. Moreover, pNiPAAm, which has an LCST around 32°C [69], has been shown to fully phase separate and precipitate at 37°C when it is in its linear, uncrosslinked state.

The first study reported in this manuscript showed increased hydrogel swelling with longer fabrication times and increased initiator concentrations (Figure V-1). When the thermal initiator system was added in a final concentration of 20 mM and the hydrogels were formed for 30 minutes at 37°C, higher swelling ratios were observed as opposed to hydrogels fabricated for shorter intervals and/or lower initiator

concentrations. The phenomenon taking place at the incubation temperature of 37°C is a complex interplay between two kinetically independent mechanisms. Covalent crosslinking of the macromolecules takes place at the same time as those chains undergo a thermally-induced phase transition and collapse. The results suggest that longer fabrication intervals and higher initiator concentrations decreased the degree of pNiPAAm-driven collapse of the hydrogels during fabrication and also upon immersion in water at 37°C due to the network structure formed.

The effect of temperature on the swelling of the hydrogels in water was investigated at temperatures below (4°C) and above (37°C) the LCST of the macromers (Figure V-2). The phenomenon of increased swelling below the transition temperature has been reported for NiPAAm-based systems and the water content has been shown to decrease as the temperature approaches and surpasses the LCST [155, 159, 160]. In our studies, the swelling ratio for both hydrogel formulations was significantly higher at 4°C than at 37°C and both hydrogel types expelled water when incubated at 37°C. An interesting observation was the higher temperature-responsiveness exhibited for the acrylated as opposed to the methacrylated formulation. Acrylated hydrogels swelled more than methacrylated at 4°C but exhibited higher shrinkage at 37°C. This may be attributed to the higher flexibility of the polymer chains having an acrylate end group. The additional methyl group of the methacrylated formulations may hinder the chains from fully undergoing the pNiPAAm-associated, temperature driven collapse above the LCST, and also from their complete hydration below the LCST. It is also likely that due to the higher hydrophobicity of the methacrylated chains a "skin layer" is formed at the polymer-

aqueous medium interface which does not allow for water to be fully expelled from the interior of the hydrogel once the temperature increases [213]. Factors that have been demonstrated to control the swelling behavior of hydrophilic, crosslinked hydrogel systems is the crosslinking density [65] or the difference between the incubation temperature and the LCST for uncrosslinked, pNiPAAm-based hydrogels [181]. In the present system, there is an interrelation between the hydrophobic, pNiPAAm-driven chain aggregation and the presence of chemical crosslinks but these mechanisms do not seem to be the governing forces determining the hydrogel swelling.

Further swelling and degradation studies were performed over eight weeks in complete osteogenic media and PBS. Lower swelling was observed for samples immersed in cell culture media as compared to PBS. The presence of solutes such as monosaccharides, amino acids and serum proteins in the complete osteogenic media may have decreased the affinity of the polymer chains for water, leading to higher shrinking. Additionally, the experimental temperature was above the hydrogels' LCST, which renders them more hydrophobic. This may facilitate protein adsorption from the serum on the hydrogels which can enhance hydrophobic interactions and lead to lower swelling. In both immersing media, the swelling at 1h was generally different from subsequent time points suggesting that equilibrium had not yet been reached (Figure V-3). After this time point, there were no notable differences in swelling for each formulation, which is also consistent with the fact that no hydrogel degradation was observed (Figure V-4). Hydrogel chain degradation translates in an altered mesh structure and allows for changes in hydrogel swelling [204, 214]. The degradation of this hydrogel system is expected to occur

via hydrolysis of the ester bonds on pentaerythritol diacrylate monostearate and hydroxyethyl acrylate and its (meth)acrylated end groups. The present study showed that the time interval of eight weeks *in vitro* at 37°C was not sufficient for chain hydrolysis. As mentioned previously, the incubation temperature is above the LCST and the chains are partially dehydrated which likely shields esters from hydrolytic degradation. No mass loss was noted in the hydrogels incubated in PBS, as expressed with a constant sol fraction and dry mass. In addition, solid state NMR analysis (data not shown) did not detect any acidic compounds which would have resulted from ester hydrolysis.

Mesenchymal stem cell encapsulation

One advantage of an *in situ* forming hydrogel is the three-dimensional incorporation of cells and the potential control over their spatial distribution. In our system, homogeneous cellular distribution could be observed throughout the hydrogels for both formulations over three weeks of culture (Figure V-5). Hydrogel sections were taken both from the center and the edge of the hydrogels and stained with calcein AM and ethidium homodimer-1, markers for live and dead cells, respectively. Cells retained their viability over the entire period of the culture (Figure V-6). The cytocompatibility of the macromers for various times of crosslinking was evaluated in a previous study [206]. In this case, the reaction rate of macromer crosslinking was fast enough as not to cause any significant adverse effects to encapsulated cells. The hydrogel systems presented in this study have relatively lower swelling ratios compared to purely hydrophilic systems. However, the water retained by both hydrogel types seemed to facilitate nutrient and

oxygen diffusion into the hydrogel as well as waste product removal, a fact evidenced by viable cells.

One problem encountered in these studies was the incomplete DNA extraction from the cells and/or the gels. Double-stranded DNA could be detected until the first day of culture, but not at later time points. The presence of live cells however was confirmed with the Live/Dead staining. Possible interactions of the material and matrix components with DNA as well as material autofluorescence were accounted for. Moreover, the presence of single- and double-stranded DNA was evaluated with the Oli-Green assay kit [215] with minimal detection. Therefore, quantitative DNA assay results (included as Supplemental Figure V-I) may not accurately reflect the total number of live cells.

Mesenchymal stem cells can undergo osteogenic differentiation when cultured in the presence of supplements such as dexamethasone [216]. The osteogenic marker alkaline phosphatase (ALP) was detected when the cell-laden gels were cultured in complete osteogenic media (Supplemental Figure V-II). Calcium, another marker for osteogenic differentiation, was present in the cell-laden gels as early as after one week of culture. There did not seem to be an effect of (meth)acrylated end group on mineralization. At 14 days, cell-free hydrogels had started to accumulate calcium, but at a significantly lower amount than cell-laden gels. At 21 days however, the calcium content of cell-laden and cell-free hydrogels was not statistically different (Figure V-7). Mineralized extracellular matrix has been shown to enhance osteogenic differentiation of mesenchymal stem cells [210]. Future *in vivo* studies could determine whether the mineralization of the hydrogels is a parameter that could further promote cell osteogenic differentiation in this system.

Cell –free hydrogel mineralization

The mechanism of hydrogel mineralization was further evaluated with cell-free hydrogels immersed in three different mineralizing media, namely complete osteogenic medium, the same osteogenic medium but without the addition of fetal bovine serum (FBS) and simulated body fluid (SBF). SBF has a slightly higher concentration of calcium ions (2.5 mM) than the complete osteogenic medium (1.8 mM). Both contain inorganic phosphate (1 mM), whereas the latter also contains organic phosphate in the form of β-glycerol phosphate (10 mM). Hydrogel mineralization in the absence of cells generally occurs through the addition of anionic, calcium-binding functional groups on the polymer chains, the incorporation of inorganic particles into the matrix or the formation of nucleation sites by methods that mimic the physiological mineralization process [217].

The results from the present studies indicate that the hydrogel mineralization here is mediated by the fetal bovine serum (Figure V-8). Fetal bovine serum can be extremely variable in composition [218] and often contains salts of calcium and phosphate [219, 220]. It has been reported that certain serum proteins act as calcification factors in the presence of adequate amounts of phosphate salts [221, 222]. There is also evidence in the literature that proteins found in serum exhibit endogenous alkaline phosphatase activity and can therefore hydrolyze the organic β-glycerol phosphate [223, 224]. These reports are in agreement with our studies, which showed that serum in the presence of inorganic calcium and phosphate salts as well as high amounts of β-glycerol phosphate initiated mineralization. Since the incubation temperature of 37°C is higher than their LCST, the hydrogels are in a hydrophobic state, which likely favors protein adsorption from the

serum. This fact is evidenced also by the lower swelling observed in hydrogels immersed in complete osteogenic cell culture medium, which contains proteins, as opposed to samples immersed in PBS as previously discussed. Inorganic salts alone, as in SBF, or organic phosphate in the absence of serum, as in FBS-free media, did not result in hydrogel mineralization.

Conclusions

These studies demonstrated the fabrication of hydrogels with a dual solidification mechanism, namely lower critical solution behavior and covalent crosslinking. Parameters that control the swelling behavior of the hydrogels are the chemistry of the macromer end group (acrylate or methacrylate), the concentration of the initiator system used, the fabrication interval as well as the incubation temperature and medium. The hydrogels exhibited constant swelling and no degradation over an eight-week incubation period *in vitro* at 37°C. Encapsulated mesenchymal stem cells showed uniform distribution and viability throughout the hydrogels over a culture period of 21 days. Markers for cell osteogenic differentiation, alkaline phosphatase and calcium, were detected when the hydrogels were cultured in the presence of osteogenic supplements. Additionally, the hydrogels showed mineralization in the absence of cells but with addition of osteogenic cell culture medium supplemented with fetal bovine serum and β-glycerol phosphate.

SUPPLEMENTAL FIGURES

(I)

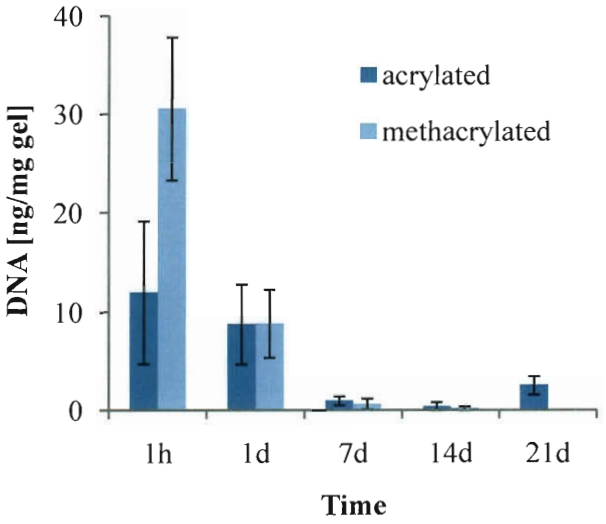

(II)

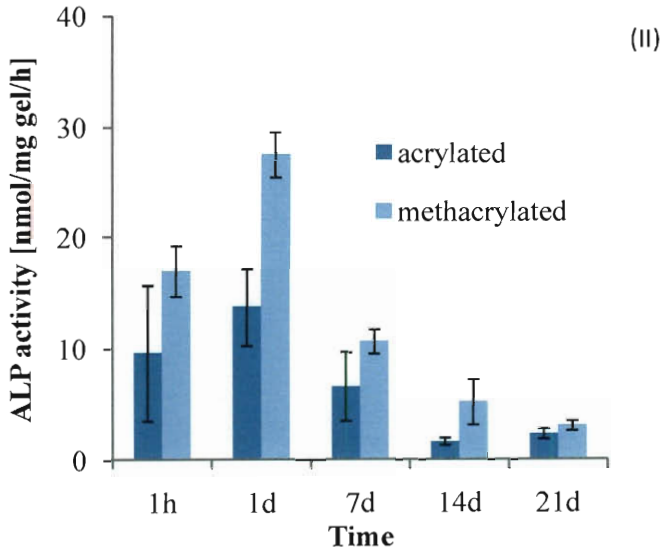

(III)

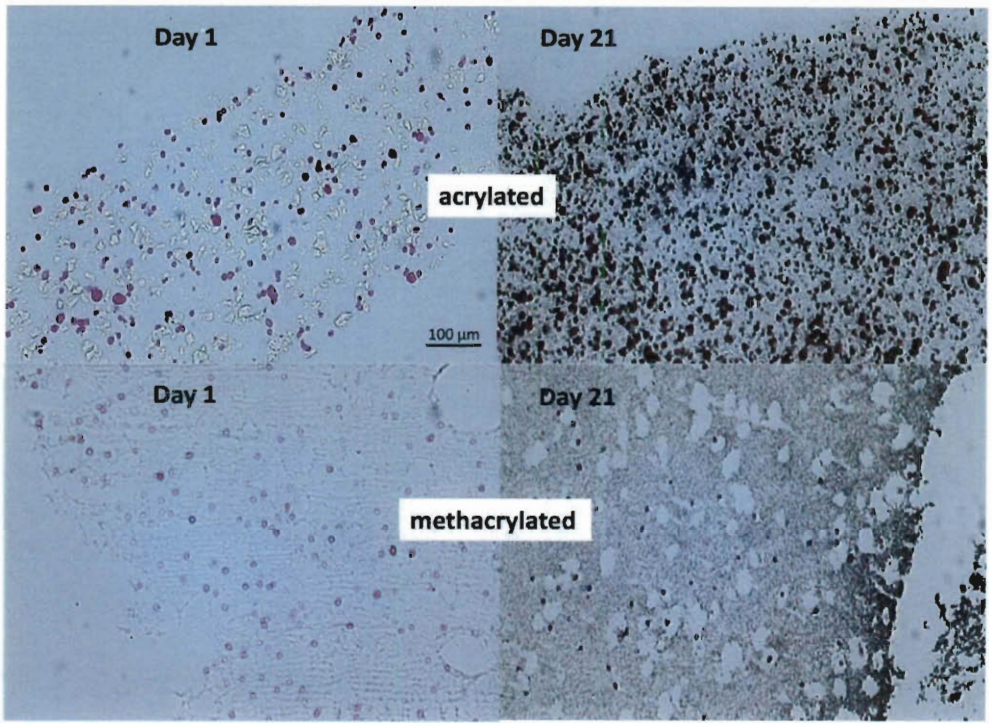
Day 1
Day 21
acrylated
100 µm
Day 1
Day 21
methacrylated

(IV)

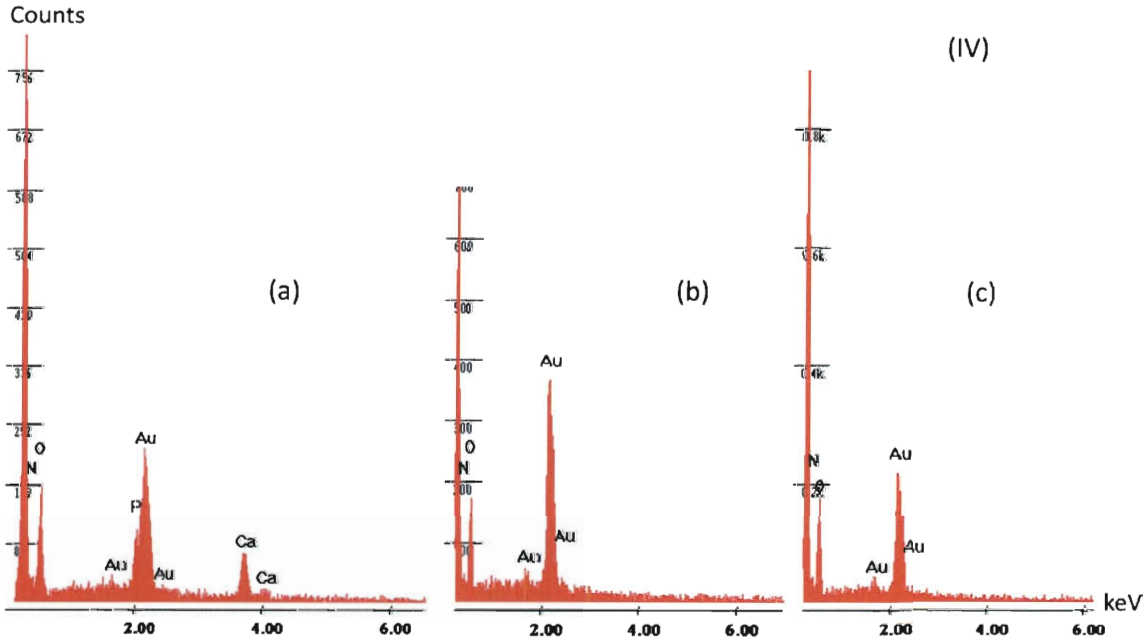
Counts
(a)
(b)
(c)
O
N
Au
Ca
keV
2.00
4.00
6.00

Supplemental figures-V: (I) and (II): Biochemical assays performed on cell-laden hydrogels cultured in osteogenic media over 21d (n=3-5). Assay readings were corrected for with blank hydrogels. (I) DNA content as determined with PicoGreen reagent. (II) Alkaline phosphatase activity. (III) Histological sections of cell-laden hydrogels stained with von Kossa reagent. Acrylated and methacrylated hydrogel sections after one-day and 21-day culture are presented. (IV) Energy dispersive spectra of cell-free hydrogels immersed for 28 days in (a) complete osteogenic media containing FBS, (b) FBS-free media, (c) SBF. Samples were sputter-coated in gold prior to SEM-EDS analysis. The signals for carbon and nitrogen derive from the polymer. Calcium and phosphorus are only detected for the samples in FBS-containing media. The calcium to phosphorus ratio for these samples was 1.10±0.23 and was determined for n=3.

CHAPTER VI

SUMMARY AND OVERALL CONCLUSIONS

This work focused on the synthesis of amphiphilic, thermoresponsive macromers and the fabrication of hydrogels that form *in situ* in response to two solidification mechanisms, a lower critical phase separation phenomenon and covalent crosslinking. The potential of these hydrogels for cell delivery was investigated in a series of cytocompatibility studies and with the encapsulation of mesenchymal stem cells.

The first aim of the work was the synthesis of amphiphilic, thermally responsive macromers with chemically modifiable groups which would allow for the addition of covalently crosslinkable moieties. Structure-property correlations for thermogelling macromers were established and the hydrophilic-hydrophobic balance was found to be an important criterion in controlling the gelation temperature of macromer solutions and thermodynamic stability of the resulting gels. As a next step, the free hydroxyls on the macromers were modified towards acrylate or methacrylate groups. A second gelation mechanism could be achieved by covalently linking these groups with the addition of a free radical thermal initiator system. The combination of physical thermogelation and thermally induced chemical crosslinking was shown to yield hydrogels with higher viscosity and stability.

The second aim of the work was to evaluate the cytocompatibility of the macromers. A first series of studies examined the cytocompatibility of unmodified

thermogelling macromers. Macromers of different molecular compositions and molecular weights were tested *in vitro* for their effect on cell viability in a hydrogel leachables as well as in a direct contact assay. An additional parameter investigated was the effect of the lower critical solution temperature on cytocompatibility. Overall, high cell viabilities were observed over a 24-h time interval. A second series of studies focused on the cytocompatibility characterization of macromers modified with the addition of (meth)acrylate groups. The effect of the (meth)acrylate derivatization on the toxicity of uncrosslinked macromers was examined and it was determined that cell viability decreased significantly after a 6-h exposure period for most formulations. In addition to the time-dependent effect, a dose-dependent effect of the macromers on cell viability was pronounced. Increased degrees of modification were shown to decrease the thermal transition temperature as well as the cytocompatibility of the macromers. These studies gave important information on the parameters that allow for high cell viability during encapsulation in these hydrogels, such as time frame for crosslinking completion.

The third and last aim was the fabrication of hydrogels from the thermoresponsive and chemically crosslinkable macromers. The swelling behavior of the hydrogels was characterized and it was found to be controlled by the chemistry of the macromer end group (acrylate or methacrylate), the concentration of the initiator system used, the fabrication interval as well as the incubation temperature and medium. When the hydrogels were incubated *in vitro* at 37°C, constant swelling and no degradation were observed over eight weeks. Mesenchymal stem cells were encapsulated and the hydrogels were cultured with osteogenic supplements over 21 days. Cells showed uniform distribution and viability throughout the hydrogels over the duration of the culture.

Markers for cell osteogenic differentiation, alkaline phosphatase and calcium, were detected. Interestingly, cell-free hydrogels showed mineralization in the presence of fetal bovine serum and β-glycerol phosphate when cultured *in vitro* at 37°C.

Overall, these studies demonstrated the successful synthesis and characterization of a thermoresponsive and chemically crosslinkable hydrogel system with controllable properties. These hydrogels may be hold promise as injectable, minimally invasive carriers for cells into a defect, encompassing a mild solidification process which would not cause damage to cells and bioactive molecules to be delivered as well as to the surrounding tissues. The design criteria in terms of hydrogel mechanical properties and hydrogel stability were realized by chemically crosslinking the hydrogel in addition to its physical thermogelation. The cytocompatibility of the macromers and the hydrogel system was found to be high and correlations between structure and properties were established. The biodegradation of the hydrogels is a parameter that may need to be optimized for future applications. In these studies, no degradation was observed *in vitro* over a period of eight weeks. The desired rate of biodegradation is strongly application dependent, but ideally, scaffold degradation should start taking place during the time cells differentiate and produce extracellular matrix.

In order to tailor the degradation rate of the polymer, the hydrophilicity of the hydrogels is one parameter that could be modified. This could be achieved by the addition of more hydrophilic monomers in the polymer. An increase in the overall hydrophilicity is likely to influence the swelling characteristics of the hydrogels, and the contact with the aqueous medium could accelerate degradation. This factor may be

further beneficial in terms of diffusional properties and cell encapsulation. Another strategy for future studies could be the incorporation of more hydrolytically labile bonds in the backbone of the polymer which would enhance the degradability of the hydrogels. However, the properties of the resulting macromers are expected to change significantly with any of these modifications in composition. A new set of studies to characterize the thermal gelation and stability properties would be necessary, as well as the characterization of the hydrogels fabricated with these macromers.

CHAPTER VII

BIBLIOGRAPHY

1. Nussenbaum B, Krebsbach PH. The role of gene therapy for craniofacial and dental tissue engineering. Adv Drug Deliv Rev 2006;58:577-591.

2. Artico M, Ferrante L, Pastore FS, Ramundo EO, Cantarelli D, Scopelliti D, Iannetti G. Bone autografting of the calvaria and craniofacial skeleton: historical background, surgical results in a series of 15 patients, and review of the literature. Surg Neurol 2003;60:71-79.

3. Mao JJ, Giannobile WV, Helms JA, Hollister SJ, Krebsbach PH, Longaker MT, Shi S. Craniofacial tissue engineering by stem cells. J Dent Res 2006;85:966-979.

4. Mercuri LG, Giobbie-Hurder A. Long-term outcomes after total alloplastic temporomandibular joint reconstruction following exposure to failed materials. J Oral Maxillofac Surg 2004;62:1088-1096.

5. Pou AM. Update on new biomaterials and their use in reconstructive surgery. Curr Opin Otolaryngol Head Neck Surg 2003;11:240-244.

6. Alsberg E, Hill EE, Mooney DJ. Craniofacial tissue engineering. Crit Rev Oral Biol Med 2001;12:64-75.

7. Costantino PD, Hiltzik D, Govindaraj S, Moche J. Bone healing and bone substitutes. Facial Plast Surg 2002;18:13-26.

8. Langer R, Vacanti JP. Tissue engineering. Science 1993;260:920-926.

9. Atala A, Bauer SB, Soker S, Yoo JJ, Retik AB. Tissue-engineered autologous bladders for patients needing cystoplasty. Lancet 2006;367:1241-1246.

10. Warren SM, Fong KD, Chen CM, Loboa EG, Cowan CM, Lorenz HP, Longaker MT. Tools and techniques for craniofacial tissue engineering. Tissue Eng 2003;9:187-200.

11. Downey PA, Siegel MI. Bone biology and the clinical implications for osteoporosis. Phys Ther 2006;86:77-91.

12. Habibovic P, de Groot K. Osteoinductive biomaterials--properties and relevance in bone repair. J Tissue Eng Regen Med 2007;1:25-32.

13. Holland TA, Mikos AG. Biodegradable polymeric scaffolds. Improvements in bone tissue engineering through controlled drug delivery. Adv Biochem Eng Biotechnol 2006;102:161-185.

14. Khan Y, Yaszemski MJ, Mikos AG, Laurencin CT. Tissue engineering of bone: material and matrix considerations. J Bone Joint Surg Am 2008;90 Suppl 1:36-42.

15. Kretlow JD, Mikos AG. Review: mineralization of synthetic polymer scaffolds for bone tissue engineering. Tissue Eng 2007;13:927-938.

16. Salgado AJ, Oliveira JT, Pedro AJ, Reis RL. Adult stem cells in bone and cartilage tissue engineering. Curr Stem Cell Res Ther 2006;1:345-364.

17. Mikos AG, et al. Engineering complex tissues. Tissue Eng 2006;12:3307-3339.

18. Villanueva JE, Nimni ME. Promotion of calvarial cell osteogenesis by endothelial cells. J Bone Miner Res 1990;5:733-739.

19. Huang YC, Kaigler D, Rice KG, Krebsbach PH, Mooney DJ. Combined angiogenic and osteogenic factor delivery enhances bone marrow stromal cell-driven bone regeneration. J Bone Miner Res 2005;20:848-857.

20. Leach JK, Kaigler D, Wang Z, Krebsbach PH, Mooney DJ. Coating of VEGF-releasing scaffolds with bioactive glass for angiogenesis and bone regeneration. Biomaterials 2006;27:3249-3255.

21. Patel ZS, Young S, Tabata Y, Jansen JA, Wong ME, Mikos AG. Dual delivery of an angiogenic and an osteogenic growth factor for bone regeneration in a critical size defect model. Bone 2008;43:931-940.

22. Jeon O, Song SJ, Kang SW, Putnam AJ, Kim BS. Enhancement of ectopic bone formation by bone morphogenetic protein-2 released from a heparin-conjugated poly(L-lactic-co-glycolic acid) scaffold. Biomaterials 2007;28:2763-2771.

23. Kroese-Deutman HC, Ruhe PQ, Spauwen PH, Jansen JA. Bone inductive properties of rhBMP-2 loaded porous calcium phosphate cement implants inserted at an ectopic site in rabbits. Biomaterials 2005;26:1131-1138.

24. Castano-Izquierdo H, Alvarez-Barreto J, van den Dolder J, Jansen JA, Mikos AG, Sikavitsas VI. Pre-culture period of mesenchymal stem cells in osteogenic media influences their in vivo bone forming potential. J Biomed Mater Res A 2007;82:129-138.

25. Dadsetan M, Hefferan TE, Szatkowski JP, Mishra PK, Macura SI, Lu L, Yaszemski MJ. Effect of hydrogel porosity on marrow stromal cell phenotypic expression. Biomaterials 2008;29:2193-2202.

26. Na K, Kim SW, Sun BK, Woo DG, Yang HN, Chung HM, Park KH. Osteogenic differentiation of rabbit mesenchymal stem cells in thermo-reversible hydrogel constructs containing hydroxyapatite and bone morphogenic protein-2 (BMP-2). Biomaterials 2007;28:2631-2637.

27. Sumanasinghe RD, Osborne JA, Loboa EG. Mesenchymal stem cell-seeded collagen matrices for bone repair: Effects of cyclic tensile strain, cell density, and media conditions on matrix contraction in vitro. J Biomed Mater Res A 2008.

28. Vogel G. Harnessing the power of stem cells. Science 1999;283:1432-1434.

29. Caplan AI. Mesenchymal stem cells. J Orthop Res 1991;9:641-650.

30. Caplan AI. Review: mesenchymal stem cells: cell-based reconstructive therapy in orthopedics. Tissue Eng 2005;11:1198-1211.

31. Park H, Temenoff JS, Tabata Y, Caplan AI, Mikos AG. Injectable biodegradable hydrogel composites for rabbit marrow mesenchymal stem cell and growth factor delivery for cartilage tissue engineering. Biomaterials 2007;28:3217-3227.

32. Temenoff JS, Park H, Jabbari E, Sheffield TL, LeBaron RG, Ambrose CG, Mikos AG. In vitro osteogenic differentiation of marrow stromal cells encapsulated in biodegradable hydrogels. J Biomed Mater Res A 2004;70:235-244.

33. Wang DA, Williams CG, Yang F, Cher N, Lee H, Elisseeff JH. Bioresponsive phosphoester hydrogels for bone tissue engineering. Tissue Eng 2005;11:201-213.

34. Yamada Y, Ueda M, Naiki T, Takahashi M, Hata K, Nagasaka T. Autogenous injectable bone for regeneration with mesenchymal stem cells and platelet-rich plasma: tissue-engineered bone regeneration. Tissue Eng 2004;10:955-964.

35. Alhadlaq A, et al. Adult stem cell driven genesis of human-shaped articular condyle. Ann Biomed Eng 2004;32:911-923.

36. Williams DF. The Williams Dictionary of Biomaterials: Liverpool University Press, UK, 1999.

37. Williams D. Revisiting the definition of biocompatibility. Med Device Technol 2003;14:10-13.

38. Suggs LJ, Shive MS, Garcia CA, Anderson JM, Mikos AG. In vitro cytotoxicity and in vivo biocompatibility of poly(propylene fumarate-co-ethylene glycol) hydrogels. J Biomed Mater Res 1999;46:22-32.

39. Timmer MD, Ambrose CG, Mikos AG. In vitro degradation of polymeric networks of poly(propylene fumarate) and the crosslinking macromer poly(propylene fumarate)-diacrylate. Biomaterials 2003;24:571-577.

40. Zein I, Hutmacher DW, Tan KC, Teoh SH. Fused deposition modeling of novel scaffold architectures for tissue engineering applications. Biomaterials 2002;23:1169-1185.

41. Pham QP, Sharma U, Mikos AG. Electrospinning of polymeric nanofibers for tissue engineering applications: a review. Tissue Eng 2006;12:1197-1211.

42. Brandl F, Sommer F, Goepferich A. Rational design of hydrogels for tissue engineering: impact of physical factors on cell behavior. Biomaterials 2007;28:134-146.

43. Shi X, Hudson JL, Spicer PP, Tour JM, Krishnamoorti R, Mikos AG. Injectable nanocomposites of single-walled carbon nanotubes and biodegradable polymers for bone tissue engineering. Biomacromolecules 2006;7:2237-2242.

44. Pierschbacher MD, Ruoslahti E. Influence of stereochemistry of the sequence Arg-Gly-Asp-Xaa on binding specificity in cell adhesion. J Biol Chem 1987;262:17294-17298.

45. Griffith LG, Naughton G. Tissue engineering--current challenges and expanding opportunities. Science 2002;295:1009-1014.

46. Hench LL, Polak JM. Third-generation biomedical materials. Science 2002;295:1014-1017.

47. Gridelli B, Panarello G, Gruttadauria S, Marcos A, Grossi P. Infections after living-donor liver transplantation. Surgical infections 2006;7 Suppl 2:S105-108.

48. Weitz J, et al. Living-donor kidney transplantation: risks of the donor--benefits of the recipient. Clinical transplantation 2006;20 Suppl 17:13-16.

49. Gridelli B, Panarello G, Gruttadauria S, Marcos A, Grossi P. Infections after Living-Donor Liver Transplantation. Surg Infect 2006;7:s-105-s-108.

50. Weitz J, et al. Living-donor kidney transplantation: risks of the donor - benefits of the recipient. Clin Transplant 2006;20:13-16.

51. Fox MD. The Price Is Wrong: The Moral Cost of Living Donor Inducements. Am J Transplant 2006;6:2529-2530.

52. Gaston RS, Danovitch GM, Epstein RA, Kahn JP, Matas AJ, Schnitzler MA. Limiting Financial Disincentives in Live Organ Donation: A Rational Solution to the Kidney Shortage. Am J Transplant 2006;6:2548-2555.

53. Kaserman DL. On the Feasibility of Resolving the Organ Shortage. Inquiry 2006;43:160-166.

54. Quante M, Wiedebusch S. Overcoming the shortage of transplantable organs: ethical and psychological aspects. Swiss Med Wkly 2006;136:523-528.

55. Higgins RSD, Fishman JA. Disparities in Solid Organ Transplantation for Ethnic Minorities: Facts and Solutions. Am J Transplant 2006;6:2556-2562.

56. Hoffman AS. Hydrogels for biomedical applications. Advanced drug delivery reviews 2002;54:3-12.

57. Peppas NA. Hydrogels. Biomaterials Science, An Introduction to Materials in Medicine. San Diego, California: Academic Press, 1996. p. 60-64.

58. Peppas NA, Mikos AG. Preparation methods and structure of hydrogels. In: Peppas NA, editor. Hydrogels in Medicine and Pharmacy. Boca Raton, Florida: CRC Press, 1986. p. 1-25.

59. Burdick JA, Frankel D, Dernell WS, Anseth KS. An initial investigation of photocurable three-dimensional lactic acid based scaffolds in a critical-sized cranial defect. Biomaterials 2003;24:1613-1620.

60. Burkoth AK, Anseth KS. A review of photocrosslinked polyanhydrides: in situ forming degradable networks. Biomaterials 2000;21:2395-2404.

61. Ossipov DA, Hilborn J. Poly(vinyl alcohol)-based hydrogels formed by "click chemistry". Macromolecules 2006;39:1709-1718.

62. Shu XZ, Ahmad S, Liu Y, Prestwich GD. Synthesis and evaluation of injectable, in situ crosslinkable synthetic extracellular matrices for tissue engineering. J Biomed Mater Res A 2006;79:902-912.

63. Kuo CK, Ma PX. Ionically crosslinked alginate hydrogels as scaffolds for tissue engineering: part 1. Structure, gelation rate and mechanical properties. Biomaterials 2001;22:511-521.

64. Peppas NA. Physiologically responsive gels. J Bioact Compat Polym 1991;6:241-246.

65. Peppas NA, Bures P, Leobandung W, Ichikawa H. Hydrogels in pharmaceutical formulations. Eur J Pharm Biopharm 2000;50:27-46.

66. Li L, Shan H, Yue CY, Lam YC, Tam KC, Hu X. Thermally induced association and dissociation of methylcellulose in aqueous solutions. Langmuir 2002;18:7291-7298.

67. Liu YY, Shao YH, Lu J. Preparation, properties and controlled release behaviors of pH-induced thermosensitive amphiphilic gels. Biomaterials 2006;27:4016-4024.

68. Yin X, Hoffman AS, Stayton PS. Poly(N-isopropylacrylamide-co-propylacrylic acid) copolymers that respond sharply to temperature and pH. Biomacromolecules 2006;7:1381-1385.

69. Schild HG. Poly(N-isopropylacrylamide): Experiment, Theory and Application. Prog Polym Sci 1992;17:163-249.

70. Southall NT, Dill KA, Haymet AD. A view of the hydrophobic effect. J Phys Chem B 2002;106:521-533.

71. Kabanov AV, Batrakova EV, Alakhov VY. Pluronic block copolymers as novel polymer therapeutics for drug and gene delivery. J Control Release 2002;82:189-212.

72. Joly-Duhamel C, Hellio D, Djabourov M. All gelatin networks: 1. Biodiversity and physical chemistry. Langmuir 2002;18:7208-7217.

73. Jeong B, Kim SW, Bae YH. Thermosensitive sol-gel reversible hydrogels. Advanced drug delivery reviews 2002;54:37-51.

74. Ruel-Gariepy E, Leroux JC. In situ-forming hydrogels--review of temperature-sensitive systems. Eur J Pharm Biopharm 2004;58:409-426.

75. Takahashi M, Shimazaki M, Yamamoto J. Thermoreversible gelation and phase separation in aqueous methyl cellulose solutions. J Polym Sci B 2001;39:91-100.

76. Liu W, et al. A rapid temperature-responsive sol-gel reversible poly(N-isopropylacrylamide)-g-methylcellulose copolymer hydrogel. Biomaterials 2004;25:3005-3012.

77. Stabenfeldt SE, Garcia AJ, LaPlaca MC. Thermoreversible laminin-functionalized hydrogel for neural tissue engineering. J Biomed Mater Res A 2006;77:718-725.

78. Tate MC, Shear DA, Hoffman SW, Stein DG, LaPlaca MC. Biocompatibility of methylcellulose-based constructs designed for intracerebral gelation following experimental traumatic brain injury. Biomaterials 2001;22:1113-1123.

79. Bhattarai N, Matsen FA, Zhang M. PEG-grafted chitosan as an injectable thermoreversible hydrogel. Macromolecular bioscience 2005;5:107-111.

80. Bhattarai N, Ramay HR, Gunn J, Matsen FA, Zhang M. PEG-grafted chitosan as an injectable thermosensitive hydrogel for sustained protein release. J Control Release 2005;103:609-624.

81. Cho JH, et al. Chondrogenic differentiation of human mesenchymal stem cells using a thermosensitive poly(N-isopropylacrylamide) and water-soluble chitosan copolymer. Biomaterials 2004;25:5743-5751.

82. Dang JM, Sun DD, Shin-Ya Y, Sieber AN, Kostuik JP, Leong KW. Temperature-responsive hydroxybutyl chitosan for the culture of mesenchymal stem cells and intervertebral disk cells. Biomaterials 2006;27:406-418.

83. Chenite A, et al. Novel injectable neutral solutions of chitosan form biodegradable gels in situ. Biomaterials 2000;21:2155-2161.

84. Crompton KE, Goud JD, Bellamkonda RV, Gengenbach TR, Finkelstein DI, Horne MK, Forsythe JS. Polylysine-functionalised thermoresponsive chitosan hydrogel for neural tissue engineering. Biomaterials 2007;28:441-449.

85. Zhang X, Wu D, Chu CC. Synthesis and characterization of partially biodegradable, temperature and pH sensitive Dex-MA/PNIPAAm hydrogels. Biomaterials 2004;25:4719-4730.

86. Huang X, Lowe TL. Biodegradable thermoresponsive hydrogels for aqueous encapsulation and controlled release of hydrophilic model drugs. Biomacromolecules 2005;6:2131-2139.

87. Shirakawa M, Yamotoya K, Nishinari K. Tailoring of xyloglucan properties using an enzyme. Food Hydrocoll 1998;12:25-28.

88. Nisbet DR, et al. Morphology and gelation of thermosensitive xyloglucan hydrogels. Biophysical chemistry 2006;121:14-20.

89. Yang H, Kao WJ. Thermoresponsive gelatin/monomethoxy poly(ethylene glycol)-poly(D,L-lactide) hydrogels: formulation, characterization, and antibacterial drug delivery. Pharmaceutical research 2006;23:205-214.

90. Ohya S, Matsuda T. Poly(N-isopropylacrylamide) (PNIPAM)-grafted gelatin as thermoresponsive three-dimensional artificial extracellular matrix: molecular and formulation parameters vs. cell proliferation potential. Journal of biomaterials science 2005;16:809-827.

91. Gil ES, Frankowski DJ, Spontak RJ, Hudson SM. Swelling behavior and morphological evolution of mixed gelatin/silk fibroin hydrogels. Biomacromolecules 2005;6:3079-3087.

92. Coughlan DC, Quilty FP, Corrigan OI. Effect of drug physicochemical properties on swelling/deswelling kinetics and pulsatile drug release from thermoresponsive poly(N-isopropylacrylamide) hydrogels. J Control Release 2004;98:97-114.

93. Nakayama M, Okano T, Miyazaki T, Kohori F, Sakai K, Yokoyama M. Molecular design of biodegradable polymeric micelles for temperature-responsive drug release. J Control Release 2006;115:46-56.

94. Hacker MC, Ma BB, Kretlow JD, Mikos AG. Novel macromers for the fabrication of injectable, calcium-binding hydrogels. Annual Meeting of the Society for Biomaterials. Pittsburgh, PA, 2006.

95. Na K, Park JH, Kim SW, Sun BK, Woo DG, Chung HM, Park KH. Delivery of dexamethasone, ascorbate, and growth factor (TGF beta-3) in thermo-reversible hydrogel constructs embedded with rabbit chondrocytes. Biomaterials 2006;27:5951-5957.

96. Hatakeyama H, Kikuchi A, Yamato M, Okano T. Bio-functionalized thermoresponsive interfaces facilitating cell adhesion and proliferation. Biomaterials 2006;27:5069-5078.

97. Pei Y, Chen J, Yang L, Shi L, Tao Q, Hui B, Li J. The effect of pH on the LCST of poly(N-isopropylacrylamide) and poly(N-isopropylacrylamide-co-acrylic acid). Journal of biomaterials science 2004;15:585-594.

98. Zhang XZ, Yang YY, Chung TS, Ma KX. Preparation and characterization of fast response macroporous poly(N-isopropylacrylamide) hydrogels. Langmuir 2001;17:6094-6099.

99. Feil H, Bae YH, Feijen J, Kim SW. Effect of comonomer hydrophilicity and ionization on the lower critical solution temperature of N-isopropylacrylamide copolymers. Macromolecules 1993;26:2496-2500.

100. Liu XM, Wang LS, Wang L, Huang J, He C. The effect of salt and pH on the phase-transition behaviors of temperature-sensitive copolymers based on N-isopropylacrylamide. Biomaterials 2004;25:5659-5666.

101. Liu YY, Fan XD, Wei BR, Si QF, Chen WX, Sun L. pH-responsive amphiphilic hydrogel networks with IPN structure: a strategy for controlled drug release. International journal of pharmaceutics 2006;308:205-209.

102. Xu FJ, Kang ET, Neoh KG. pH- and temperature-responsive hydrogels from crosslinked triblock copolymers prepared via consecutive atom transfer radical polymerizations. Biomaterials 2006;27:2787-2797.

103. Song SC, Lee SB, Jin JI, Sohn YS. A new class of biodegradable thermosensitive polymers. I. Synthesis and characterization of poly(organophosphazenes) with methoxy-poly(ethylene glycol) and amino acid esters as side groups. Macromolecules 1999;32:2188-2193.

104. Okano T, Yamada N, Sakai H, Sakurai Y. A novel recovery system for cultured cells using plasma-treated polystyrene dishes grafted with poly(N-isopropylacrylamide). J Biomed Mater Res 1993;27:1243-1251.

105. Alexandridis P, Hatton TA. Poly(ethylene oxide)-poly(propylene oxide)-poly(ethylene oxide) block copolymer surfactants in aqueous solutions and interfaces: thermodynamics, structure, dynamics and modeling. Colloids Surf A 1995;96:1-46.

106. Ahmed F, Alexandridis P, Shankaran H, Neelamegham S. The ability of poloxamers to inhibit platelet aggregation depends on their physicochemical properties. Thrombosis and haemostasis 2001;86:1532-1539.

107. Steinleitner A, Lambert H, Kazensky C, Cantor B. Poloxamer 407 as an intraperitoneal barrier material for the prevention of postsurgical adhesion formation and reformation in rodent models for reproductive surgery. Obstetrics and gynecology 1991;77:48-52.

108. Nalbandian RM, Henry RL, Balko KW, Adams DV, Neuman NR. Pluronic F-127 gel preparation as an artificial skin in the treatment of third-degree burns in pigs. J Biomed Mater Res 1987;21:1135-1148.

109. Schmolka IR. Artificial skin. I. Preparation and properties of pluronic F-127 gels for treatment of burns. J Biomed Mater Res 1972;6:571-582.

110. Kabanov A, Zhu J, Alakhov V. Pluronic block copolymers for gene delivery. Advances in genetics 2005;53:231-261.

111. Higuchi A, et al. Serum protein adsorption and platelet adhesion on pluronic-adsorbed polysulfone membranes. Biomaterials 2003;24:3235-3245.

112. Higuchi A, et al. Bioinert surface of pluronic-immobilized flask for preservation of hematopoietic stem cells. Biomacromolecules 2006;7:1083-1089.

113. Higuchi A, et al. Temperature-induced cell detachment on immobilized pluronic surface. J Biomed Mater Res A 2006;79:380-392.

114. Weinand C, et al. Hydrogel-beta-TCP scaffolds and stem cells for tissue engineering bone. Bone 2006;38:555-563.

115. Cortiella J, et al. Tissue-engineered lung: an in vivo and in vitro comparison of polyglycolic acid and pluronic F-127 hydrogel/somatic lung progenitor cell constructs to support tissue growth. Tissue Eng 2006;12:1213-1225.

116. Cohn D, Sosnik A, Levy A. Improved reverse thermo-responsive polymeric systems. Biomaterials 2003;24:3707-3714.

117. Sosnik A, Cohn D. Ethoxysilane-capped PEO-PPO-PEO triblocks: a new family of reverse thermo-responsive polymers. Biomaterials 2004;25:2851-2858.

118. Sosnik A, Cohn D, San Roman J, Abraham GA. Crosslinkable PEO-PPO-PEO-based reverse thermo-responsive gels as potentially injectable materials. Journal of biomaterials science 2003;14:227-239.

119. Cohn D, Sosnik A, Garty S. Smart hydrogels for in situ generated implants. Biomacromolecules 2005;6:1168-1175.

120. Sosnik A, Cohn D. Reverse thermo-responsive poly(ethylene oxide) and poly(propylene oxide) multiblock copolymers. Biomaterials 2005;26:349-357.

121. Cohn D, Lando G, Sosnik A, Garty S, Levi A. PEO-PPO-PEO-based poly(ether ester urethane)s as degradable reverse thermo-responsive multiblock copolymers. Biomaterials 2006;27:1718-1727.

122. Cellesi F, Tirelli N. A new process for cell microencapsulation and other biomaterial applications: Thermal gelation and chemical cross-linking in "tandem". Journal of materials science 2005;16:559-565.

123. Cellesi F, Tirelli N, Hubbell JA. Materials for cell encapsulation via a new tandem approach combining reverse thermal gelation and covalent crosslinking. Macromol Chem Phys 2002;203:1466-1472.

124. Cellesi F, Tirelli N, Hubbell JA. Towards a fully-synthetic substitute of alginate: development of a new process using thermal gelation and chemical cross-linking. Biomaterials 2004;25:5115-5124.

125. Jeong B, Bae YH, Lee DS, Kim SW. Biodegradable block copolymers as injectable drug-delivery systems. Nature 1997;388:860-862.

126. Jeong B, Bae YH, Kim SW. In situ gelation of PEG-PLGA-PEG triblock copolymer aqueous solutions and degradation thereof. J Biomed Mater Res 2000;50:171-177.

127. Chen S, Singh J. Controlled delivery of testosterone from smart polymer solution based systems: in vitro evaluation. International journal of pharmaceutics 2005;295:183-190.

128. Zitzmann M, Nieschlag E. Hormone substitution in male hypogonadism. Molecular and cellular endocrinology 2000;161:73-88.

129. Lee J, Bae YH, Sohn YS, Jeong B. Thermogelling aqueous solutions of alternating multiblock copolymers of poly(L-lactic acid) and poly(ethylene glycol). Biomacromolecules 2006;7:1729-1734.

130. Behravesh E, Shung AK, Jo S, Mikos AG. Synthesis and characterization of triblock copolymers of methoxy poly(ethylene glycol) and poly(propylene fumarate). Biomacromolecules 2002;3:153-158.

131. Fisher JP, Jo S, Mikos AG, Reddi AH. Thermoreversible hydrogel scaffolds for articular cartilage engineering. Journal of biomedical materials research 2004;71:268-274.

132. Kang GD, Cheon SH, Khang G, Song SC. Thermosensitive poly(organophosphazene) hydrogels for a controlled drug delivery. Eur J Pharm Biopharm 2006;63:340-346.

133. Kang GD, Cheon SH, Song SC. Controlled release of doxorubicin from thermosensitive poly(organophosphazene) hydrogels. International journal of pharmaceutics 2006;319:29-36.

134. Park KH, Song SC. Morphology of spheroidal hepatocytes within injectable, biodegradable, and thermosensitive poly(organophosphazene) hydrogel as cell delivery vehicle. Journal of bioscience and bioengineering 2006;101:238-242.

135. Sohn YS, Kim JK, Song R, Jeong B. The relationship of thermosensitive properties with structure of organophosphazenes. Polymer 2004;45:3081-3084.

136. Gutowska A, Jeong B, Jasionowski M. Injectable gels for tissue engineering. The Anatomical record 2001;263:342-349.

137. Temenoff JS, Mikos AG. Injectable biodegradable materials for orthopedic tissue engineering. Biomaterials 2000;21:2405-2412.

138. Nguyen KT, West JL. Photopolymerizable hydrogels for tissue engineering applications. Biomaterials 2002;23:4307-4314.

139. Lutolf MP, Weber FE, Schmoekel HG, Schense JC, Kohler T, Muller R, Hubbell JA. Repair of bone defects using synthetic mimetics of collagenous extracellular matrices. Nature biotechnology 2003;21:513-518.

140. Ifkovits JL, Burdick JA. Review: photopolymerizable and degradable biomaterials for tissue engineering applications. Tissue engineering 2007;13:2369-2385.

141. Elisseeff J, Anseth K, Sims D, McIntosh W, Randolph M, Langer R. Transdermal photopolymerization for minimally invasive implantation. Proceedings of the

National Academy of Sciences of the United States of America 1999;96:3104-3107.

142. Temenoff JS, Shin H, Conway DE, Engel PS, Mikos AG. In vitro cytotoxicity of redox radical initiators for cross-linking of oligo(poly(ethylene glycol) fumarate) macromers. Biomacromolecules 2003;4:1605-1613.

143. Shin H, Temenoff JS, Mikos AG. In vitro cytotoxicity of unsaturated oligo[poly(ethylene glycol) fumarate] macromers and their cross-linked hydrogels. Biomacromolecules 2003;4:552-560.

144. Galaev IY, Mattiasson B. 'Smart' polymers and what they could do in biotechnology and medicine. Trends in biotechnology 1999;17:335-340.

145. Qiu Y, Park K. Environment-sensitive hydrogels for drug delivery. Advanced drug delivery reviews 2001;53:321-339.

146. Dong LC, Hoffman AS. Synthesis and application of thermally reversible heterogels for drug delivery. Journal of Controlled Release 1990;13:21-31.

147. Gutowska A, Seok Bark J, Chan Kwon I, Han Bae Y, Cha Y, Wan Kim S. Squeezing hydrogels for controlled oral drug delivery. Journal of Controlled Release 1997;48:141-148.

148. Klouda L, Mikos AG. Thermoresponsive hydrogels in biomedical applications. Eur J Pharm Biopharm 2008;68:34-45.

149. Ron ES, Bromberg LE. Temperature-responsive gels and thermogelling polymer matrices for protein and peptide delivery. Advanced drug delivery reviews 1998;31:197-221.

150. Stile RA, Healy KE. Thermo-responsive peptide-modified hydrogels for tissue regeneration. Biomacromolecules 2001;2:185-194.

151. Saim AB, Cao Y, Weng Y, Chang CN, Vacanti MA, Vacanti CA, Eavey RD. Engineering autogenous cartilage in the shape of a helix using an injectable hydrogel scaffold. The Laryngoscope 2000;110:1694-1697.

152. Jeong B, Lee KM, Gutowska A, An YH. Thermogelling biodegradable copolymer aqueous solutions for injectable protein delivery and tissue engineering. Biomacromolecules 2002;3:865-868.

153. Seong JY, Jun YJ, Jeong B, Sohn YS. New thermogelling poly(organophosphazenes) with methoxypoly(ethylene glycol) and oligopeptide as side groups. Polymer 2005;46:5075-5081.

154. Ibusuki S, Iwamoto Y, Matsuda T. System-engineered cartilage using poly(N-isopropylacrylamide)-grafted gelatin as in situ-formable scaffold: in vivo performance. Tissue engineering 2003;9:1133-1142.

155. Stile RA, Burghardt WR, Healy KE. Synthesis and Characterization of Injectable Poly(N-isopropylacrylamide)-Based Hydrogels That Support Tissue Formation in Vitro. Macromolecules 1999;32:7370-7379.

156. Gil ES, Hudson SM. Stimuli-reponsive polymers and their bioconjugates. Prog Polym Sci 2004;29:1173-1222.

157. Ohya S, Nakayama Y, Matsuda T. Thermoresponsive artificial extracellular matrix for tissue engineering: hyaluronic acid bioconjugated with poly(N-isopropylacrylamide) grafts. Biomacromolecules 2001;2:856-863.

158. Vernon B, Kim SW, Bae YH. Thermoreversible copolymer gels for extracellular matrix. Journal of biomedical materials research 2000;51:69-79.

159. Lee BH, West B, McLemore R, Pauken C, Vernon BL. In-situ injectable physically and chemically gelling NIPAAm-based copolymer system for embolization. Biomacromolecules 2006;7:2059-2064.

160. Robb SA, Lee BH, McLemore R, Vernon BL. Simultaneously physically and chemically gelling polymer system utilizing a poly(NIPAAm-co-cysteamine)-based copolymer. Biomacromolecules 2007;8:2294-2300.

161. Odian G. Principles of polymerization: John Wiley & Sons, Inc., 1991.

162. Boutris C, Chatzi EG, Kiparissides C. Characterization of the LCST behaviour of aqueous poly(N-isopropylacrylamide) solutions by thermal and cloud point techniques. Polymer 1997;38:2567-2570.

163. Jansen EJ, et al. Hydrophobicity as a design criterion for polymer scaffolds in bone tissue engineering. Biomaterials 2005;26:4423-4431.

164. Guse C, et al. Biocompatibility and erosion behavior of implants made of triglycerides and blends with cholesterol and phospholipids. International journal of pharmaceutics 2006;314:153-160.

165. Lindblad MS, Liu Y, Albertsson AC, Ranucci E, Karlsson S. Polymers from renewable resources. Adv Polym Sci 2002;157:139-161.

166. Seniha Guner F, Yagci Y, Tuncer Erciyes A. Polymers from triglyceride oils. Prog Polym Sci 2006;31:633-670.

167. Fulzele SV, Satturwar PM, Dorle AK. Study of the biodegradation and in vivo biocompatibility of novel biomaterials. Eur J Pharm Sci 2003;20:53-61.

168. Braunecker WA, Matyjazewski K. Controlled/living radical polymerization: Features, developments, and perspectives. Prog Polym Sci 2007;32:93-146.

169. Yoshioka H, Mori Y, Tsukikawa S, Kubota S. Thermoreversible gelation on cooling and on heating of an aqueous gelatin-poly(N-isopropylacrylamide) conjugate. Polym Adv Technol 1998;9:155-158.

170. Shim MS, et al. Poly(D,L-lactic acid-co-glycolic acid)-b-poly(ethylene glycol)-b-poly (D,L-lactic acid-co-glycolic acid) triblock copolymer and thermoreversible phase transition in water. Journal of biomedical materials research 2002;61:188-196.

171. Pelton R. Temperature-sensitive aqueous microgels. Advances in colloid and interface science 2000;85:1-33.

172. Peter SJ, Suggs LJ, Yaszemski MJ, Engel PS, Mikos AG. Synthesis of poly(propylene fumarate) by acylation of propylene glycol in the presence of a proton scavenger. Journal of biomaterials science 1999;10:363-373.

173. Hu X, Zhang Z, Zhang X, Li Z, Zhu XX. Selective acylation of cholic acid derivatives with multiple methacrylate groups. Steroids 2005;70:531-537.

174. Timmer MD, Jo S, Wang C, Ambrose CG, Mikos AG. Characterization of the cross-linked structure of fumarate-based degradable polymer networks. Macromolecules 2002;35:4373-4379.

175. Elisseeff J, McIntosh W, Anseth K, Riley S, Ragan P, Langer R. Photoencapsulation of chondrocytes in poly(ethylene oxide)-based semi-interpenetrating networks. Journal of biomedical materials research 2000;51:164-171.

176. Mann BK, Gobin AS, Tsai AT, Schmedlen RH, West JL. Smooth muscle cell growth in photopolymerized hydrogels with cell adhesive and proteolytically

degradable domains: synthetic ECM analogs for tissue engineering. Biomaterials 2001;22:3045-3051.

177. Bryant SJ, Anseth KS. The effects of scaffold thickness on tissue engineered cartilage in photocrosslinked poly(ethylene oxide) hydrogels. Biomaterials 2001;22:619-626.

178. Kretlow JD, Klouda L, Mikos AG. Injectable matrices and scaffolds for drug delivery in tissue engineering. Adv Drug Deliv Rev 2007;59:263-273.

179. Temenoff JS, Park H, Jabbari E, Conway DE, Sheffield TL, Ambrose CG, Mikos AG. Thermally cross-linked oligo(poly(ethylene glycol) fumarate) hydrogels support osteogenic differentiation of encapsulated marrow stromal cells in vitro. Biomacromolecules 2004;5:5-10.

180. Vermonden T, Fedorovich NE, van Geemen D, Alblas J, van Nostrum CF, Dhert WJ, Hennink WE. Photopolymerized thermosensitive hydrogels: synthesis, degradation, and cytocompatibility. Biomacromolecules 2008;9:919-926.

181. Hacker MC, Klouda L, Ma BB, Kretlow JD, Mikos AG. Synthesis and characterization of injectable, thermally and chemically gelable, amphiphilic poly(N-isopropylacrylamide)-based macromers. Biomacromolecules 2008;9:1558-1570.

182. Betz MW, Modi PC, Caccamese JF, Coletti DP, Sauk JJ, Fisher JP. Cyclic acetal hydrogel system for bone marrow stromal cell encapsulation and osteodifferentiation. J Biomed Mater Res A 2008;86:662-670.

183. Nicodemus GD, Bryant SJ. Cell encapsulation in biodegradable hydrogels for tissue engineering applications. Tissue Eng Part B Rev 2008;14:149-165.

184. Southall NT, Dill KA, Haymet ADJ. A View of the Hydrophobic Effect. Journal of Physical Chemistry B 2002;106:521-533.

185. Kim NS, Lee GM. Response of recombinant Chinese hamster ovary cells to hyperosmotic pressure: effect of Bcl-2 overexpression. J Biotechnol 2002;95:237-248.

186. Mockridge JW, Benton EC, Andreeva LV, Latchman DS, Marber MS, Heads RJ. IGF-1 regulates cardiac fibroblast apoptosis induced by osmotic stress. Biochem Biophys Res Commun 2000;273:322-327.

187. Zhu MM, Goyal A, Rank DL, Gupta SK, Vanden Boom T, Lee SS. Effects of elevated pCO2 and osmolality on growth of CHO cells and production of antibody-fusion protein B1: a case study. Biotechnol Prog 2005;21:70-77.

188. Kaihara S, Matsumura S, Fisher JP. Cellular responses to degradable cyclic acetal modified PEG hydrogels. J Biomed Mater Res A 2008.

189. Du JZ, Sun TM, Weng SQ, Chen XS, Wang J. Synthesis and characterization of photo-cross-linked hydrogels based on biodegradable polyphosphoesters and poly(ethylene glycol) copolymers. Biomacromolecules 2007;8:3375-3381.

190. Timmer MD, Shin H, Horch RA, Ambrose CG, Mikos AG. In vitro cytotoxicity of injectable and biodegradable poly(propylene fumarate)-based networks: unreacted macromers, cross-linked networks, and degradation products. Biomacromolecules 2003;4:1026-1033.

191. De Groot CJ, Van Luyn MJ, Van Dijk-Wolthuis WN, Cadee JA, Plantinga JA, Den Otter W, Hennink WE. In vitro biocompatibility of biodegradable dextran-based hydrogels tested with human fibroblasts. Biomaterials 2001;22:1197-1203.

192. Yoshii E. Cytotoxic effects of acrylates and methacrylates: relationships of monomer structures and cytotoxicity. J Biomed Mater Res 1997;37:517-524.

193. Atsumi T, Fujisawa S, Tonosaki K. (Meth)acrylate monomer-induced cytotoxicity and intracellular Ca(2+) mobilization in human salivary gland carcinoma cells and human gingival fibroblast cells related to monomer hydrophobicity. Biomaterials 2006;27:5794-5800.

194. Fujisawa S, Atsumi T, Kadoma Y. Cytotoxicity of methyl methacrylate (MMA) and related compounds and their interaction with dipalmitoylphosphatidylcholine (DPPC) liposomes as a model for biomembranes. Oral Dis 2000;6:215-221.

195. Fujisawa S, Kadoma Y, Komoda Y. 1H and 13C NMR studies of the interaction of eugenol, phenol, and triethyleneglycol dimethacrylate with phospholipid liposomes as a model system for odontoblast membranes. J Dent Res 1988;67:1438-1441.

196. Schweikl H, Spagnuolo G, Schmalz G. Genetic and cellular toxicology of dental resin monomers. J Dent Res 2006;85:870-877.

197. Chan K, O'Brien PJ. Structure-activity relationships for hepatocyte toxicity and electrophilic reactivity of alpha,beta-unsaturated esters, acrylates and methacrylates. J Appl Toxicol 2008;28:1004-1015.

198. Fundueanu G, Constantin M, Stanciu C, Theodoridis G, Ascenzi P. pH- and temperature-sensitive polymeric microspheres for drug delivery: the dissolution of copolymers modulates drug release. Journal of materials science 2009;20:2465-2475.

199. Misra GP, Singh RS, Aleman TS, Jacobson SG, Gardner TW, Lowe TL. Subconjunctivally implantable hydrogels with degradable and thermoresponsive properties for sustained release of insulin to the retina. Biomaterials 2009;30:6541-6547.

200. Tang Z, Akiyama Y, Yamato M, Okano T. Comb-type grafted poly(N-isopropylacrylamide) gel modified surfaces for rapid detachment of cell sheet. Biomaterials 31:7435-7443.

201. Gant RM, Abraham AA, Hou Y, Cummins BM, Grunlan MA, Cote GL. Design of a self-cleaning thermoresponsive nanocomposite hydrogel membrane for implantable biosensors. Acta biomaterialia 6:2903-2910.

202. Fujimoto KL, Ma Z, Nelson DM, Hashizume R, Guan J, Tobita K, Wagner WR. Synthesis, characterization and therapeutic efficacy of a biodegradable, thermoresponsive hydrogel designed for application in chronic infarcted myocardium. Biomaterials 2009;30:4357-4368.

203. Guan J, Hong Y, Ma Z, Wagner WR. Protein-reactive, thermoresponsive copolymers with high flexibility and biodegradability. Biomacromolecules 2008;9:1283-1292.

204. Censi R, Fieten PJ, di Martino P, Hennink WE, Vermonden T. In Situ Forming Hydrogels by Tandem Thermal Gelling and Michael Addition Reaction between Thermosensitive Triblock Copolymers and Thiolated Hyaluronan. Macromolecules 2010;43:5771–5778.

205. Cheng V, Lee BH, Pauken C, Vernon BL. Poly(N-isopropylacrylamide-co-Poly(ethylene glycol))-Acrylate Simultaneously Physically and Chemically Gelling Polymer Systems. Journal of Applied Polymer Science 2007;106:1201-1207.

206. Klouda L, Hacker MC, Kretlow JD, Mikos AG. Cytocompatibility evaluation of amphiphilic, thermally responsive and chemically crosslinkable macromers for in situ forming hydrogels. Biomaterials 2009;30:4558-4566.

207. Thibault RA, Scott Baggett L, Mikos AG, Kasper FK. Osteogenic differentiation of mesenchymal stem cells on pregenerated extracellular matrix scaffolds in the absence of osteogenic cell culture supplements. Tissue engineering 16:431-440.

208. Guo X, et al. In vitro generation of an osteochondral construct using injectable hydrogel composites encapsulating rabbit marrow mesenchymal stem cells. Biomaterials 2009;30:2741-2752.

209. Liao J, Guo X, Nelson D, Kasper FK, Mikos AG. Modulation of osteogenic properties of biodegradable polymer/extracellular matrix scaffolds generated with a flow perfusion bioreactor. Acta biomaterialia 6:2386-2393.

210. Datta N, Pham QP, Sharma U, Sikavitsas VI, Jansen JA, Mikos AG. In vitro generated extracellular matrix and fluid shear stress synergistically enhance 3D osteoblastic differentiation. Proceedings of the National Academy of Sciences of the United States of America 2006;103:2488-2493.

211. Kokubo T, Takadama H. How useful is SBF in predicting in vivo bone bioactivity? Biomaterials 2006;27:2907-2915.

212. Brazel CS, Peppas NA. Synthesis and Characterization of Thermo-and Chemomechanically Responsive Poly(N-isopropylacrylamide-co-methacrylic acid) Hydrogels. Macromolecules 1995;28:8016-8020.

213. Yoshida R, Uchida K, Kaneko Y, Sakai K, Kikuchi A, Sakurai Y, Okano T. Comb-type grafted hydrogels with rapid de-swelling response to temperature changes. Nature 1995;374:240-242.

214. Temenoff JS, Park H, Jabbari E, Conway DE, Sheffield TL, Ambrose CG, Mikos AG. Thermally Cross-linked Oligo(poly(ethylene glycol) fumarate) Hydrogels Support Osteogenic Differentiation of Encapsulated Marrow Stromal Cells in Vitro. Biomacromolecules 2004;5:5-10.

215. Kasper FK, Seidlits SK, Tang A, Crowther RS, Carney DH, Barry MA, Mikos AG. In vitro release of plasmid DNA from oligo(poly(ethylene glycol) fumarate) hydrogels. J Control Release 2005;104:521-539.

216. Jager M, Feser T, Denck H, Krauspe R. Proliferation and osteogenic differentiation of mesenchymal stem cells cultured onto three different polymers in vitro. Annals of biomedical engineering 2005;33:1319-1332.

217. Gkioni C, Leeuwenburgh S, Douglas T, Mikos AG, Jansen J. Mineralization of Hydrogels for Bone Regeneration. Tissue Eng Part B Rev.

218. Honn KV, Singley JA, Chavin W. Fetal bovine serum: a multivariate standard. Proceedings of the Society for Experimental Biology and Medicine Society for Experimental Biology and Medicine (New York, NY 1975;149:344-347.

219. Boskey AL, Roy R. Cell culture systems for studies of bone and tooth mineralization. Chemical reviews 2008;108:4716-4733.

220. Pedraza CE, Chien YC, McKee MD. Calcium oxalate crystals in fetal bovine serum: implications for cell culture, phagocytosis and biomineralization studies in vitro. Journal of cellular biochemistry 2008;103:1379-1393.

221. Price PA, Chan WS, Jolson DM, Williamson MK. The elastic lamellae of devitalized arteries calcify when incubated in serum: evidence for a serum calcification factor. Arteriosclerosis, thrombosis, and vascular biology 2006;26:1079-1085.

222. Price PA, June HH, Hamlin NJ, Williamson MK. Evidence for a serum factor that initiates the re-calcification of demineralized bone. The Journal of biological chemistry 2004;279:19169-19180.

223. Hamlin NJ, Price PA. Mineralization of decalcified bone occurs under cell culture conditions and requires bovine serum but not cells. Calcified tissue international 2004;75:231-242.

224. Khouja HI, Bevington A, Kemp GJ, Russell RG. Calcium and orthophosphate deposits in vitro do not imply osteoblast-mediated mineralization: mineralization by betaglycerophosphate in the absence of osteoblasts. Bone 1990;11:385-391.